WAVE DISPERSION AND ABSORPTION

IN PARTIALLY SATURATED ROCKS.

A DISSERTATION

SUBMITTED TO THE DEPARTMENT OF GEOPHYSICS

AND THE COMMITTEE ON GRADUATE STUDIES

OF STANFORD UNIVERSITY

IN PARTIAL FULFILLMENT OF THE REQUIREMENTS

FOR THE DEGREE OF

DOCTOR OF PHILOSOPHY

By

John Wesley DeVilbiss Muñoz

January 1980

THESIS ABSTRACT

The exploration for underground steam is an important field of research in our times. Results from our laboratory experiments suggest that the ratio of compressional to shear acoustic wave amplitude is a practical and usefull diagnostic for underground steam. The compressional to shear wave propagation velocity ratio is also an indicator of partial pore saturation but the changes expected for this parameter are shown to be small in sedimentary regimes although it may be usefull in volcanic or igneous intrusive geological provinces. The large changes in the amplitude ratio are such that the measurement of the velocity ratio will be difficult in partially saturated rocks in situ.

The amplitude ratio is found to be sensitive to the amount of gas in the partially saturated rock in contrast to the velocity ratio which is insensitive to the degree of saturation in these rocks.

Shear wave amplitude was found to be a good indicator of the approximate amount of steam or gas in a rock and may be useful as a estimator of gas or steam reserves.

Compressional wave amplitude was found to be very sensitive to the appearance of a small amount of gas or steam in the pores in an originally saturated rock. The attenuation was found to increase significantly at low values of gas saturation and then decrease to values above those corresponding to complete saturation.

The presence of clays in a sandstone was seen to decrease the wave propagation velocities by a large percentage for a saturated sandstone but increase them in the dry condition. Its presence also decreased the attenuation of the rock as it dried.

Compressional and Shear waves propagation velocities have been measured accurately at a temperature of 150 degrees centigrade with respect to varying degree of saturation. It was found that the variations of compressional wave propagation velocities agree qualitatively with published theories of wave propagation in rocks. The variations of shear wave propagation velocities indicate that at the frequency of the measurements the effective shear modulus is sensitive to the presence of water in the pores. This has not been recognized experimentally or quantitatively in theory in the past. The magnitude of the change in effective shear modulus of the rock was found to vary with the permeability of the sample suggesting a possible fluid flow mechanism for the effect. Nevertheless, another mechanism, viscous shear relaxation, also can explain the phenomenon.

We present laboratory empirical results of dispersion phenomena in porous rocks. The results provide insight into the nature of the frequency dependence of attenuation in porous media and permit identification of the dominant mechanisms at high frequencies.

Comparison between measurements at sonic and ultrasonic frequencies of attenuation and propagation velocities in granite and sandstone suggests that Q is constant with frequency over this range in low pososity rocks but decreases with frequency for high porosity rocks. The behavior on the sandstone could also be related to the presence of clays

in the rock. A constant Q theoretical model was seen to fit the data for the granite but not the data for the sandstone. A generalized Voigt model was fitted to the sandstone data and was seen to predict very low values of Q for ultrasonic frequencies.

An empirical relationship between dispersion and permeability is presented. The permeability in constant porosity sandstones is shown to be related to dispersion experienced by acoustic waves in the frequency interval between 1-200 KHz.

The development of high quality transducer mosaics for acoustic pulse sources at elevated temperatures was critical to our research. Detailed procedures for their construction are included in this work.

TABLE OF CONTENTS

LIST OF TABLES

LIST OF FIGURES

Chapter I

THE EFFECTS OF PORE FLUIDS ON DISPERSION AND ABSORPTION.

1.1 ABSTRACT

Measurements of acoustic wave P and S velocities at ultrasonic frequencies indicate that, at these frequencies, pore fluids can have a large effect on the effective shear modulus for the rock. The velocities and attenuation changes for three different, important rock structures have been measured accuratelly as the pore water changes into steam. The results show that the ratio of P wave amplitude to S wave amplitude can be very valuable as an indicator of underground steam. The velocity ratio under the same varying conditions may be usefull in geothermal exploration in low porosity rocks. The attenuation of P wave was found to be largest for partially saturated rocks with high degrees of water saturation, significantly smaller in fully saturated rocks and lowest in dry rocks. S wave attenuation increases with the amount of liquid water in the pores.

1.2 INTRODUCTION

Acoustical properties of rocks are known to depend strongly on original lithology, history of the rock and present conditions of pressure and temperature. The effect of the type of pore fluids and

saturation on seismic velocities and attenuation is important to geophysical exploration since it has potential as an indicator of pore fluid type, degree of saturation or lithology. Understanding the nature of the processes involved and developing techniques for predicting the behavior of acoustic properties of porous rocks under natural conditions is therefore important. Laboratory measurements can aid in the identification of the dominant mechanisms that operate under specific conditions and this knowledge can provide testable and useful predictions.

The purpose of this study has been to verify certain theoretical conclusions and accurately measure, at ultrasonic frequencies, the changes in compressional and shear acoustic wave propagation velocities (nominated here as P and S velocities, viz., Vp and Vs) and the corresponding changes in attenuation as the water saturation of the rock decreases.

There are several ways to decrease the saturation of a rock sample. One is to saturate and weigh the sample and then apply air pressure to drive the water out. Then the sample is weighed to determine the bulk degree of saturation. This procedure was used by Gregory, [1976]. By this procedure the small thin cracks remain saturated until very dry conditions are achieved and it does not guarantee homogeneity in the distribution of pore fluid. The Pulse-Transmission method of velocity determination has the important advantage that only small specimens are required. This is at the same time a disadvantage since the velocity

value will be representative of a very local part of the rock and not an average value. Nevertheless, the small sample dimension and the simplicity of the technique is specially adaptable to elevated temperature measurements above 100°C. The evaporation process of water in rock pores is not yet well understood. The effect of capillary forces and small communicating channels makes the process very different than in other conditions. Theories of wave propagation in partially saturated rocks require precise knowledge of the distribution of liquid and gaseous phases in the pores [Toksoz, 1976]. There is no reason to believe that this distribution is the same in a rock that becomes undersaturated due to an increase in the pore volume, as in the case of rocks under shearing stresses near fault zones, to that in a rock that is undersaturated by forcing the water out with air, to that of a rock where gas is released out of solution, and to that of a rock that is heated until the pore fluid evaporates.

For geothermal exploration applications it is important to determine under natural conditions of evaporation the behavior of acoustic wave propagation velocities and attenuation. This can be achieved only by subjecting the rock to elevated temperatures and then letting the water in the pores evaporate gradually.

Ito, et al.[1979] have presented pulse transmission ultrasonic data for low permeability Berea Sandstone at approximately 150°C and 200°C with respect to saturation. In that paper we have reported our observations of Vp/Vs changes and the corresponding amplitude ratio

changes that are particularly interesting for the possible distinction between steam bearing and hot water domains. We now know that, although the observations are qualitatively valid, the sample was probably undersaturated at the beginning of the experiment and therefore the changes observed in P waves were smaller than they would have been if the sample had been completely saturated. In addition, other effects were completely absent. We have improved our saturation scheme to insure very high degrees of saturation, and some experimental procedures are revised.

Several past investigations have suggested a statistically significant difference between dynamic and static measurements of the effective elastic constants of porous rocks or between dynamic measurements at different frequencies [Thill,1974, Simmons and Brace,1965, Auberger and Rinehart,1961, Birch,1961]. Since rocks are notoriously lossy the difference in dry rocks is expected from the the dispersion that accompanies attenuation if Q does not depend on the first power or the inverse power of frequency [Kanamori and Anderson, 1977]. But different rocks show different magnitudes of dispersion. Linear theories of wave propagation predict significant dispersion for low Q rocks [Kjartansson,1979]. But the predicted dispersion has never been studied sistematically with these theories in mind.

Walsh [1968] derived the frequency dependence of the elastic constants of a solid with a dilute concentration of penny-shaped inclusions of small aspect ratio. He found that both the effective bulk

modulus and the effective shear modulus of the material depend on the product of the frequency of the wave propagating through the media and the viscocity of the pore fluid. His theory also predicts, at ultrasonic frequencies, as will be shown later, a significant difference between the effective shear modulus of a dry rock with small aspect ratio inclusions, and that of the same rock, but saturated with water. This difference has not been given adequate attention in empirical investigations in the past [Nur and Simmons, 1969]. Low porosity rock with low aspect ratio cracks has been considered insensitive to saturation even at ultrasonic frequencies.

Ultrasonic methods of velocity determination have for many years been used to study effects of pore fluids, pressure, temperature, etc. on seismic velocities without the assurance that the dispersion associated with the attenuation of the rock is insignificant at ultrasonic frequencies [Gregory,1976, King,1966]. It is very important to verify whether this assumption is justified or under what conditions it is justified.

The role of pore fluids on attenuation has been studied recently by Winkler and Nur [1979]. We present results of changes in attenuation at ultrasonic frequencies that agree with his results at frequencies below 1 KHz, and extend the range of observation where pore fluid mechanisms are found to be important, several orders of magnitude in frequency.

1.3 EXPERIMENTAL PROCEDURES

The samples are cylindrical with diameter ~19 mm and length ~33 mm. The cylindrical surfaces are ground parallel to within .03 mm and soaked in slowly circulating deionized water for 24 hours to remove the water-soluble grinding-coolant dilute solution (Mirror-Grind 4916, ArBest Corp.). They are dried in a vacuum oven (60°C, 760mm Hg) for several days and then saturated with deionized, distilled, degassed water according to a technique described by Ito et al.,[1979]. Our equipment permits complete drying of the chamber before the sample is introduced, relatively high vacuums by means of a cold trap between the vacuum pump and the chamber, immediate filling of the chamber with degassed (heated to 100°C and cooled to room temperature) dionized water, and application of up to 1800 psi of pore pressure to push the water into the very small cracks. The pore pressure in the saturation chamber is continually measured in order to determine when the maximum possible volume of water has been admitted by the sample.

Within a sealed, seamless, annealed copper jacket the sample is subjected to a constant confining pressure, Pc, of 100 bars and pore pressure of 15 bars in an externally heated pressure vessell with silicon fluid as the pressure medium [after Ito,et al.1979]. After slowly raising the temperature to 150°C the pore pressure is decreased stepwise at constant Pc and pulse-transmission velocity and first arrival zero-to-peak amplitude measurements are made after waiting for pore pressure equilibrium. At a pore pressure of approximately 4.7 bars, the saturation pressure of water at this temperature, most of the water

in the pores evaporates or is displaced by steam. Upon reaching atmospheric pressure the procedure is reversed.

1 MHz piezoelectric PZT-5A transducer mosaics eupoxied unto stainless steel end-plugs, that seal the copper jacket, are used as sources and receivers of compressional and torsional waves. The torsional transducers are composites of smaller shear plates aligned closely around the circunference of the compressional transducer. Transit times are measured with a time counter by superimposing a variable delayed pulse and the first break of the wave on synchronous channels of an oscilloscope. The counter is started with a square pulse to the source transducer and stopped by the variable delayed pulse.

The power to the source transducer is kept constant throughout the experiment to permit the comparison of the amplitude measurements. These are corrected for the change in acoustic impedance at the boundary between the transducer mounts and the sample, produced by changes in velocity. The similar correction due to the density change is negligible.

The pore pressure is controled to within .07 bars through two capillary tubes that are silver soldered into the cylindrical end plugs from the side. They communicate through an axial conduit to the ends of the sample. A thermocouple measures the temperature of the silicon fluid next to the copper jacket to within 0.5°C, and another one close by is utilized to provide feedback to the temperature controller.

1.4 OBSERVATIONS AND ANALISIS

We have data for three different rock structures: a clean sandstone known as St.Peter's Sandstone; a sandstone with approximately 5% Kaolinite known as Berea Sandstone; and a thermally fractured Westerly Granite quenched from 400°C in room temperature water. Some sample charateristics are given in table 1.

1.4.1 VELOCITY MEASUREMENTS

Figure 1 shows the results of the velocity measurements for decreasing pore pressure. The values have been normalized with respect to the velocity at the highest pore pressure corresponding to the particular rock. The dotted line indicates where the water-steam transition occurs according to published steam tables [Keenan,1969] for the temperature of the experiment.

The P velocity in the fractured granite shows a large change at the water-steam transition. This change can be attributed to the decrease in bulk modulus of the pore fluid, and its occurrence indicates that the bulk modulus of the fluid, and therefore the degree of saturation, had started to decrease in the granite at pore pressures 10 bars higher than the saturation pressure of water. The normalized comparison of P velocities shows that the variations in velocity in the fractured granite are much greater than the those in the sandstones. The decrease in density in the sandstones acts to counteract the effect of the decrease of the bulk modulus of the fluid.

TABLE 1

ROCK	POROSITY %	PERMEABILITY md	%CLAY	DENSITY: SATURATED g/cc	DRY
St. Peter's Sandstone	19.3	940	1	2.41	2.21
Berea Sandstone	19.8	620	4	2.32	2.12
fractured Westerly Granite	1.2	-	0	2.65	2.64

ROCK	ORIGIN	COMMENTS
St. Peter's Sandstone	Klondike Plant of Pennsylvania Glass Sand Corp. Augusta, Mo. U.S.A	well sorted,clean
Berea Sandstone	Cleveland Quarries, Amherst,Ohio,U.S.A	fine to medium grained
fractured Westerly Granite	Rhode Island, U.S.A	thermally fractured by quenching in room temperature water from 400 deg. C

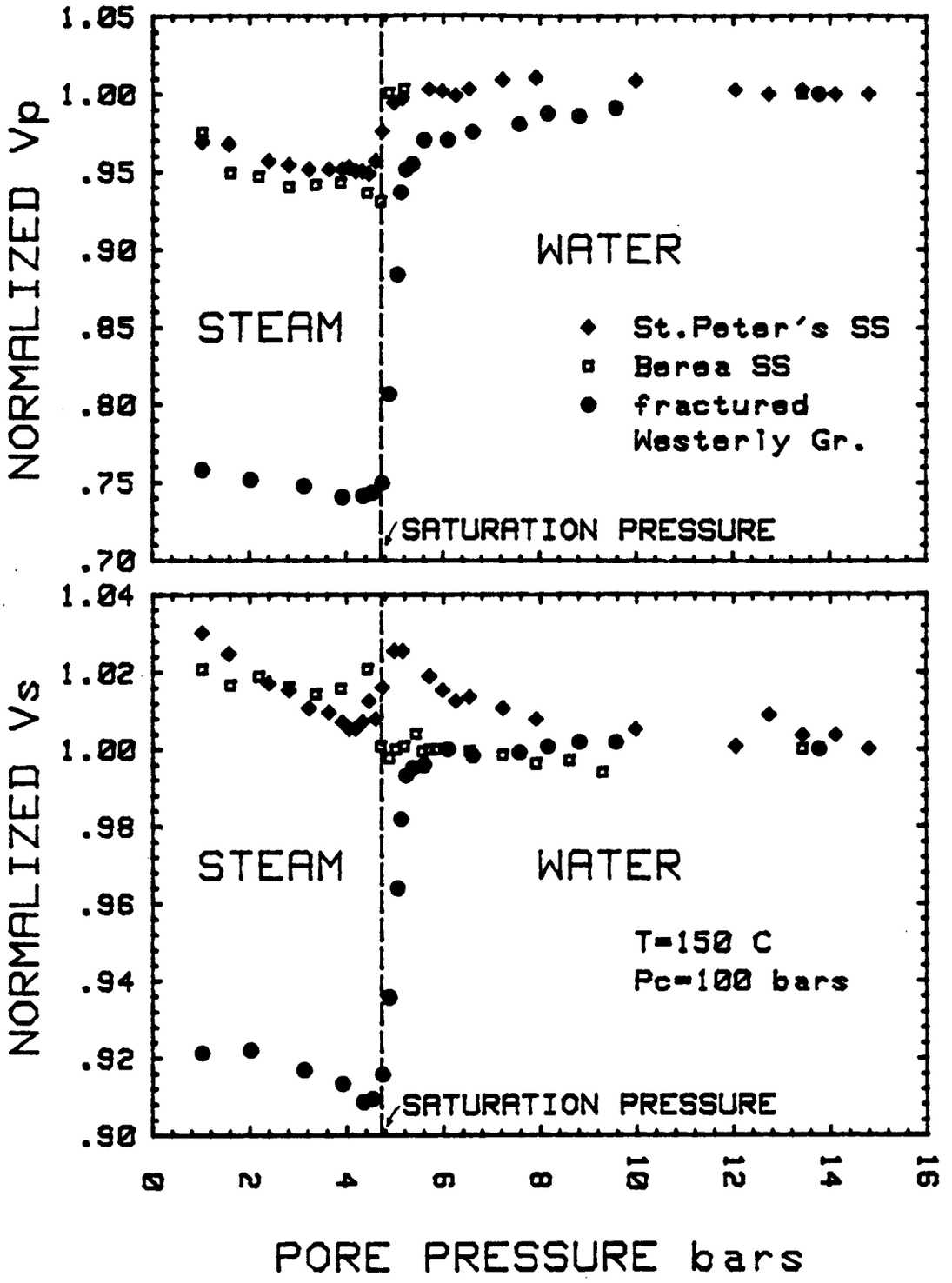

Figure 1: Wave velocities with decreasing pore pressure. The data is normalized with respect to the highest pore pressure value for each rock. The slashed line marks the saturation pressure of water at 150°C.

The effect of density change on shear velocity can be approximated by assuming a constant effective shear modulus as:

$$dVs=\frac{\phi Vs}{2\rho}$$

where:

ϕ =porosity
Vs=shear velocity of saturated rock in Km/sec.
ρ =density of saturated rock in g/cc.

The results for the shear velocity measurements reveal several interesting features: In the data for Berea Sandstone, represented by squares, the abrupt increase in shear velocity at the water-steam transition is only 50% of the change expected from the total expulsion of water from the pores. This must mean that the effective shear modulus of the rock decreases as the water leaves the pores, i.e., as the viscocity of the pore fluid drops from that of water to that of steam.

The counteracting effects can be appreciated better in the shear velocity data for the clean sandstone, St.Peter's Sandstone, represented by diamonds. Notice that the P velocity for this sanstone started to decrease at a pore pressure several bars above the water-steam transition. The change suggests that the rock became undersaturated sooner, that water had started to leave the pores, and the density had

started to decrease. The effect is a very small increase in shear velocity, but larger than the estimated error in the determinations. Figure 2 shows the absolute shear velocity data for St.Peter's and Berea sandstones. The error bars represent 2/3 of the maximum estimated error in the velocity determinations.

The effect of the unrelaxed shear modulus for St.Peter's Sandstone is 30% of the expected density effect on the shear velocity and equal to .04 Km/sec. Table 2 summarizes these observations.

Comparison of our new data with that published in Ito, et al [1979] reveals that saturation at pore pressures much higher than 100 psi with degassed water is essential to observe relaxation phenomena manifested as decreases in shear velocity as the water saturation decreases. When saturation is done at low pore pressures as in the case of the low permeability Berea Sandtone utilized in Ito, et al [1979], the shear velocity variation with decrease in saturation is just the expected variation due to a decrease in density with the effective shear modulus constant.

Another effect possibly related to the presence of clay in a sandstone is the difference in velocities of the two sandstones. Distilled water is known to decrease the rigidity of clays. Brine solutions do not affect the clays as much. This can be demonstrated easily by putting samples of Kaolinite in water, NaCl and KCl solutions symultaneously. In a few days the sample in water will have

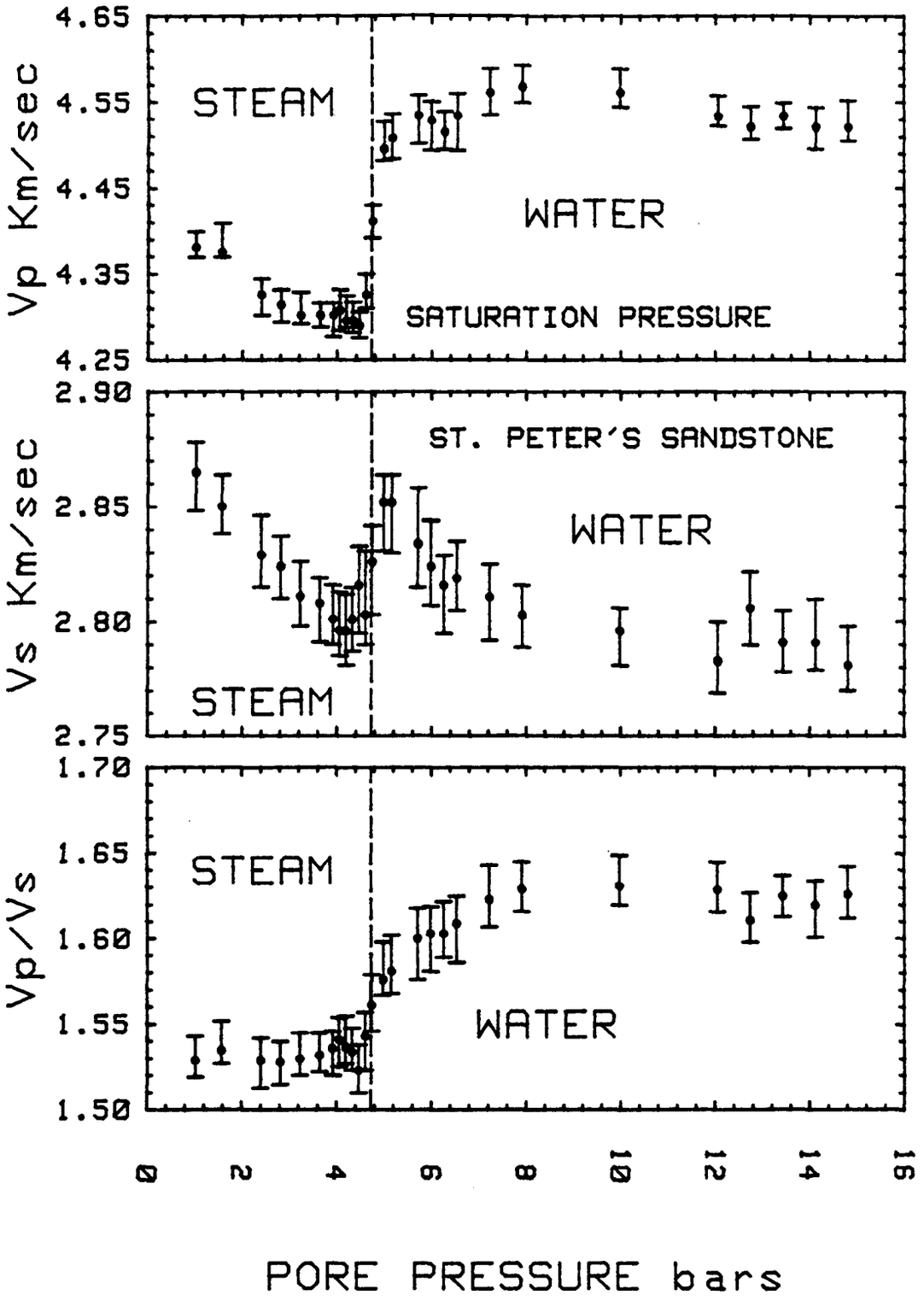

Figure 2a: Absolute wave velocities for St. Peter's Sandstone. Error bars represent 2/3 of the maximum estimated errors. Decreasing pore pressure.

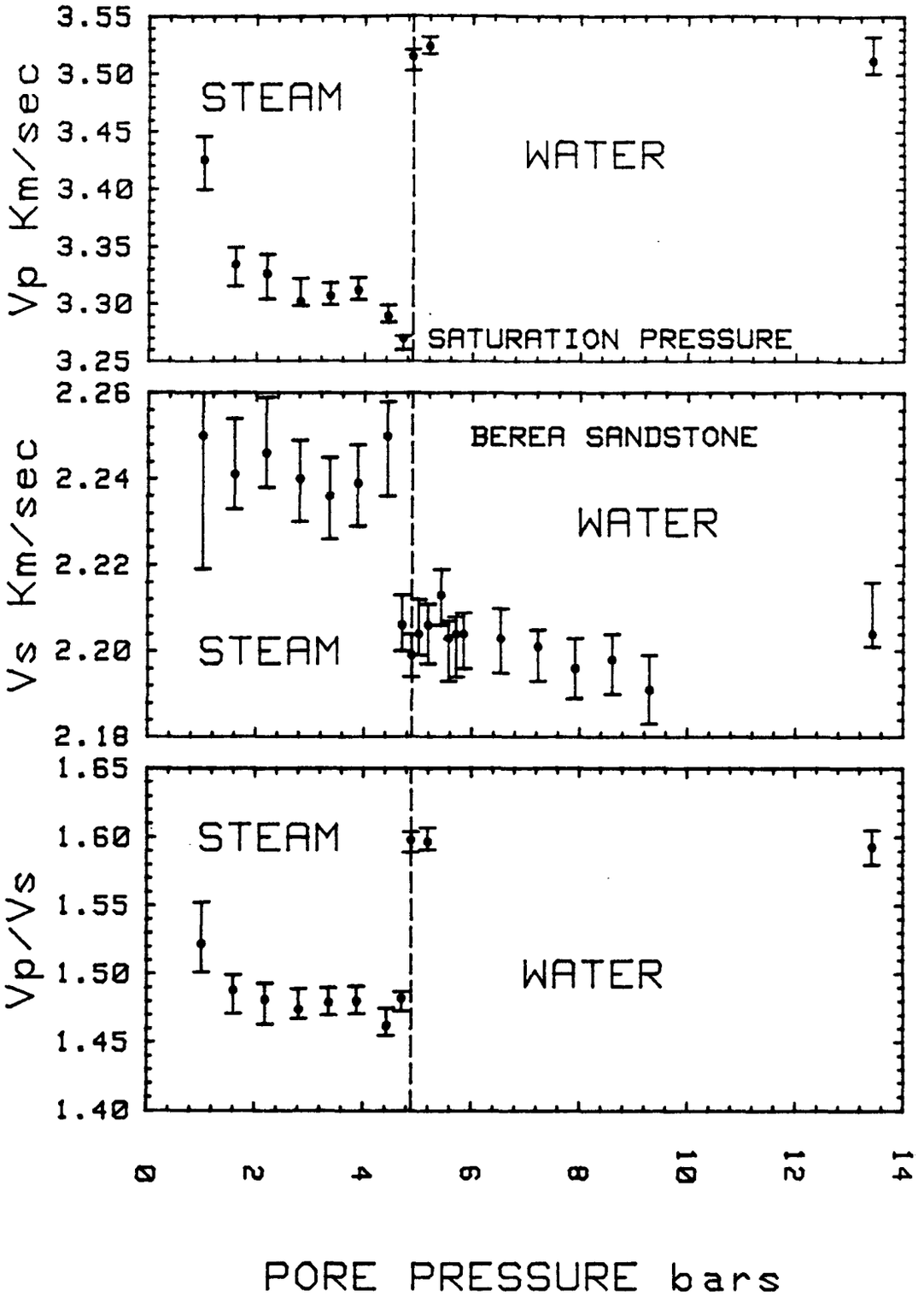

Figure 2b: Absolute wave velocities for Berea Sandstone. Error bars represent 2/3 of the maximum estimated errors. Decreasing pore pressure.

TABLE 2

ROCK	POROSITY %	PREDICTED CHANGE (Vs) Km/sec	OBSERVED CHANGE (Vs) Km/sec	OBSERVED CHANGE / PREDICTED CHANGE x100	CHANGE IN EFFECTIVE SHEAR MODULUS %
St. Peter's Sandstone	19.3	.110	.08	73%	-
Berea Sandstone	19.8	.094	.04	42%	-
fractured Westerly Granite	1.2	-	.22	-	18

disintegrated, but the samples in the brines maintain their shape. [Tosaya, 1979, personal communication]. The P and S velocities of Berea Sandstone are 1 and .5 Km/sec lower, respectively than those of St.Peter's Sandstone (at 150°C and 100 bars Pc).

An unexpected feature of the normalized velocity plot (figure 1) is the 9% change in shear velocity in the fractured granite when the pore pressure is near the water-steam transition. The calculated shear modulus change, assuming constant density, is 18%. The observation is clearly due to a change in effective shear modulus since the effect of density change is negligible. The magnitude of the change in effective shear modulus for the sandstones cannot be determined from our data. Not only does the effect of the density change mask the effect, but the increase in shear velocity due to dehydration of the clays is unknown and it reduces the difference between the shear velocity, corrected for the density change, and the observed velocity. All that can be said from the data is that the change in effective shear modulus occurs in the sandstones as the water leaves the pores.

Nur and Simmons [1969] reported large variation of Vp and a small change in Vs in low porosity rocks upon saturation. Their measurements at low effective pressures show that shear velocities for saturated Westerly granite are higher than those for dry rock, as in our measurements but, in their study, the reversed was observed at slightly higher pressures. Nevertheless, the difference between the saturated and dry shear velocities at high pressures is within the estimated

absolute error of the velocity determinations. It may also be due to fracturing or lengthening of cracks produced by the first pressure cycle required by the measurements in the dry rock.

Walsh [1969] derived expressions for the effective elastic constants of an elastic solid matrix and a viscous pore fluid. The fluid is contained in isolated penny-shaped low aspect ratio inclusions. All inclusions are assumed to have the same average diameter (major axis), d, and to be surrounded on the average by a volume, v, of solid material. When the inclusion fluid is air (viscocity vanishingly small and compressibility almost infinite) the expression for the effective shear modulus reduces to:

$$\left(\frac{\mu_o}{\mu} - 1\right)_{air} = .12\left(\frac{d}{v}^3\right) + .024\pi\left(\frac{d}{v}^3\right) \qquad (1)$$

When the inclusion fluid is water at 150°C (viscocity low but compressibility finite) the expression is:

$$\left(\frac{\mu_o}{\mu} - 1\right)_{water} = .12\left(\frac{d}{v}^3\right) \cdot \frac{1}{1+\left(.0018\,\frac{f}{\alpha}\right)^2} \qquad (2)$$

where: μ_o = shear modulus of solid matrix

$\bar{\mu}$ = effective shear modulus of solid with inclusions

$\frac{d^3}{v} = \frac{6C}{\pi\alpha}$ = crack density

f = frequency in MHz

α = aspect ratio, $\alpha << 1$

the factor:

$$\frac{1}{1+\left(.0018\ \frac{f}{\alpha}\right)^2} < 1$$

so that the right hand side of equation (1) will always be, at least, $0.024\pi\ d/v$ greater than the right hand side of equation (2). Therefore:

$$\bar{\mu}_{water} > \bar{\mu}_{air}$$

Figures 3 and 4 shows the ratio of the effective shear modulus to the shear modulus of Quartz plotted with the crack density set constant. The curves are for the pore conditions of complete 150°C water saturation or complete steam saturation. The predited change in effective shear

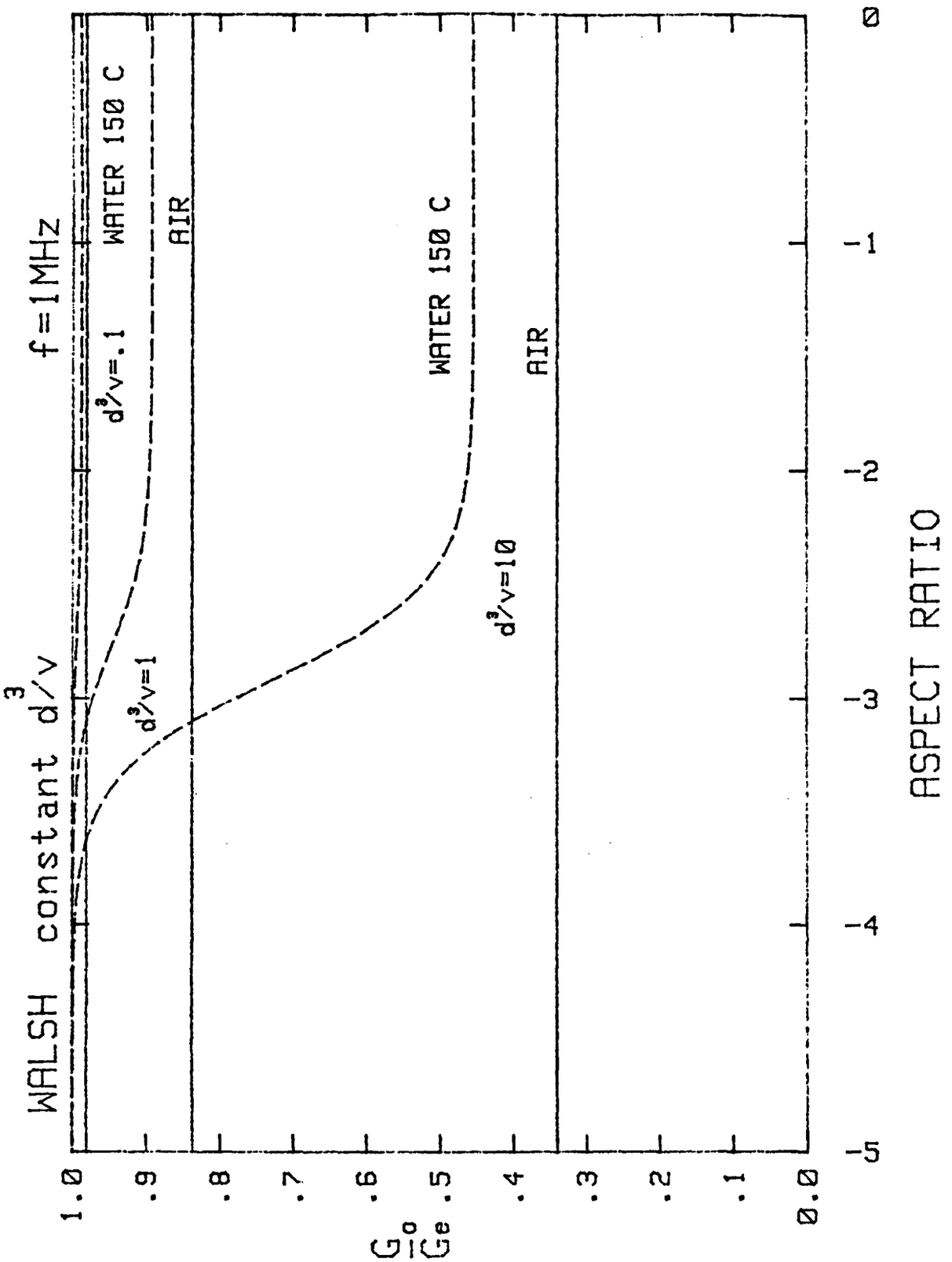

Figure 3: Results of substitutions into Walsh (1969) model for 1MHz and water at 150°C in the inclusions, or air in the inclusions.

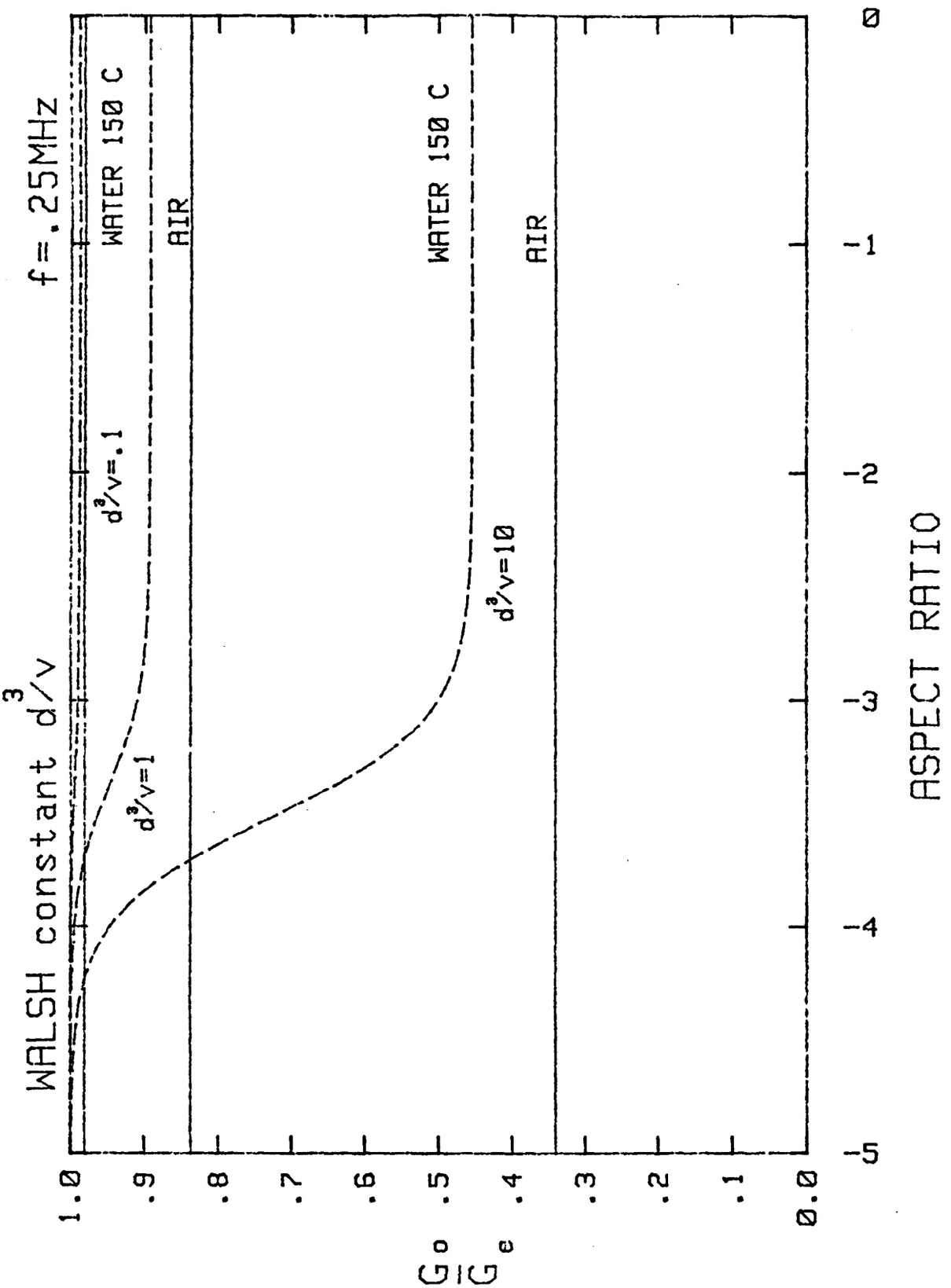

Figure 4: Results of substitutions into Walsh (1969) model for 0.25 MHz and Water or air in the inclusions.

modulus can be seen for different aspect ratios. In a natural rock, there will be a distribution of aspect ratios [Toksoz,1976]. The computation of the effective shear modulus of the saturated rock requires an integration over the concentrations of the aspect ratios.

In another paper Nur and Simmons [1969b] showed that the effective shear modulus and attenuation depend on the viscocity of the pore fluid. The results show a large change in shear velocity in the same rock for several orders of magnitude change in viscocity. Since shear modulus in Walsh's theory depends on the factor $\omega\eta$ an order of magnitude change in η is equivalent to an order of magnitude change in frequency and viceversa. Nur and Simmons reported a small positive change in Vs upon saturation with water.

O'Connell and Budiansky [1977] have proposed that a fluid-flow mechanism can also be the cause of the change of shear velocity upon saturation in a rock. They conclude, in fact, that fluid-flow in the "saturated isobaric" condition is the dominant mechanism producing the unrelaxed effective shear modulus for low porosity rocks. We find that in addition Walsh's expression predicts a significant difference in effective shear moduli between the solid with empty or steam filled inclusions and one in which they are filled with water at 150°C for a frequency of 250 KHz, aspect ratios of 10^{-4} and crack densities greater than 5. Nevertheless, the application of Walsh's equation to model a fractured granite of high crack density may be innapropiate. In the derivation it is implicitly assumed that the crack density is small since the crack is contained in

material that is not cracked. In addition, the cracks are modeled by flattened elliptical inclusions whose surfaces are almost in contact. The extremely thin films of water in these inclusions will sustain high stresses at lower frequencies than more realistic cracks filled with water. The capillary forces in the real pores, acting on the fluid may increase its resistance to flow so that the shear modulus will appear unrelaxed at ultrasonic frequencies. But this is speculation.

O'Connell and Budiansky's treatment of the problem is based, for large crack densities, on the "self consistent approximation" They presented results of the application of their theory in a water saturated rock with aspect ratios distributed (uniformly in log α) from 10^{-4} to 10^{-2} These aspect ratios may be representative of our fractured granite. The theory predicts significant dispersion due to fluid flow between 100 KHz and seismic frequencies. Since the shear velocity at seismic frequencies is insensitive to saturation [Biot, 1956] and the porosity of the fractured granite is small we can obtain a measure of the dispersion between those frequencies and the frequencies of our measurements by taking the ratio of the velocities in the saturated and dry conditions.

The important results in the comparison of our experimental results with theoretical studies is that our results can be explained qualitatively at least, by considering two mechanisms: fluid-flow between saturated cracks and viscous shear effects. Our attenuation change measurements on the same samples, made symultaneously with the

velocity measurements, provide more information on the saturation state of the samples at each pore pressure. Some insight can be gained by considering those results in conjunction with the velocity data.

1.4.2 ATTENUATION MEASUREMENTS

Figure 5 shows normalized values of the zero to peak ampitudes of the first arrival. It reflects changes of the attenuation in the sample. The values are normalized with respect to the corresponding value for the rock at the highest pore pressure. The three sets of measurements show the same minimum in P wave amplitude above the saturation pressure of water and then abrupt increases to 50% above the reference amplitude as the pore pressure decreases. The minimum in P wave amplitude occurs where the pores are partially saturated, where only a slight amount of water had been bled.

At temperatures removed below the boiling point of water, a crack that is communicated to other pores through one or several channels, will remain saturated until the pressure outside the pore is greater than:

$$\frac{2A_t}{r} + P_w$$

P_w = fluid pressure inside pore.

A_t = adhesion tension between water and air or steam.

r is the largest radius communicating the crack and Pw is the fluid pressure in the saturated pore [Amyx, 1960]. This relationship is roughly applicable when water is air-flushed from a sample and it shows

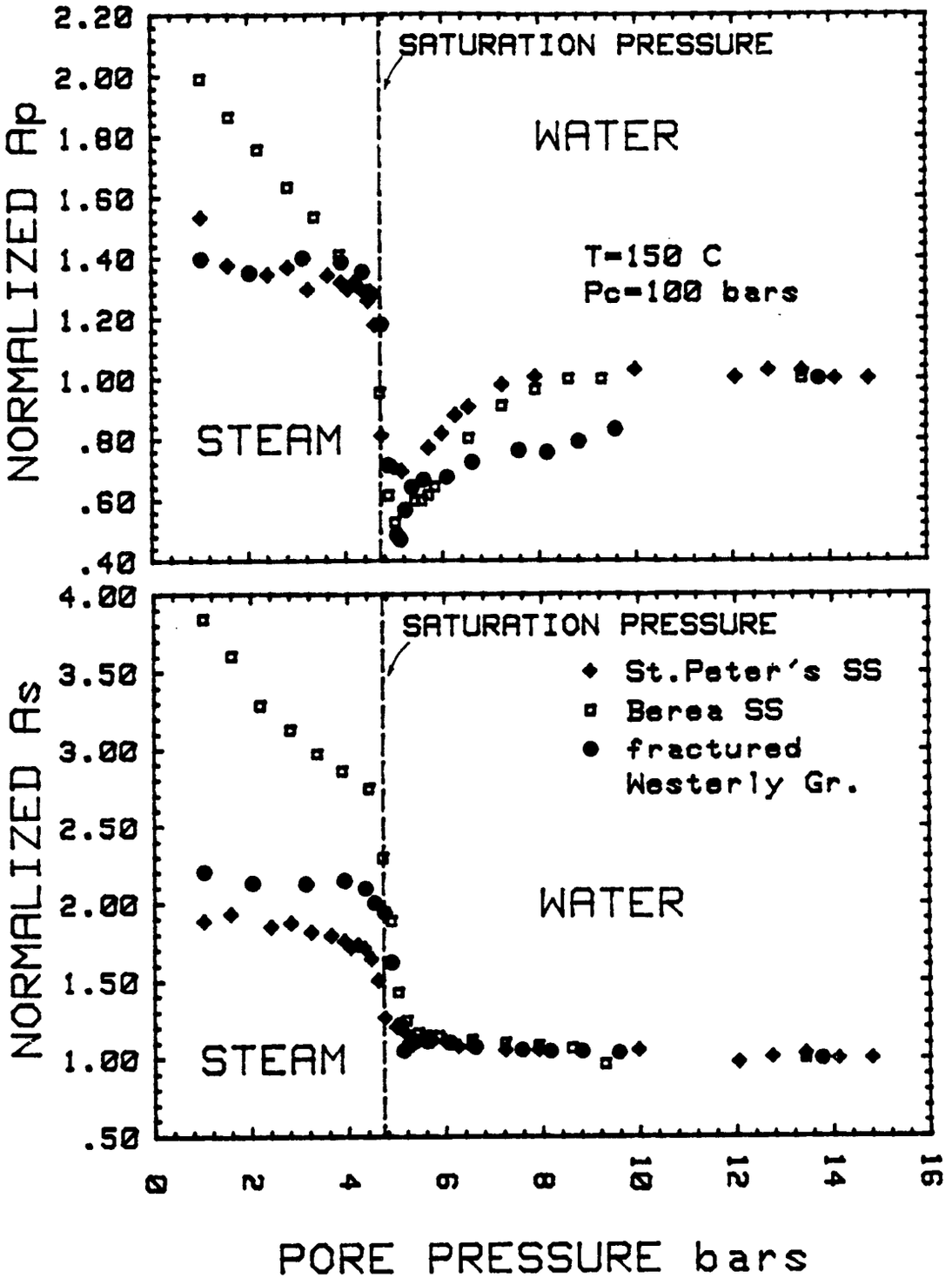

Figure 5: Measurements of the first arrival amplitudes normalized with respect to the values at the highest pore pressure for each rock. Decreasing pore pressure.

that, in this case, the cracks with the smallest radius will loose some of their water only after cracks of larger radius openings. Cracks that communicate to other pores through only one outlet will remain permanently saturated in this case. Nevertheless, at elevated temperatures, the process is very different. Hsieh [1979] has studied some aspects of the physics of the behavior of water in pores as the pore pressure decreases toward the saturation pressure of water. Pore water under these conditions is not only in one phase. It is a low compressibility mixture of water and steam in continuous change of phase. As the pore pressure approaches the saturation pressure, this mixture begins to leave the pores with larger openings, leaving a coating on the walls of the pores and remaining in the smallest pores [Collins, 1961]. It is inadequate then to speak of pore water in the liquid state in these conditions. At the saturation pressure, even the thinnest cracks will contain the mixture of water and steam, but the layers of this mixture held unto the surfaces of the crack by the strong capillary forces is thick enough to connect at the outlet or outlets of the thin cracks. Therefore, the fluid compressibility changes above the saturation pressure and the fluid in most cracks is pushed out by internal evaporation upon reaching the saturation pressure. The result is a decrease in Vp above the saturation pressure as observed for the fractured granite and St.Peter's Sandstone. According to this model of fluid distribution during evaporation, the viscocity of the pores does not change until the saturation pressure is reached and all pores are evacuated. If the shear velocity difference between the fully saturated and dry conditions of the fractured granite is due to the viscocity of

the fluid in the thin pores, then we would expect the shear velocity to remain constant until a pore pressure very close to the saturation pressure of water. Within the experimental error this is observed in the shear velocity data for the fractured granite.

It is possible that clays modify the character of the shear velocity changes at the water-steam transition. This is suggested by the abrupt decrease in effective shear modulus in Berea Sandstone and the gradual change in the almost clayless St.Peter's Sandstone. Layered clays are known to expell their water suddenly under certain conditions of pressure and temperature creating zones of overpressure that may represent potential danger zones for drillers. In the preparation for the experiments, as the temperature of the rocks was increased slowly to 150°C at approximately constant confinning pressure, the pore pressure in St.Peter's Sandstone, and to a smaller degree that in the fractured Westerly Granite decreased, while in the case of Berea Sandstone it increased notoriously and had to be bled continually down to 15 bars. This means that the pore volume increased slower than the pore fluid volume for Berea Sandstone or that the clays were expelling their water as the temperature was increased. Since the increase in Pp for this rock was very large per °C, the second explanation seems more applicable.

Our data shows that the maximum attenuation of a P wave at ultrasonic frequencies occurs above the saturation pressure of water and that the attenuation in the saturated rock is less than that for partial saturation and more than that for the steam filled or almost dry rock.

In the case of the steam filled clay sandstone the attenuation is very sensitive to the dehydration of the clay in the rock. It decreases as the clay dries.

Shear amplitude changes for the three structures of rock are distinctly different in form and magnitude from those of the P wave amplitude. The measurements of shear wave amplitude indicate that shear wave attenuation increases monotonically with the amount of water-steam mixture in the pores, and that it is almost constant above the saturation pressure of water in the pore pressure range where the P wave attenuation is decreasing, and, below the saturation pressure the changes in shear attenuation are much larger than those for P wave attenuation. It is important to note that the attenuation of ultrasonic shear waves does not change very much as the sample becomes undersaturated. That means that the mechanism operating in total water saturation produces approximately the same attenuation that the mechanism operating in the condition where P attenuation is increasing to a minimum.

Our relative attenuation results are in excellent agreement with Winkler's [1979] resonance-bar absolute measurements of attenuation at around 1 KHz (figure 6). The agreement suggests that the dominant mechanisms of compressional attenuation that produce the changes are not those related to phase changes produced by the passing of the wave, but those in which the pore fluid movement or viscous dissipation absorbes energy. It is remarkable that attenuation with respect to saturation

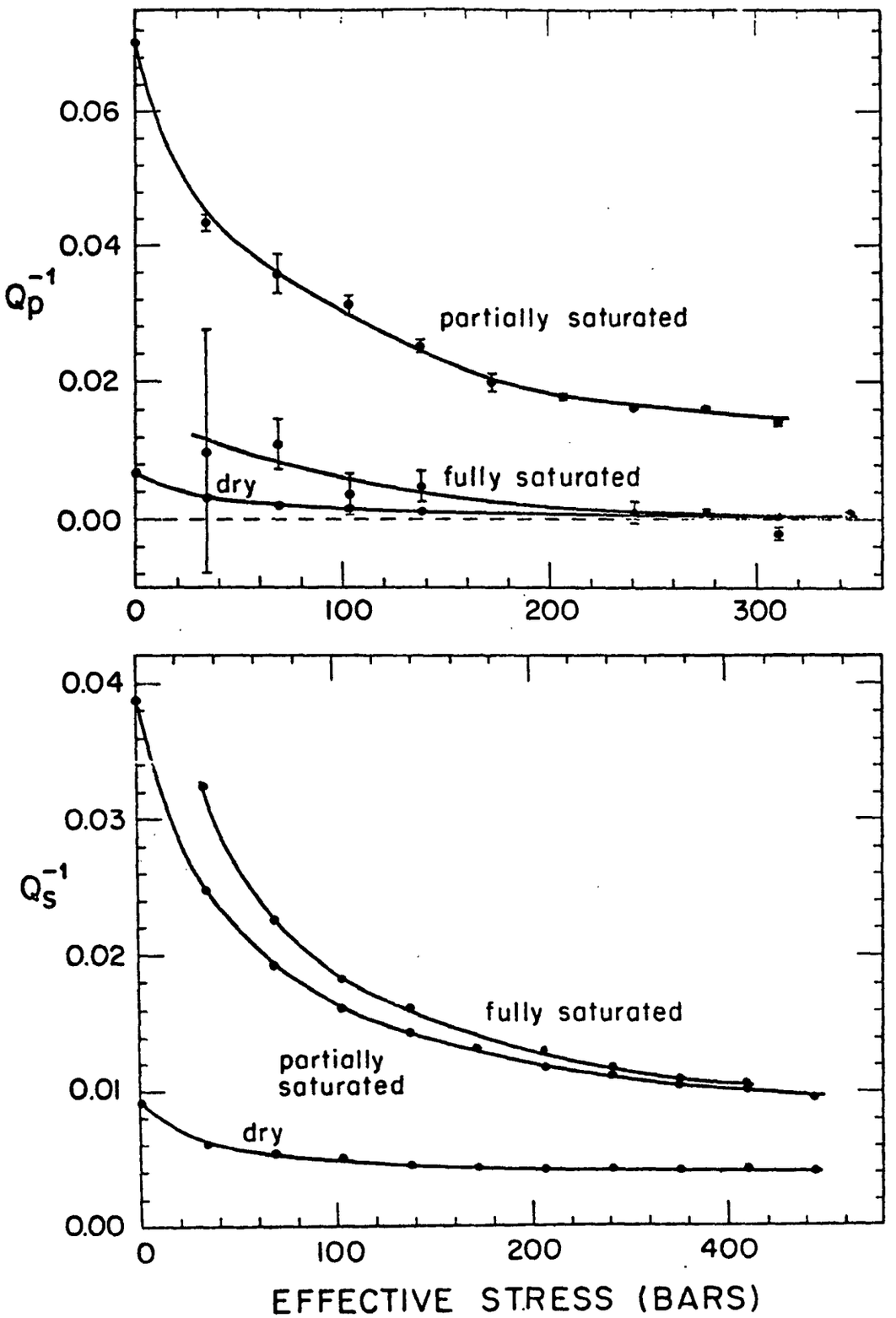

Figure 6: Winkler (1979) measurements of Q in Massillon Sandstone, a sandstone very similar to Berea Sandstone.

with water changes qualitatively in the same manner within 3 orders of magnitude in frequency even when some additional mechanisms may be operating and some may have ceased to operate at ultrasonic frequencies. In addition the temperature is different by 130°C. It shows that pore fluid mechanisms are indeed dominant over other mechanisms in saturated and partially saturated rocks.

Comparison of the velocity and relative attenuation results lead to the observation that, although the existence of partial saturation is evidenced by the behavior of the P wave amplitude and velocity at pore pressure above the saturation pressure, the shear velocity remains high, i.e., the shear modulus remains unrelaxed and shear attenuation remains high. In view of the tendency of water to coat the walls of the pores during the evaporation process, it appears that since partial saturation does not affect the shear velocity (figure 1) in the fractured Westerly granite, that, under the partially saturated conditions where the P wave amplitude is decreasing as pore pressure decreases, the mechanism for attenuation and dispersion cannot be one that is based on inter-crack squirting in saturated pores. The fluid flow mechanism is one that can operate in partially saturated pores. Mavko and Nur [1979] have proposed such mechanism. It predicts that the P wave attenuation increases substantially as the sample becomes slightly undersaturated while the shear attenuation slowly decreases. The model considers the inertial effects of water drops in the pores. Both intra-crack flow and viscous shear relaxation, the latter a mechanism that can operate on the pore water-coatings, appear applicable as an explanation of the dispersion observed in the fratured Westerly Granite at 150°C.

Our experimental results may be important in geothermal exploration since they predict that a partially saturated zone will attenuate P waves much more than S waves and that the ratio of the amplitudes of the waves is a very sensitive diagnostic of the presence of steam underground (figure 7). It is important to observe that the ratio of amplitudes, unlike the velocity ratio (shown in figure 8) can distinguish between an undersaturated zone and one that is almost dry or vapor dominated. Since the attenuation of P waves is so strong in partially saturated media it becomes very difficult to measure travel time residuals produced by changes in P velocity. For the same reason velocity ratio contrasts may not be of great utility in the detection of partially saturated rocks underground.

McEvilly [1978] has reported in situ observations of the decrease of the P wave amplitude to shear wave amplitude ratio in a caldera in La Primavera, Jalisco, Mexico (figure 9). The low values of the ratio correspond to regions where surface steam manifestations are evident. The simplicity of the field measurements assures that the ratio of compressional to shear amplitude will become a valuable tool in exploration for partially saturated steam reservoirs. Although most geothermal reservoirs may have pore pressures above the saturation pressure of the pore fluids at shallow depths at greater depths the geothermal gradient may increase enough to increase the saturation pressure above the ambient pore pressure [Kjartansson, personal communication]. In these situations a contrast in P to S attenuation will exist.

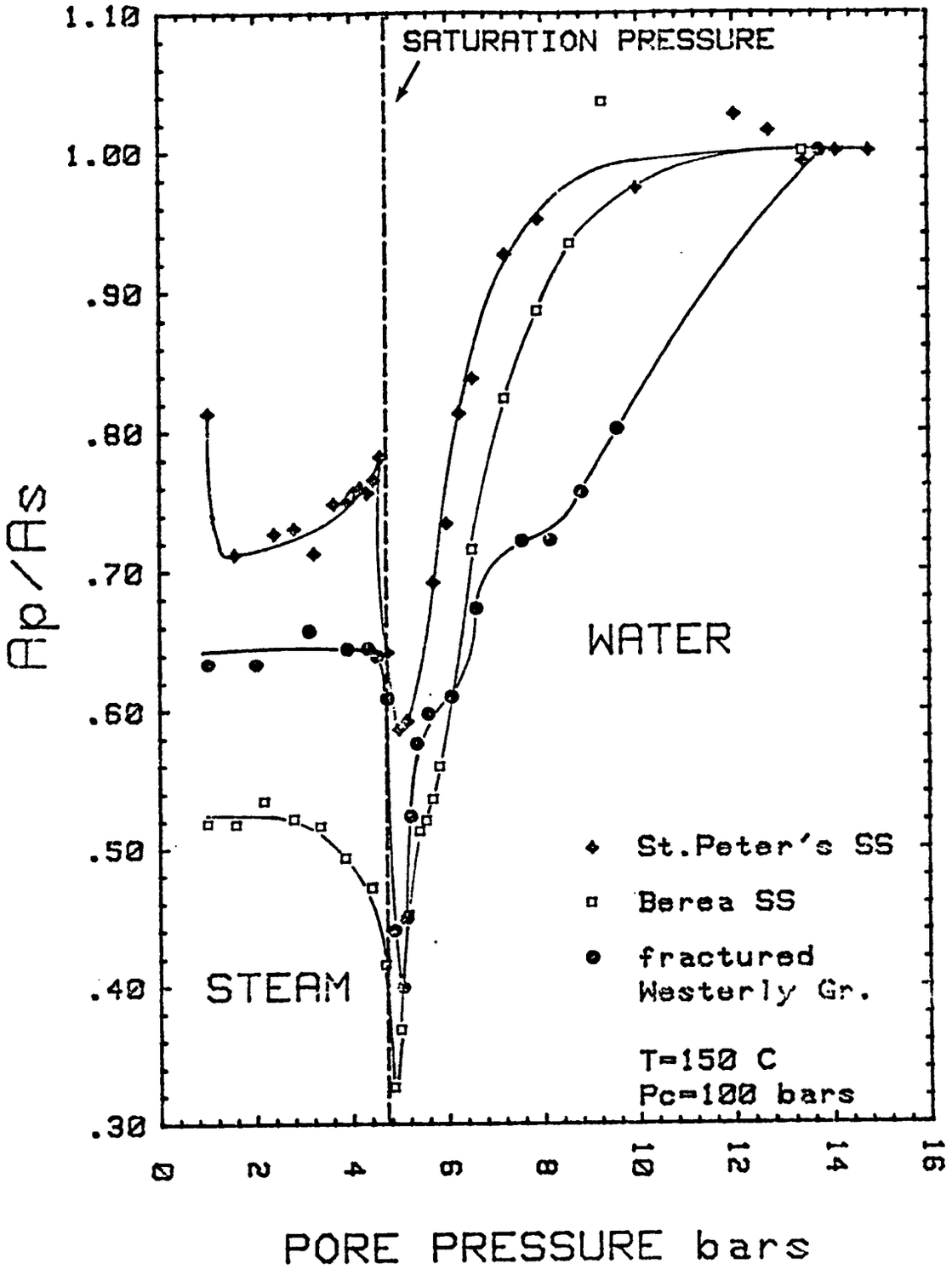

Figure 7: Ratio of the normalized amplitudes of the waves. Decreasing Pore pressurem. Note minimum above the saturation pressure of water for the three rocks.

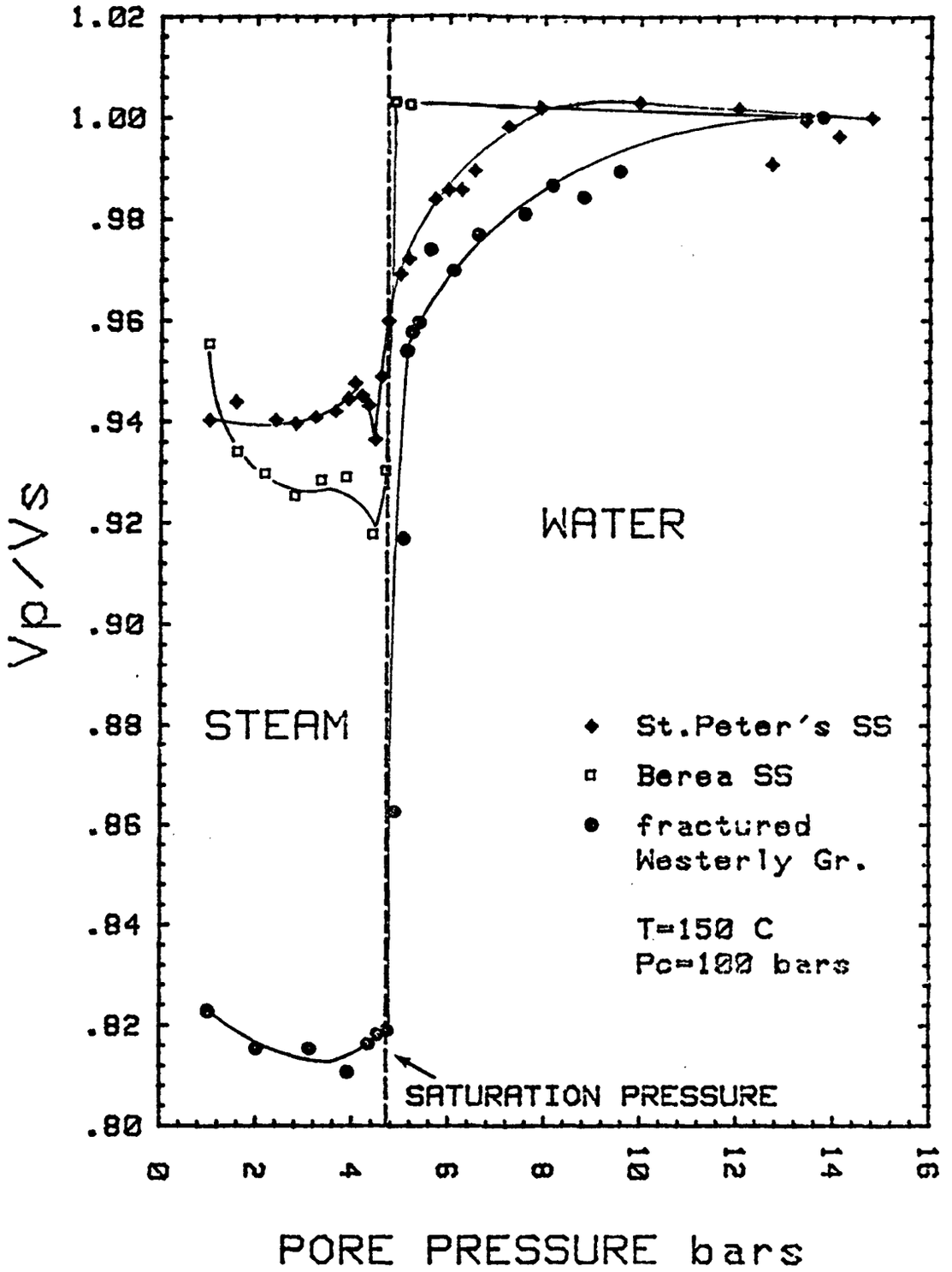

Figure 8: Ratio of Velocities. Decreasing pore pressure.All three rocks show rapid decreases close to the saturation pressure of water.

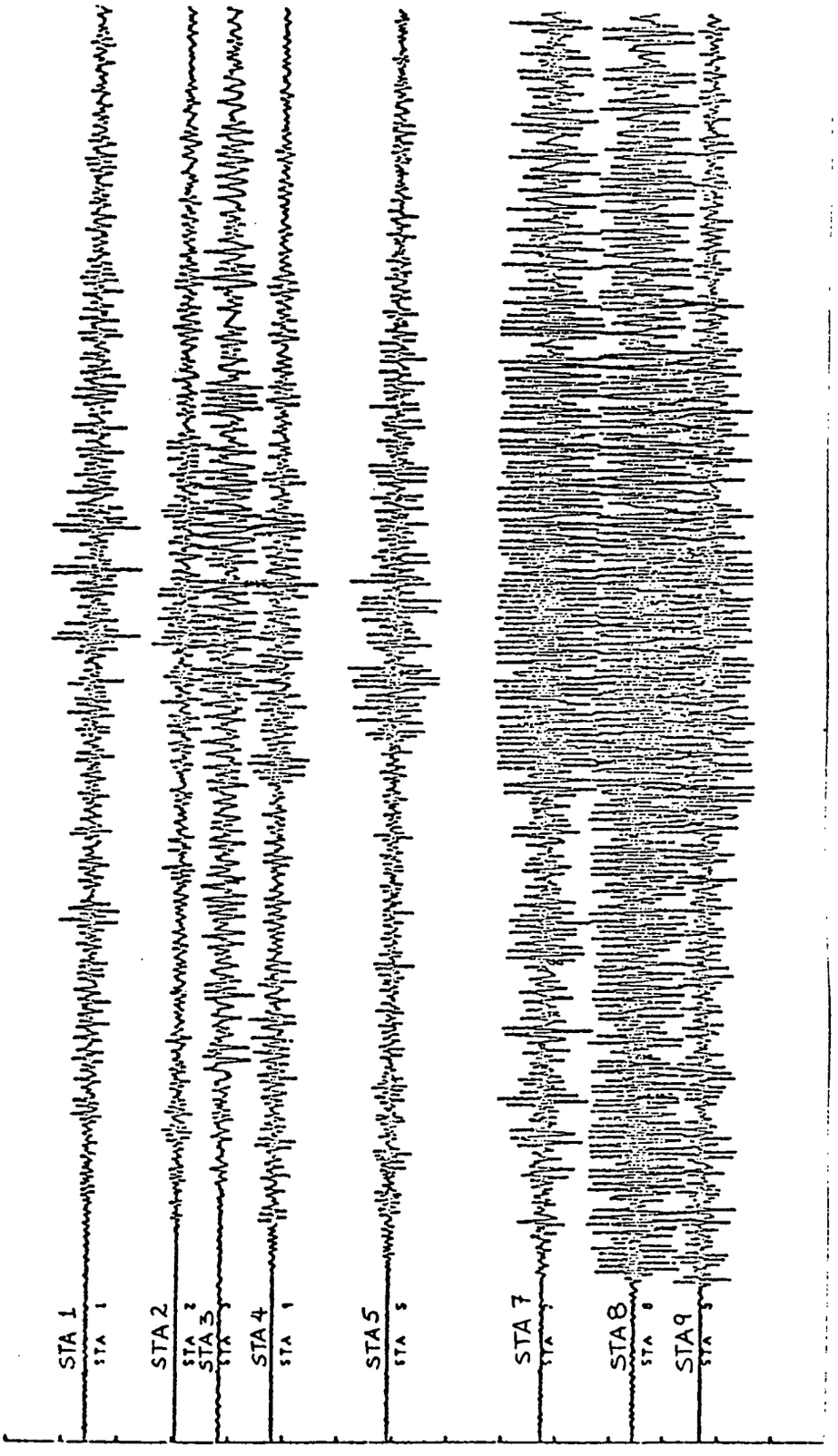

Figure 9: Seismological data from la Primavera, Jalisco, Mexico. Source is approximately 150 Km away. Station numbers decrease toward the North and into a caldera. Station three is located above a steam vent.

Chapter II

OBSERVATION OF DISPERSION PHENOMENA IN POROUS ROCKS.

2.1 ABSTRACT

Significant dispersion was observed to occur in saturated granites and sandstones between sonic and ultrasonic frequencies. For Sierra White Granite drying under room conditions from a saturated state, the shear modulus was seen to behave as predicted by a dispersion relation with Q independent of frequency. For Berea Sandstone of large permeability, the shear modulus varies with frequency much more than what the constant-Q dispersion relation predicts, suggesting that Q decreases with frequency in high porosity or permeability rocks but is constant with frequency in low porosity or low permeability rocks.

2.2 INTRODUCTION

Linear theories of wave propagation in rocks predict significant dispersion within two orders of magnitude in frequency in low Q rocks. These are known as the "Band Limited Near Constant Q", the Voigt-Ricker, and the "Linear Constant Q" models [Kjartansson, 1979]. In contrast, all the nonlinear friction mechanisms that have been proposed assume frequency independence (but predict amplitude dependence) of phase velocities. These later models rest on the basic assumption that since

Q was observed to be nearly constant with frequency in almost dry rocks [Born,1941, Birch and Bancroff,1940], then the attenuation mechanisms had to be that of friction since the heat generated per unit slip on two surfaces that slide against each other is the same regardless of the rate at which it takes place. Phase velocity was thought to be independent of frequency because frequency did not enter the theoretical derivations. There was no reason to think that the moduli of a cracked solid should be very sensitive to the rate at which slip or relaxation occurred for the same strain amplitude and the intuitive argument was thought to be supported by experimental observations for all Q values.

Some past observations of frequency independent phase velocity have been published in the past. Birch and Bancroff [1940] have measured velocities in granite over several decades of frequency and have found no dispersion within experimental uncertainty. Peselnick and Outerbridge [1961] measured velocities in limestone over 7 orders of magnitude in frequency and observed no significant dispersion. Nevertheless, these investigations have two important features in common: No attention was given to the saturation states of the samples. All the tested rocks had large Q values.

Other investigations have found that velocities are frequency dependent. Biot showed theoretically that relaxation behavior of the liquid can occur at frequencies in the low-megacycle frequency range for cracks of one micron width saturated with water [King, 1966]. Wyllie, et al [1962] and Gregory [1963] saw that shear wave velocities increased in

some samples when liquid saturated. The past chapter has shown that when a sandstone is saturated under low pore pressures that relaxation phenomena dissapears, but appears when the samples are saturated with higher vacuums and under higher pore pressures for a longer period of time. Gretner [1961] compared chuck wave velocities to sonic log velocities and found that dispersion occured within the frequencies of measurements. Simmons and Brace noted that for lossy materials the difference between the moduli calculated from ultrasonic pulse measurements and those obtained from low frequency deformation experiments was significant [Kjartansson, 1979]. Therefore, observations have suggested that in some rocks or rock conditions, dispersion is significant.

The purpose of our paper is to report our laboratory observations of dispersion, and to compare our observations with existing theories that are in agreement with past observations.

2.3 GENERAL PROCEDURE

We have measured shear velocities in Sierra White Granite and Berea Sandstone at sonic and low ultrasonic frequencies as the samples dried at room humidity, temperature and pressure from a saturated condition. Although the drying process is not homogeneous and not exactly at the same rate for all samples the simple experiments were done to test for the existence of dispersion in the two, low Qs, different rock structures.

Sierra White Granite, unlike Berea Sandstone, is not well known. Table 3 shows the principal characteristics and physical properties of the granite. Some parameters for Berea Sandstone are also given.

We have utilized composite compressional and shear transducers as sources and receivers of acoustic ultrasonic waves as described by DeVilbiss and Nur [1979]. Saturation was achieved by the same technique as described in the same paper. Long Resonant-bar samples (40"x1"x1") were saturated at pore pressures of 600 psi for several days, and ultrasonic samples were saturated at pore pressures greater than 1400 psi. The Resonant-bar samples were square in cross section. Therefore, a correction as given by Spinner [1961] was applied to the shear velocity data for this samples. The resonant bar measurements were done on a system built and described by Winkler [1979, 1979b].

2.4 EXPERIMENTAL OBSERVATIONS

2.4.1 SIERRA WHITE GRANITE EXPERIMENT

Figure 10 shows the ultrasonic data for Sierra White Granite as it dries on the bench at room conditions. P and shear velocity errors are estimates of the maximum error. Vp/Vs is also plotted along with the velocities. A gradual decrease of the shear velocity with time is observed, indicating that the effective shear modulus of the rock is decreasing with the degree of saturation. The decrease in velocity is approximately a 10% change and it stops when the saturation state of the sample is in equilibrium with room humidity. In our results for Sierra White Granite the effect of the decrease in degree of saturation is much

TABLE 3

SAMPLE DESCRIPTIONS

BEREA SANDSTONE	A fine to medium grained graywacke of Mississippian age obtained from Cleveland Quarries, Amherst, Ohio. The sandstone utilized in this study was a high permeability type of Berea, 620 md. Porosity 19.8%.
SIERRA WHITE GRANITE	A fine-grained, grayish-white muscovite-biotite granite obtained from Raymond, Cal. through the American Monument Co., Colma, Cal. Its porosity is .27%, bulk density 2.64 g/cc. An Approximate analisis is 74% silica, 15% alumina, 2% iron oxides, 3% lime, 5% soda and potash, and 0.3% combined water.

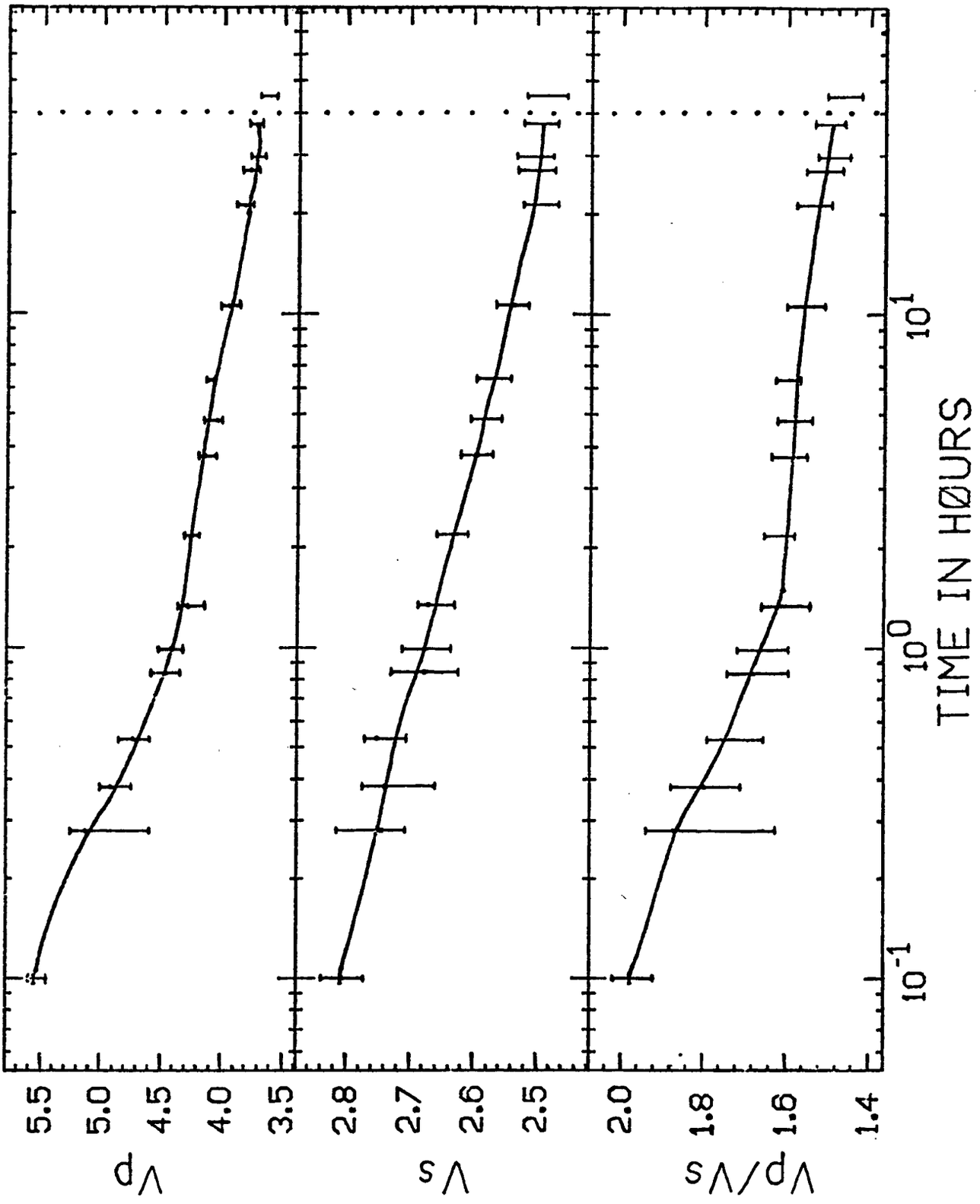

Figure 10: Ultrasonic measurements of velocities for Sierra White Granite drying under room conditions from total saturation. Data points after the dotted line are for the sample after one day in vacuum at 40°C, and filled with room air.

larger on the P velocity so that the velocity ratio still decreases by 24%.

Shear velocity in low porosity rocks is usually thought to be constant with saturation . In another paper [see chapter 1] we have investigated the causes of the change in effective shear modulus detected at ultrasonic frequencies in porous rocks upon saturation. Our concern here is to relate the effect to other measurable, macroscopic properties such as dispersion, Q and permeability.

Zero-to-peak, first arrival amplitude data was recorded during the experiment to determine the degree of saturation at the beginning of the experiment. The data is included in figure 11. The abrupt decrease in the P amplitude at the beginning of the drying process and the gradual increase of shear amplitude (proportional to 1/attenuation) is typical of rocks passing from a totally saturated to a partially saturated condition. [see chapter 1 and Winkler,1979]. The monotonic increase in shear amplitude indicates an increase in Q as the degree of saturation decreases.

Resonant-Bar data for the same rock [Winkler, personal comunication, 1979] appears in Figure 12. The samples were in close proximity in situ. Shear wave velocity is approximately constant while Qs increases monotonically as the sample dries. All strain amplitudes are smaller than 10^{-7}.

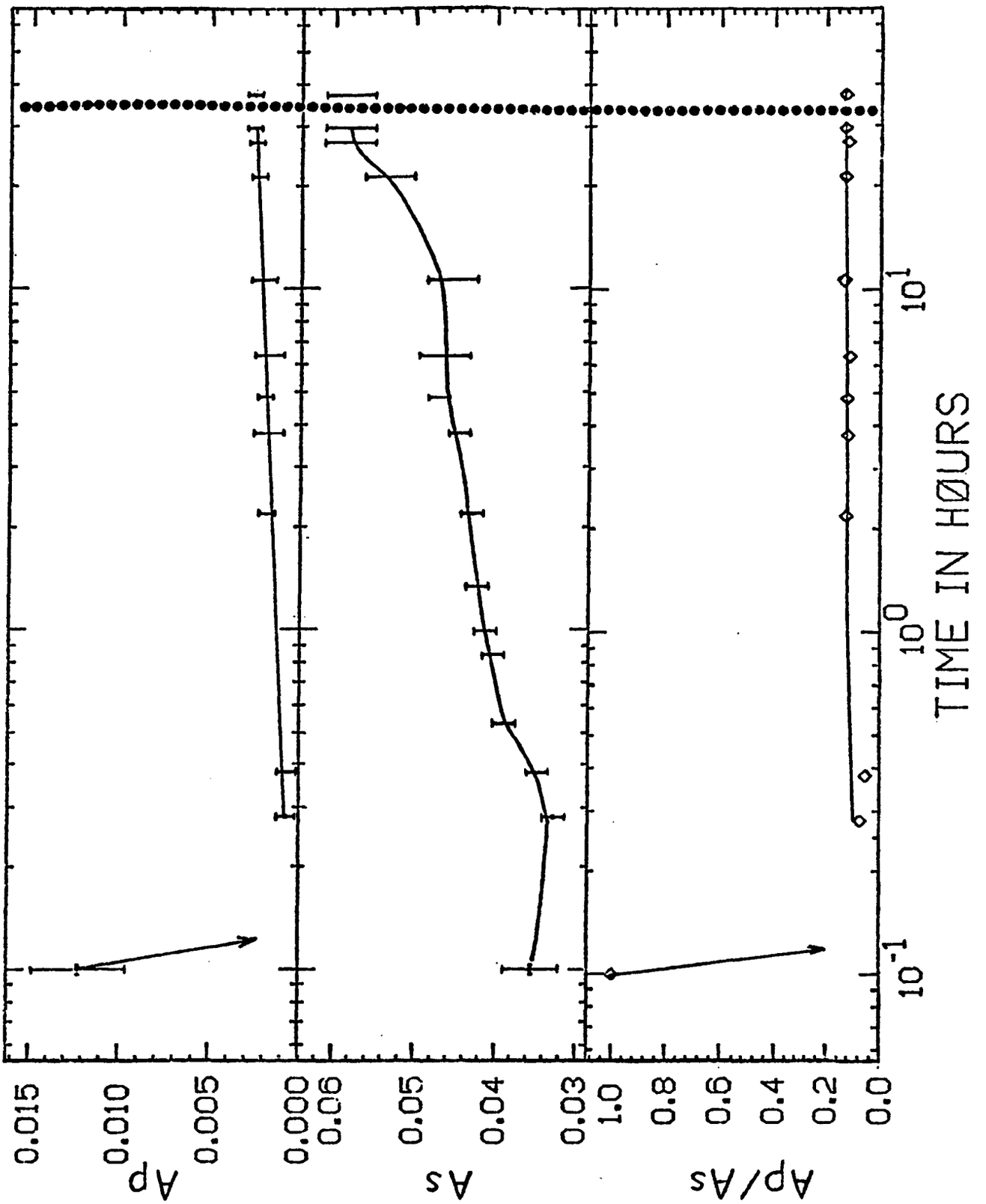

Figure 11: Amplitudes of the ultrasonic signals for Sierra White Granite drying under room conditions from total saturation. Arrows indicate the loss of signal below the noise level in the condition of partial saturation.

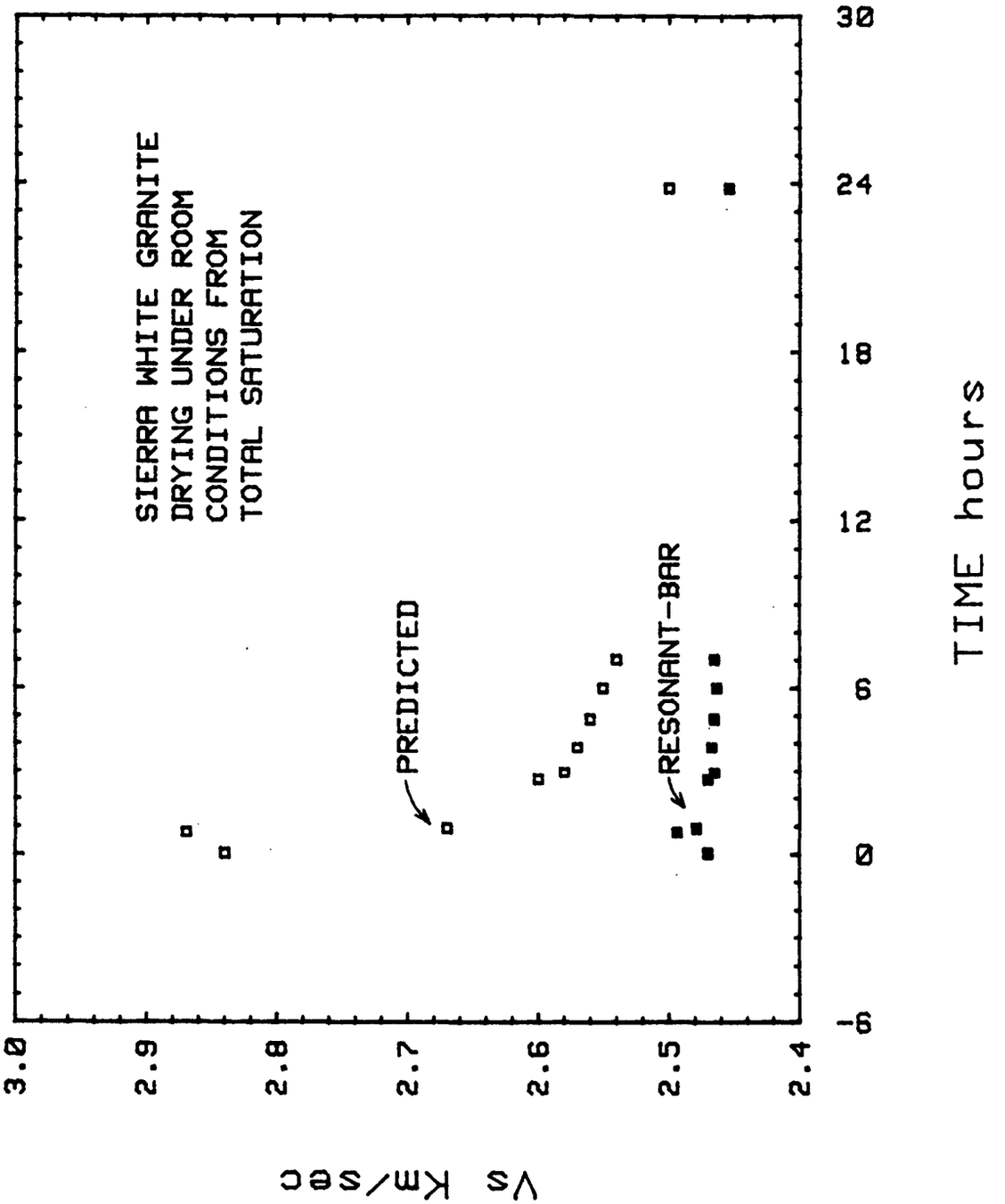

Figure 12a: Resonant-bar shear wave velocity for Sierra White Granite drying under room conditions from total saturation. The predicted values of ultrasonic shear velocity from Kjartansson (1979) are also plotted.

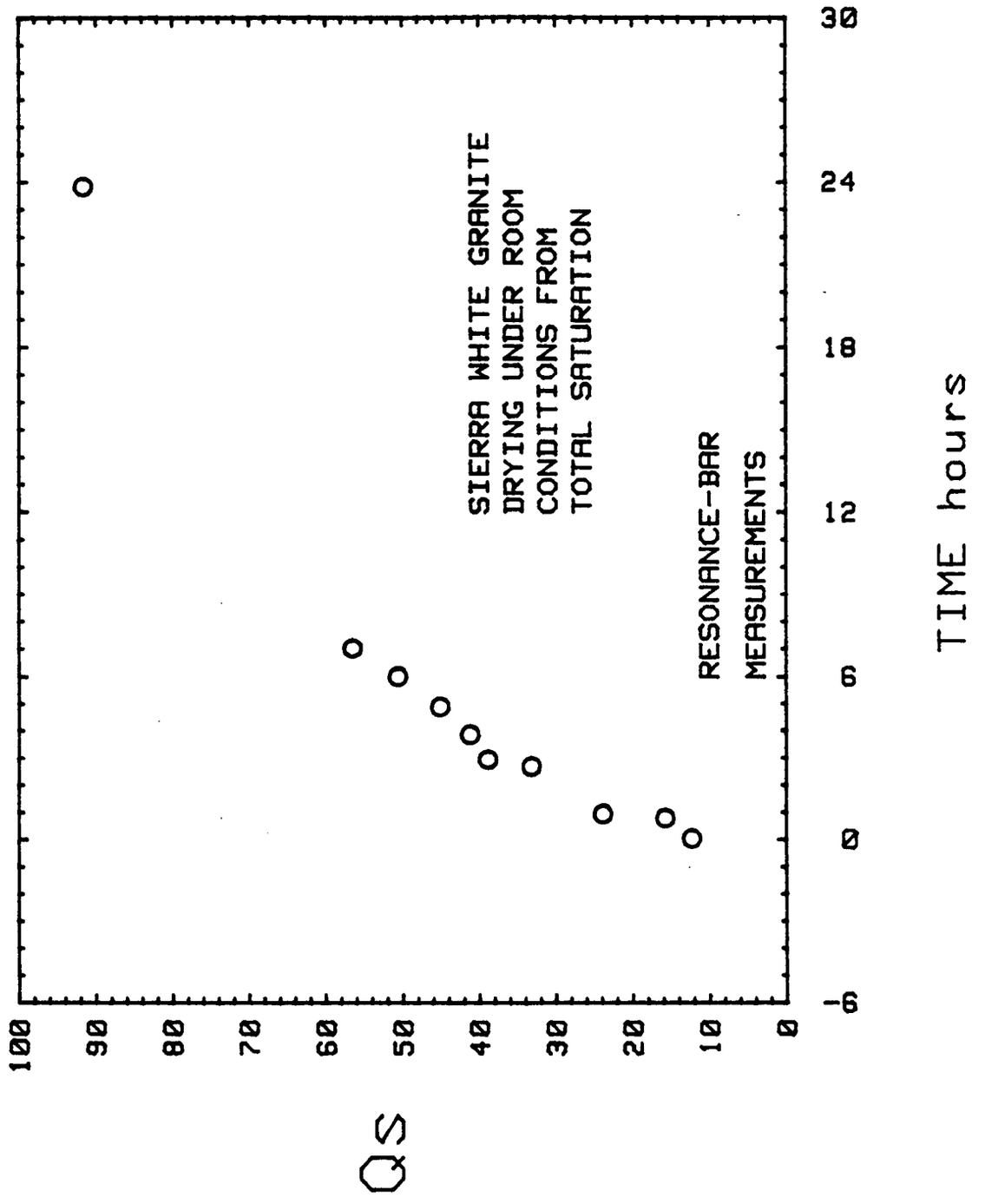

Figure 12b: Resonant-bar data for Sierra White Granite bench experiment. Sample is drying under room conditions from total saturation.

By weighing the Sierra White Granite sample used in the pulse transmission measurements of shear velocity as it dried from a saturated condition at room conditions, we have obtained the bulk degree of saturation of the sample with respect to time (Figure 13). Our resonant bar and pulse transmission data is plotted on figures 14 and 15 with respect to bulk degree of saturation. Although the distribution of the water in the rock is not known with exactness, the simple experiment gives an averaged idea of the changes in velocities and Qs with saturation.

We have utilized Kjartansson's [1979] frequency-constant Q dispersion relation to obtain predicted values of ultrasonic shear velocities based on the knowledge of Qs, Vs and the frequency of the resonant-bar measurements. The frequency of the ultrasonic measurements is calculated from the measured apparent period of the first arrival.

The dispersion relation is of the form:

$$\frac{V}{V_o} = \left(\frac{f}{f_o}\right)^{\nu} \qquad \nu = \frac{1}{\pi} \tan^{-1}\left(\frac{1}{Q}\right)$$

and predicts significant dispersion for low Q rocks. Figure 16 shows that the predicted dispersion is not too sensitive to the ratio of the frequencies of the measurements for ratios greater than 300 and Q>10.

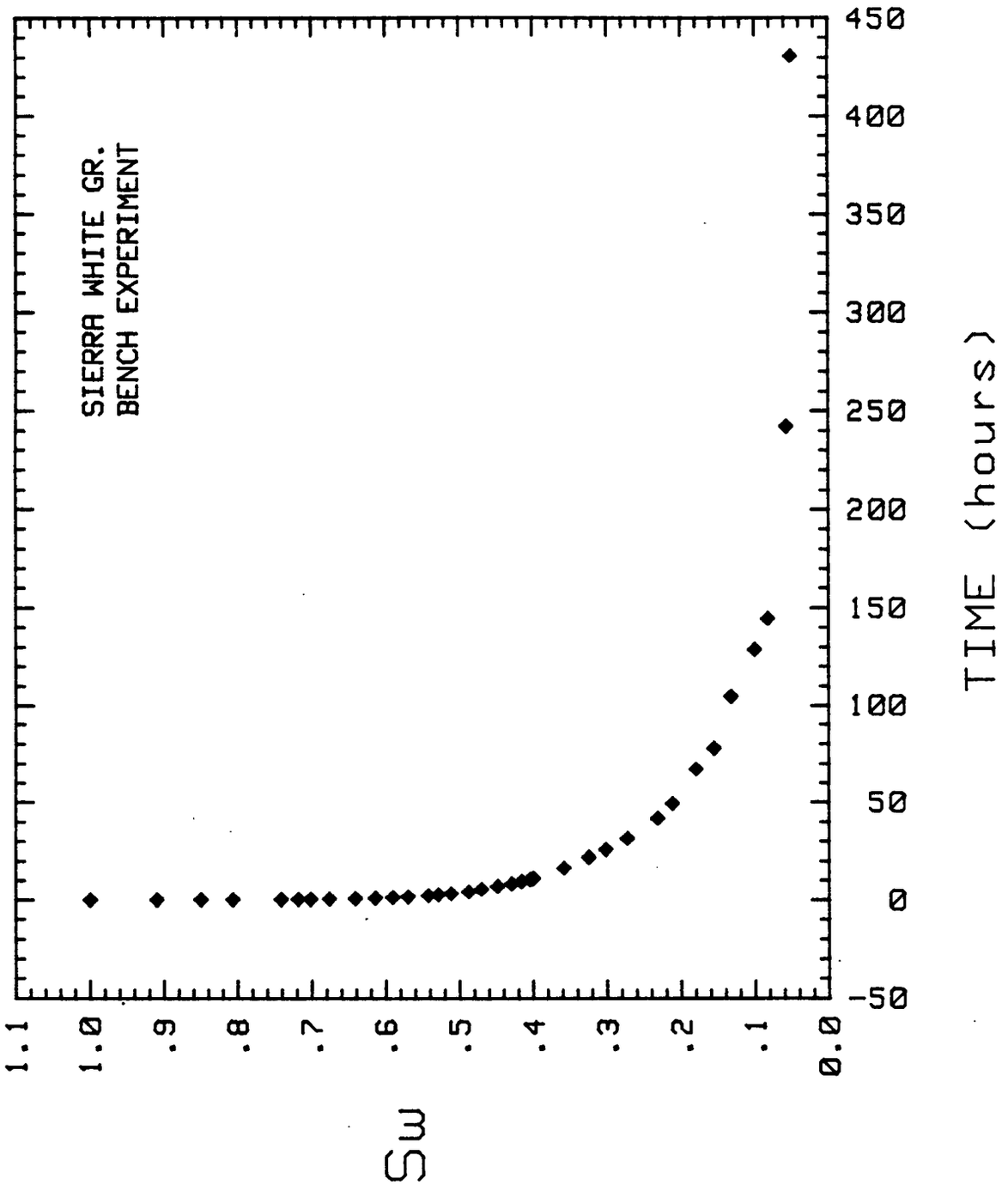

Figure 13: Bulk degree of saturation of the pulse-transmission Sierra White Granite sample as it dries under room conditions from total saturation.

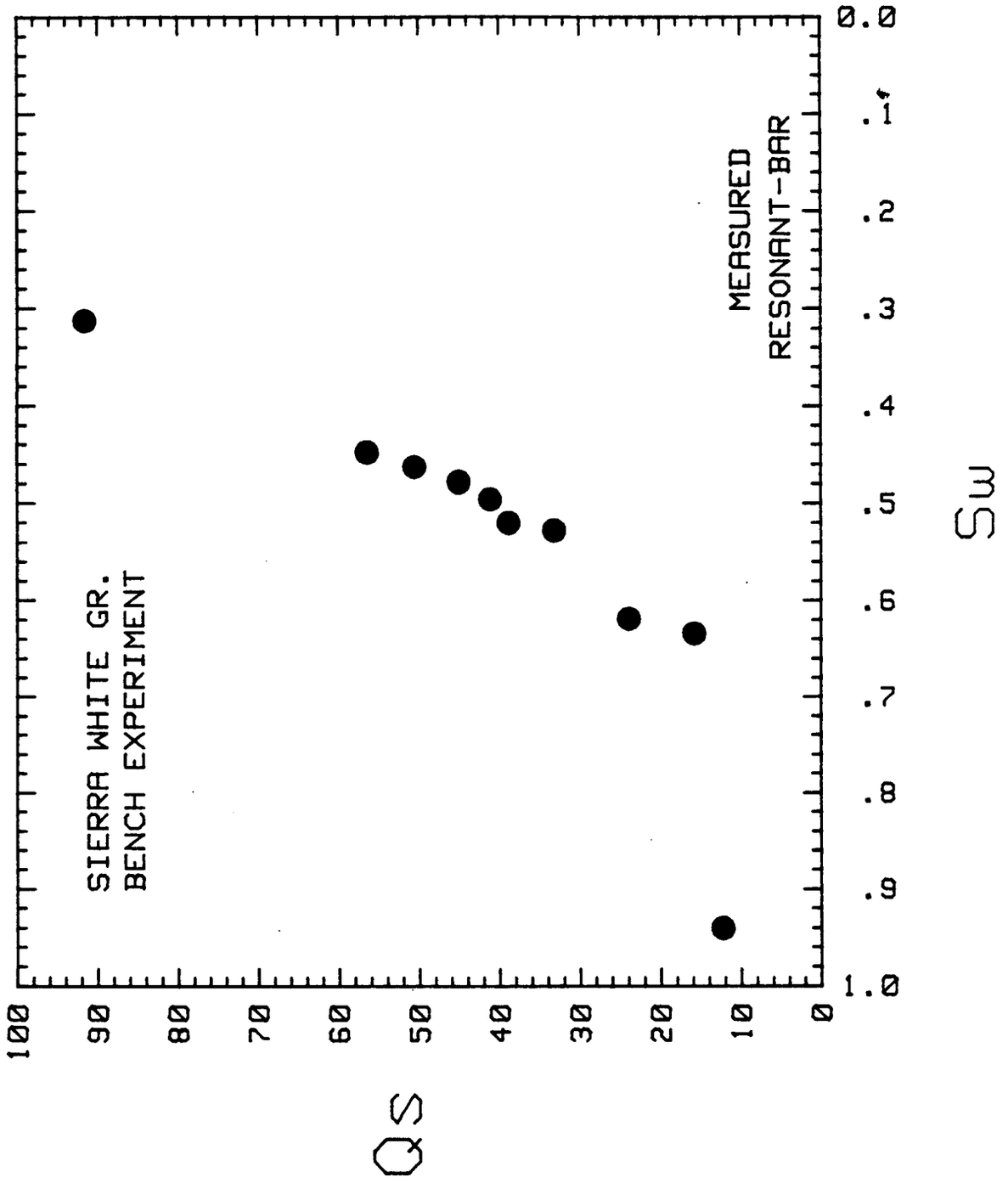

Figure 14: Resonant-bar Q data plotted as a function of bulk degree of saturation obtained from the pulse-transmission Sierra White Granite sample.

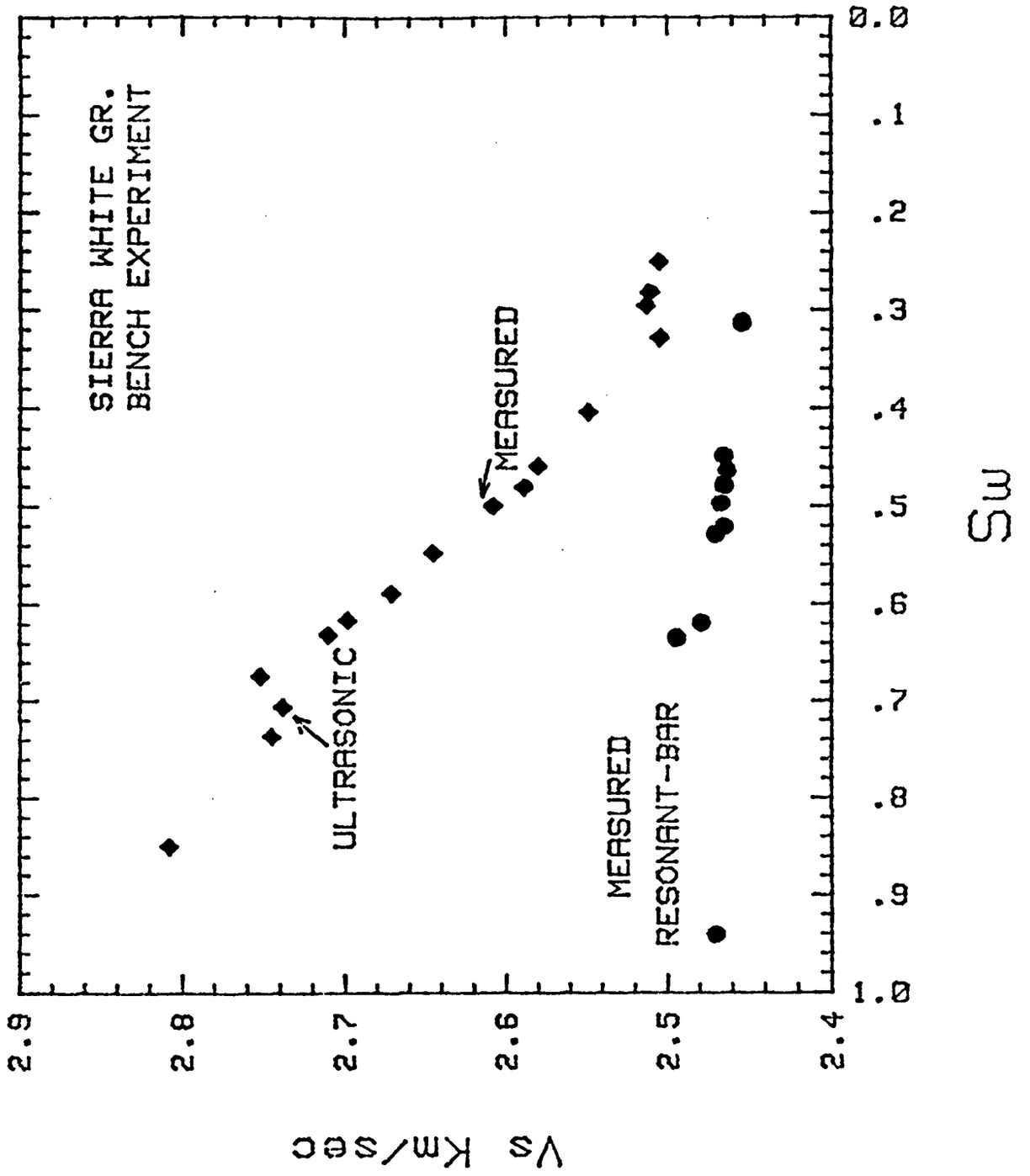

Figure 15: Shear velocities for Sierra White Granite as a function of bulk degree of saturation.

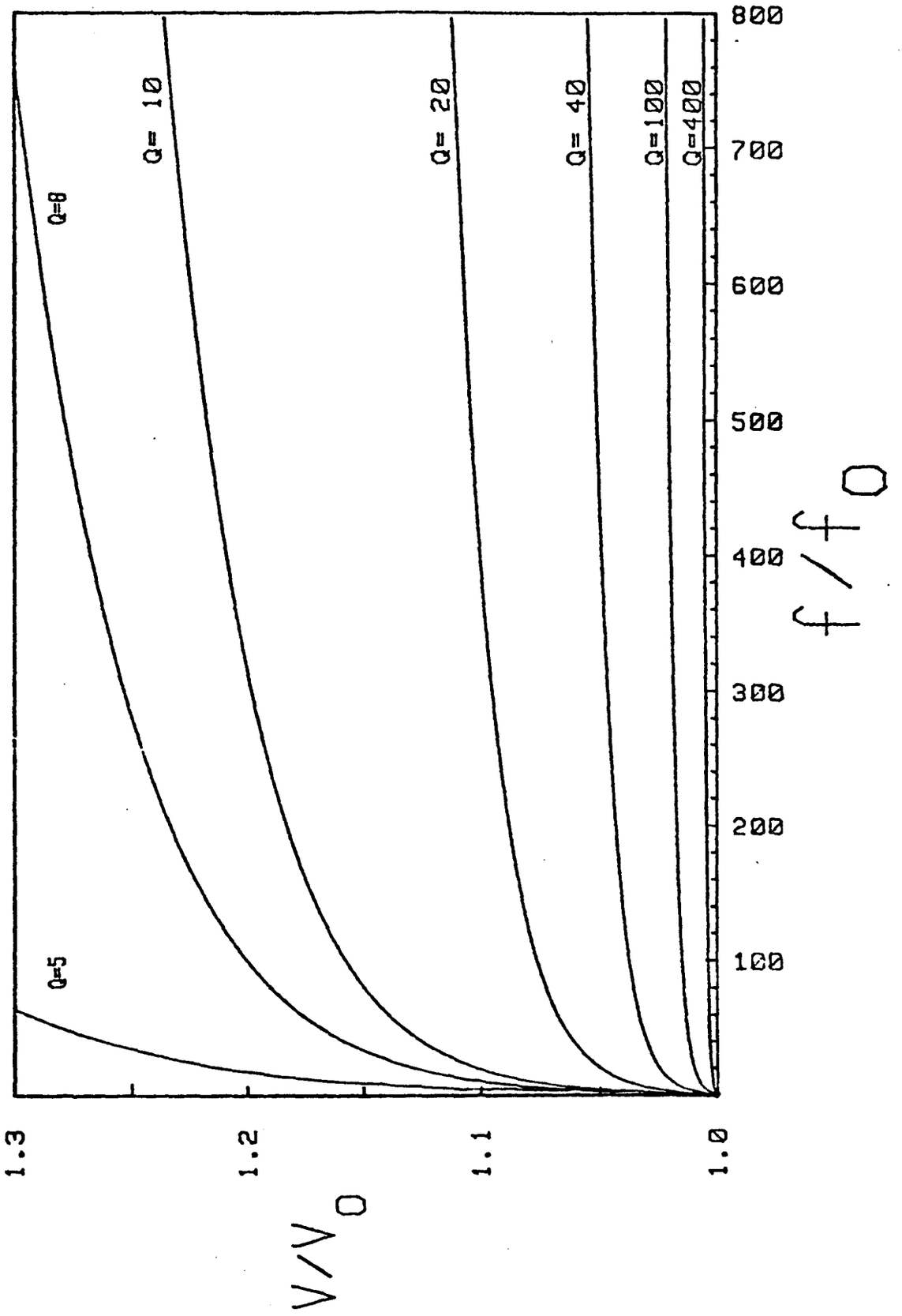

Figure 16: Plot of Kjartansson (1979) dispersion relation.

Figure 17 presents all the velocity data with respect to the bulk degree of saturation for comparison. We have included the values of shear velocity predicted by the frequency-constant Q theory.

The predicted ratio of phase velocities at the two frequencies fits the prediction very well considering that two samples were required for the measurements, and the drying rate may have been slightly different for the two samples. The data seem to agree within experimental error with the dispersion relation where Q is exactly independent of frequency. Of course, the fit does not exclude dispersion relations based on Q increasing slightly with frequency, as for example, from the generalized Maxwell model [Kjartansson, 1979], or the "Nearly constant Q" model [Liu, et al, 1976]. The conclusion is that our data indicates that Q is approximately constant within the frequency range of the measurements and the particular rock type studied in the experiment. It certainly rules out any theory that results in frequency independent shear velocity (and therefore also P wave velocity) for granite in the range between 400 Hz and 250 KHz.

It is difficult to explain the observations in the context of the friction mechanism. If water serves to "lubricate" crack surfaces and thereby enhances frictional sliding, as proposed by Johnston [1979], then we would expect Qs to increase as the sample dries and the coefficient of friction increases. This is observed. But then we would also expect the shear modulus to increase at the sonic and ultrasonic frequencies. But at 500 Hz the shear velocity is constant while Qs

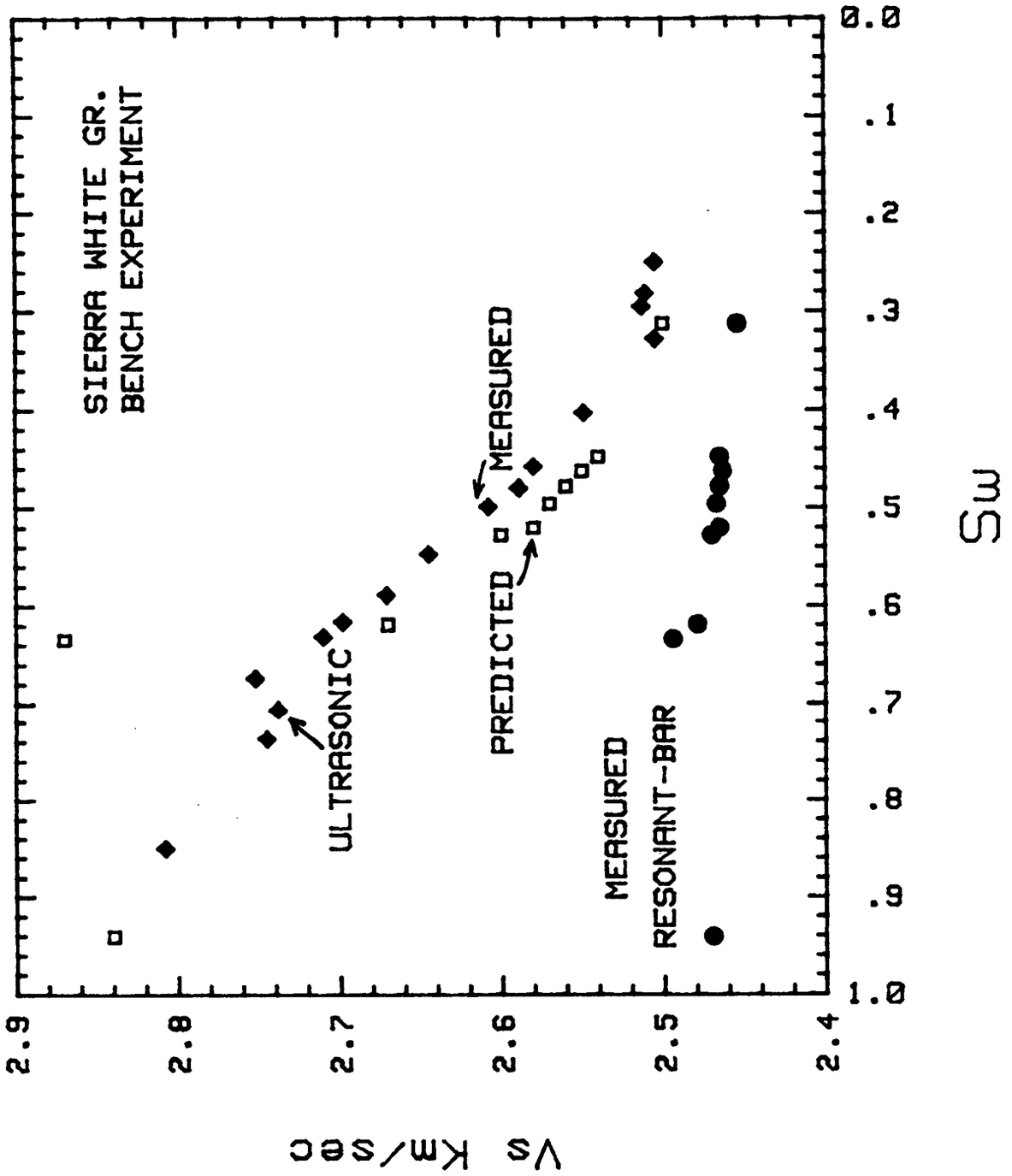

Figure 17: All shear velocity data for Sierra White Granite as a function of bulk degree of saturation. Predicted values of ultrasonic shear velocities are from Kjartansson (1979).

increases monotonically. At ultrasonic frequencies, shear velocity decreases as the sample dries, the P amplitude (or Qp) drops to a minimum, at the beginning of the drying process, and then increases again.

2.4.2 BEREA SANDSTONE EXPERIMENT

Similar data for Berea Sandstone is presented in figures 18, 19, and 20. The results show that the frequency constant Q dispersion relation does not account for the large dispersion of shear velocity in the saturated and partially saturated sandstone.

As Kjartansson has noted, "considering the complexity of solids, and rocks in particular, there is no reason to believe that the Q of all rocks is exactly independent of frequency, nor that there is any simple universal law that describes it" [Kjartansson, 1979b]. Our work is then to try to categorize rocks that show similar behavior to infer the structural and dynamic causes for the different frequency responses. This indicates that within the range studied here Q may be decreasing with frequency for rock structures similar to sandstone and nearly constant with frequency for rock that can be considered cracked solids. For both types of rocks Qs is less than 20 in the saturated condition at sonic frequencies and zero effective pressure.

We have fitted Kjartansson's [1979] generalized Voigt model to the three observations we have: the value of Qs and Vs at 388 Hz, and the value of the ultrasonic Vs in the saturated condition for Berea

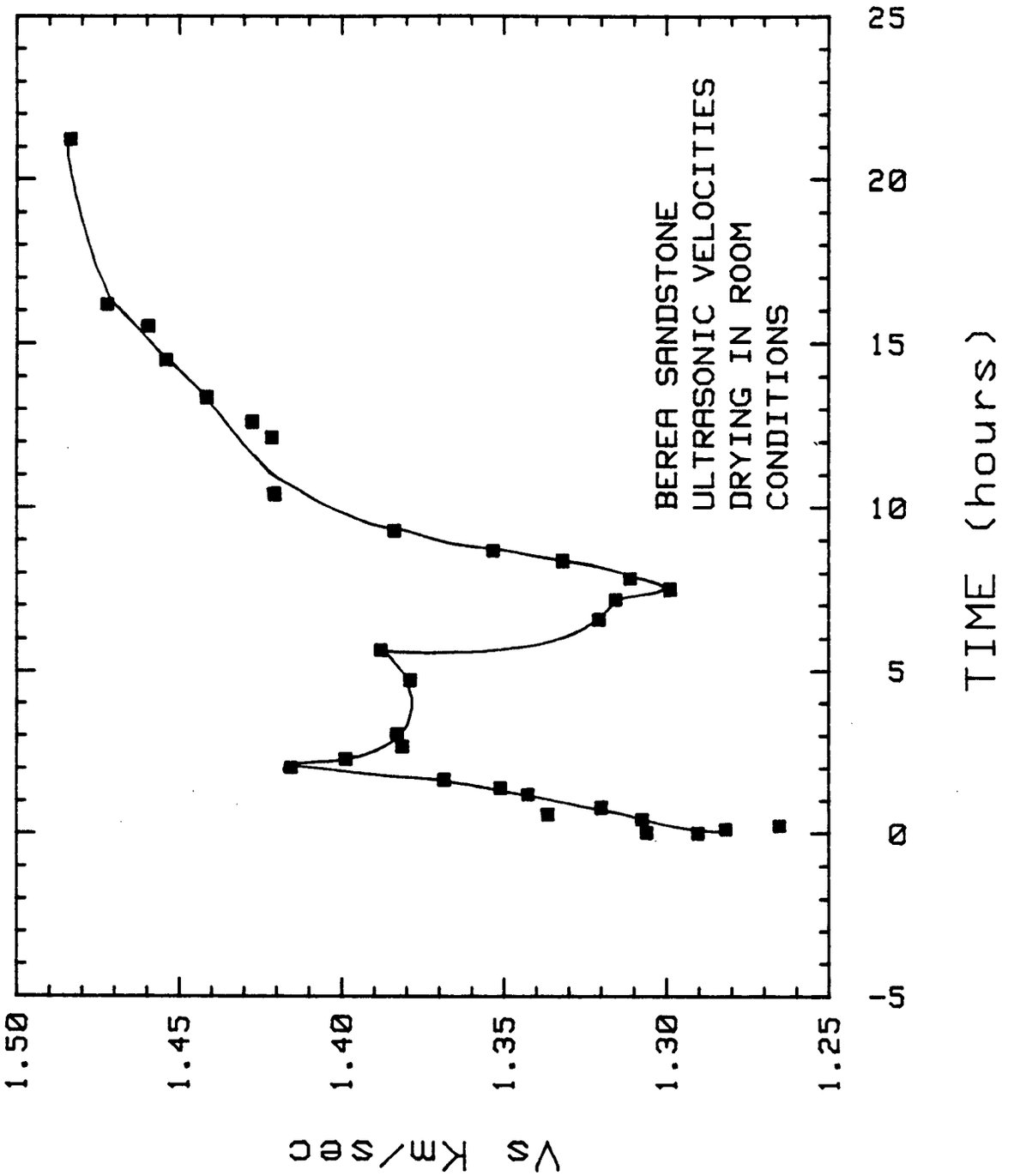

Figure 18: Ultrasonic data for Berea Sandstone drying under room conditions from a saturated condition. Note sudden decreases in effective shear modulus at 2-7 hrs.

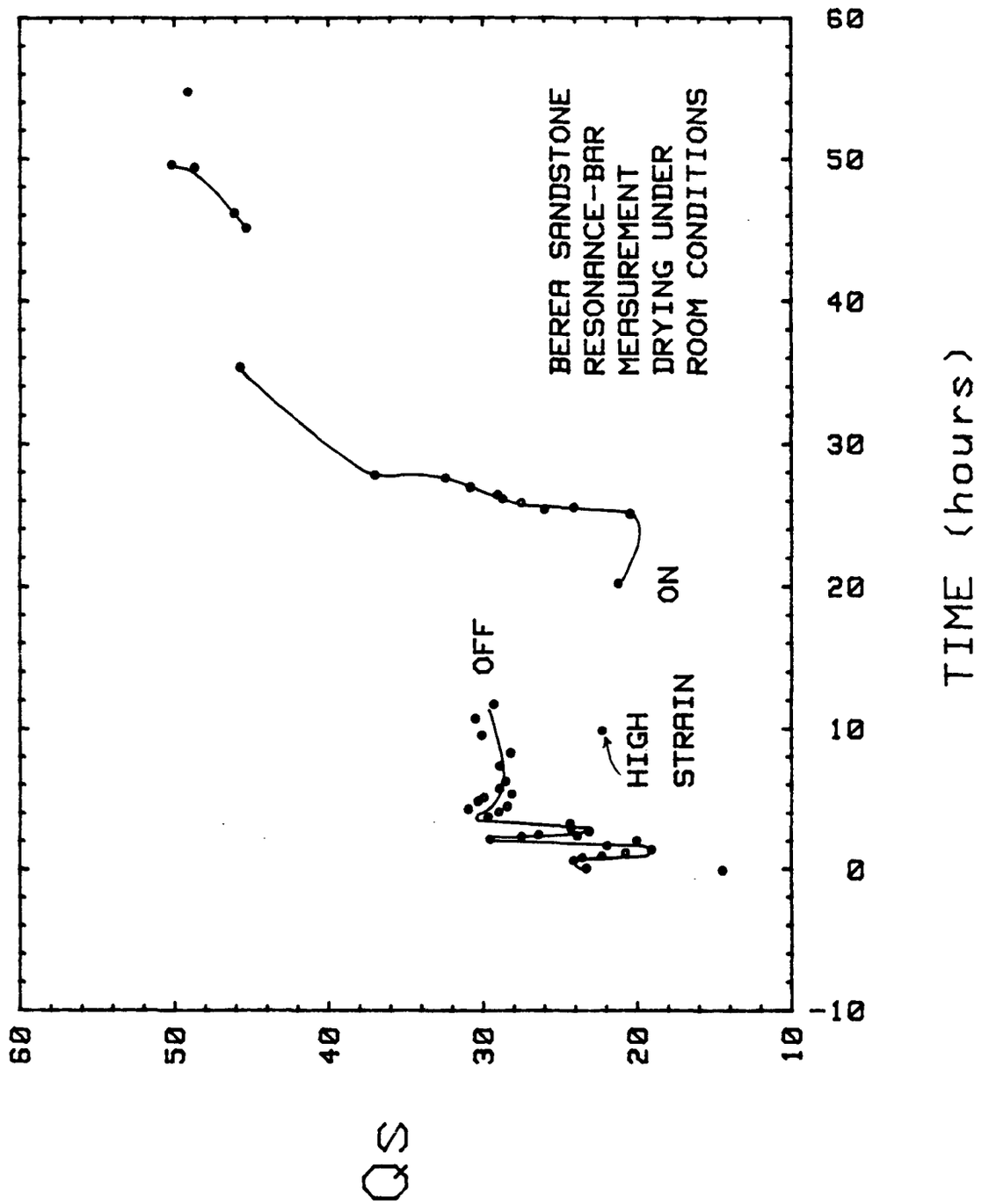

Figure 19a: Resonant-bar measurements of Qs for Berea Sandstone as it dries from total saturation under room conditions. Continuous lines indicate when the sample was under resonance vibration. The value marked "high strain" was taken, at low strain, after taking some values at higher strains.

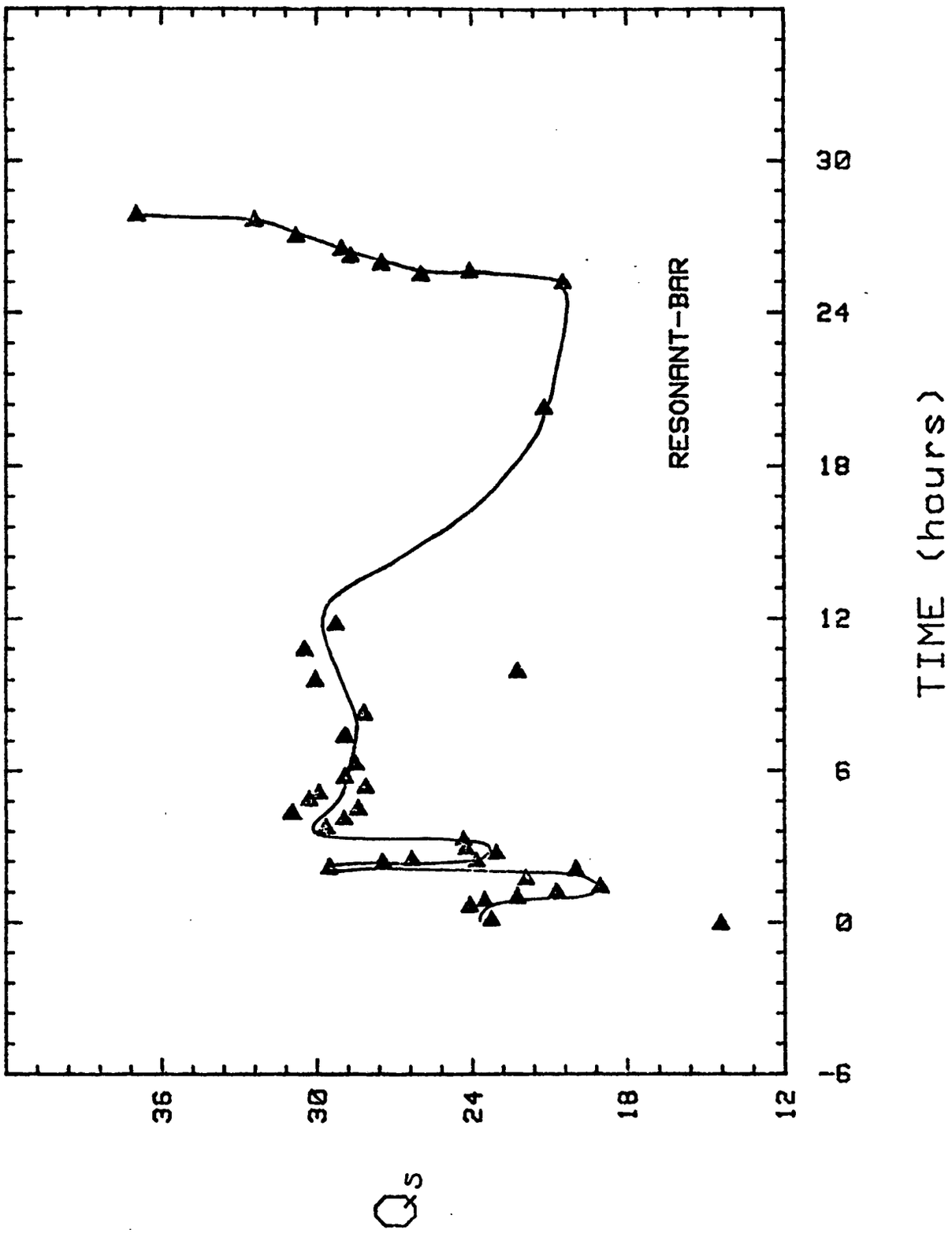

Figure 19b: Detail of figure 19a. Qs values varied at the begining of the drying process.

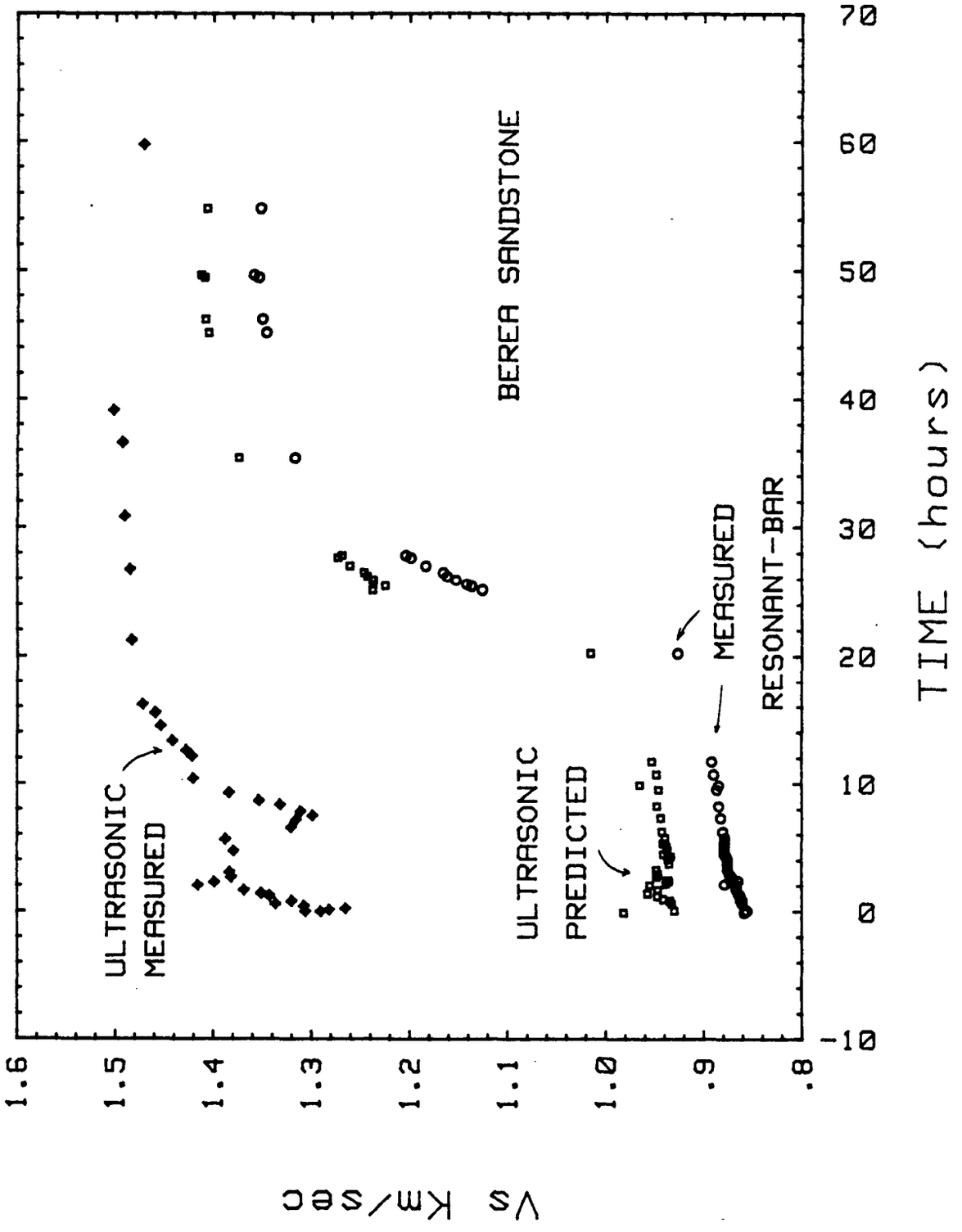

Figure 20: All shear velocity data for Berea Sandstone as it dries under room conditions from total saturation. Predicted values are from Kjartansson (1979).

Sandstone. This is the simplest model that will fit our observations. We summarize the appropiate set of equations that need be solved to find a fit of the theory to our observations:

GENERALIZED VOIGT

$$M = M_o \left| 1 + \left(\frac{i\omega}{\omega_o} \right)^{\beta} \right|$$

$$Q = Q_o + \left(\frac{\omega}{\omega_o} \right)^{-\beta} \qquad \text{where:} \quad Q_o = \cot \frac{\pi\beta}{2}$$

$$\frac{M_1}{M_2} = \frac{1 + A}{1 + A\left(\frac{\omega_1}{\omega_2} \right)^{\beta}}$$

$$Q_1 = \cot\frac{\pi\beta}{2} + A \qquad \text{where:} \quad A = Q_1 - \cot\frac{\pi\beta}{2}$$

$$Q_2 = \cot\frac{\pi\beta}{2} + A\left(\frac{\omega_2}{\omega_1} \right)^{-\beta}$$

M= modulus

ω= angular frequency

By trial and error the value of ß for the fit is 0.133, a value that indicates that a slowly decreasing Qs with frequency over the frequency range of the measurements can explain the large dispersion in the sandstone. This value for ß predicts a value of 13 for the ultrasonic Qs.

For brine saturated Berea Sandstone Toksoz, et al, [1979] have reported very low values for Q at ultrasonic frequencies. At sonic frequencies, Winkler [1979] reported higher values for water saturated Massillon Sandstone of around 25. Their results are consistent with our findings. The inference, then, is that Q dependence on frequency depends on the rock type and structure of the cracks and pores in the rock, Qs decreasing with frequency in high porosity or permeability rocks and approximately constant with frequency in low porosity or permeability rocks.

We have made measurements of shear wave velocities in three sandstones of approximately (19%) equal porosity. Two methods of velocity determination have been used to find the shear velocities at widely different frequencies. Pulse-Transmission measurements were made in small samples (1.2" long, 13/16" diameter cylinders) at frequencies of about 0.2 MHz. Resonant-bar measurements were made on 12" long, 3/4" diameter rods at frequencies of about 1.5 KHz using a record cutter head to drive the rods into resonance. The Pulse transmision samples were bonded to the transducer mounts in a dry condition and then saturated with degassed, dionized water at high* pore pressures. All measurements

* 12" bars were saturated at the same pore pressures.

were done in water saturated samples at room conditions. The samples were wrapped with either teflon tape or thin plastic wrap to minimize the evaporation of the water in them.

Figure 21 shows the results for the measurements plotted as the ratio of the ultra sonic shear wave velocity to the sonic or resonance-bar velocity with respect to the permeability of the samples as measured by Walls [Personal communication]. The measurements of shear wave velocities in saturated Sierra White Granite, which show dispersion as a 10% increase in the ultrasonic shear velocity with respect to the sonic velocity, also agrees with the dispersion-permeability relation.

The dispersion is seen to increase with the permeability of the samples. The phenomenon may be explained by considering the fluid-flow mechanism proposed by O'Connell and Budiansky [1977]. The characteristic frequency increases with the permeability of the samples so that, at ultrasonic frequencies, the more permeable samples are experiencing dispersion due to the fluid-flow mechanism apart from the viscous shear relaxation mechanism. Lower permeability sandstones would shift the characteristic frequency of the fluid flow mechanism to lower frequencies so that, at ultrasonic frequencies, the dispersion due to this mechanism is not as large. Therefore, the combination of the two mechanisms acting in the rock appears on a qualitative basis, to admit the phenomenon on theoretical basis.

Measurements on a thermally fractured Sierra White Granite, quenched from 400°C in room temperature water are shown in figure 22. The large decrease in shear velocity is a measure of the dispersion associated with this rock structure. The increase in the number and size of the

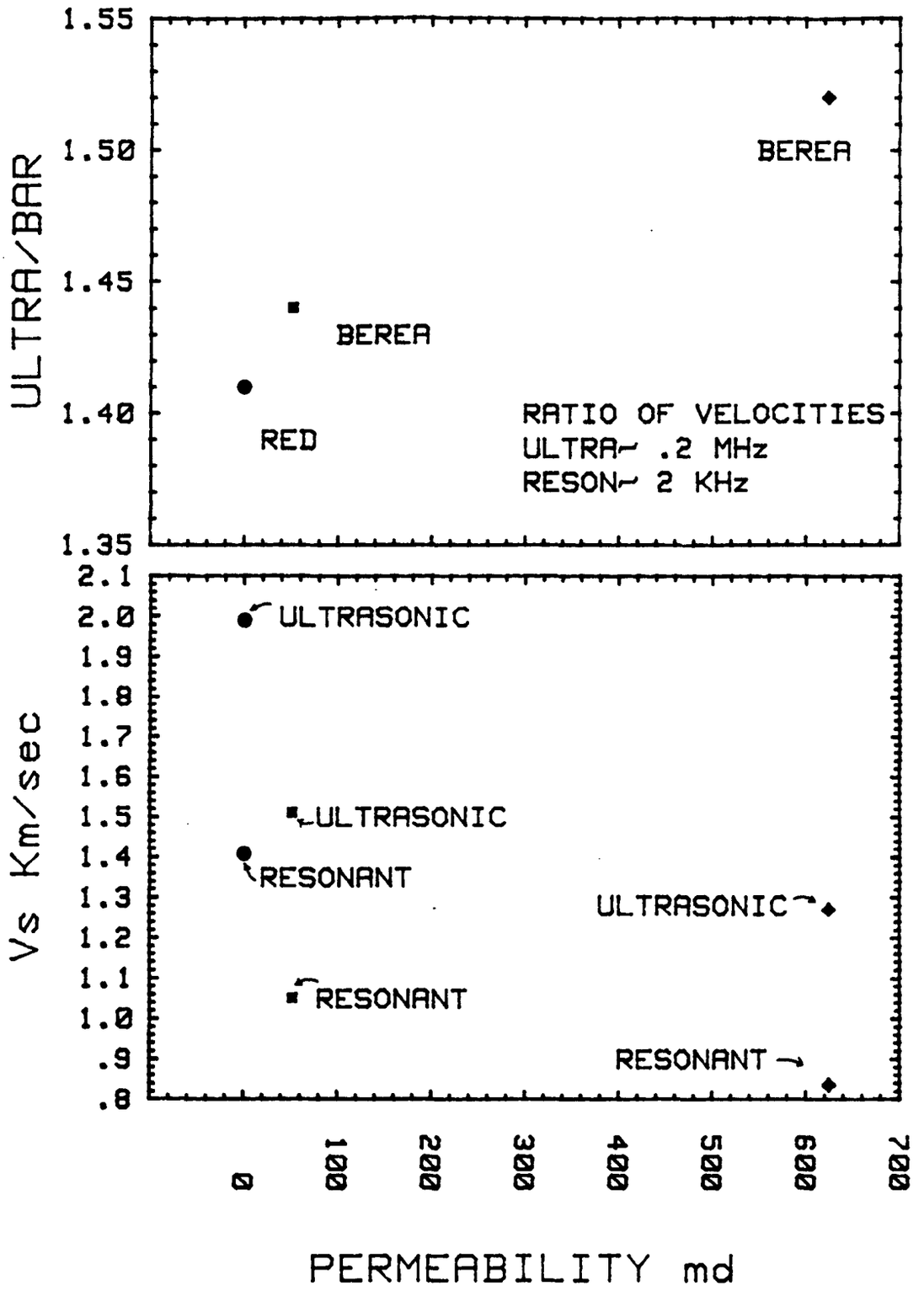

Figure 21: Experimental results of the measurement of dispersion in sandstones with different permeability.

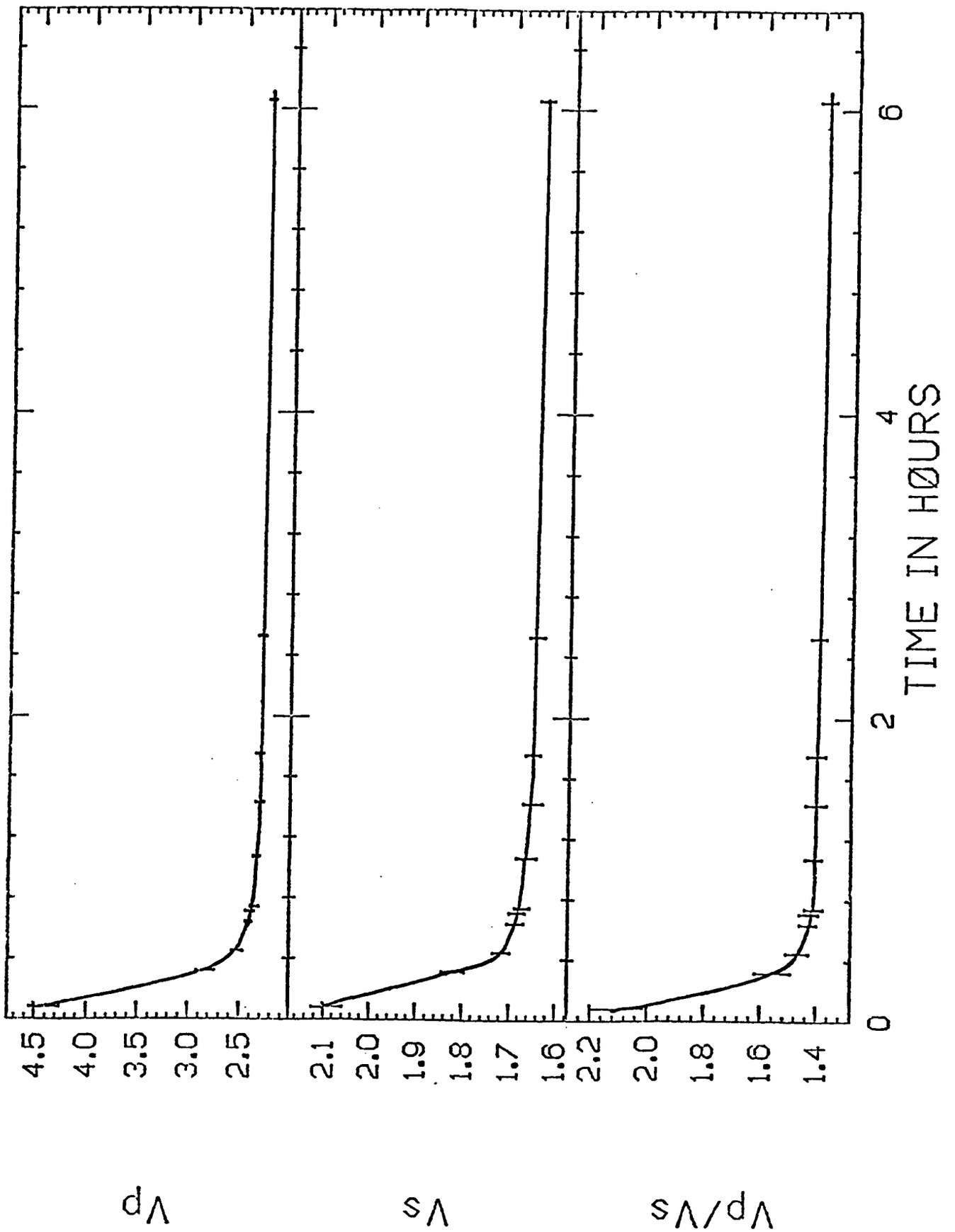

Figure 22a: Ultrasonic measurements on fractured Sierra White Granite. Drying under room conditions from total saturation.

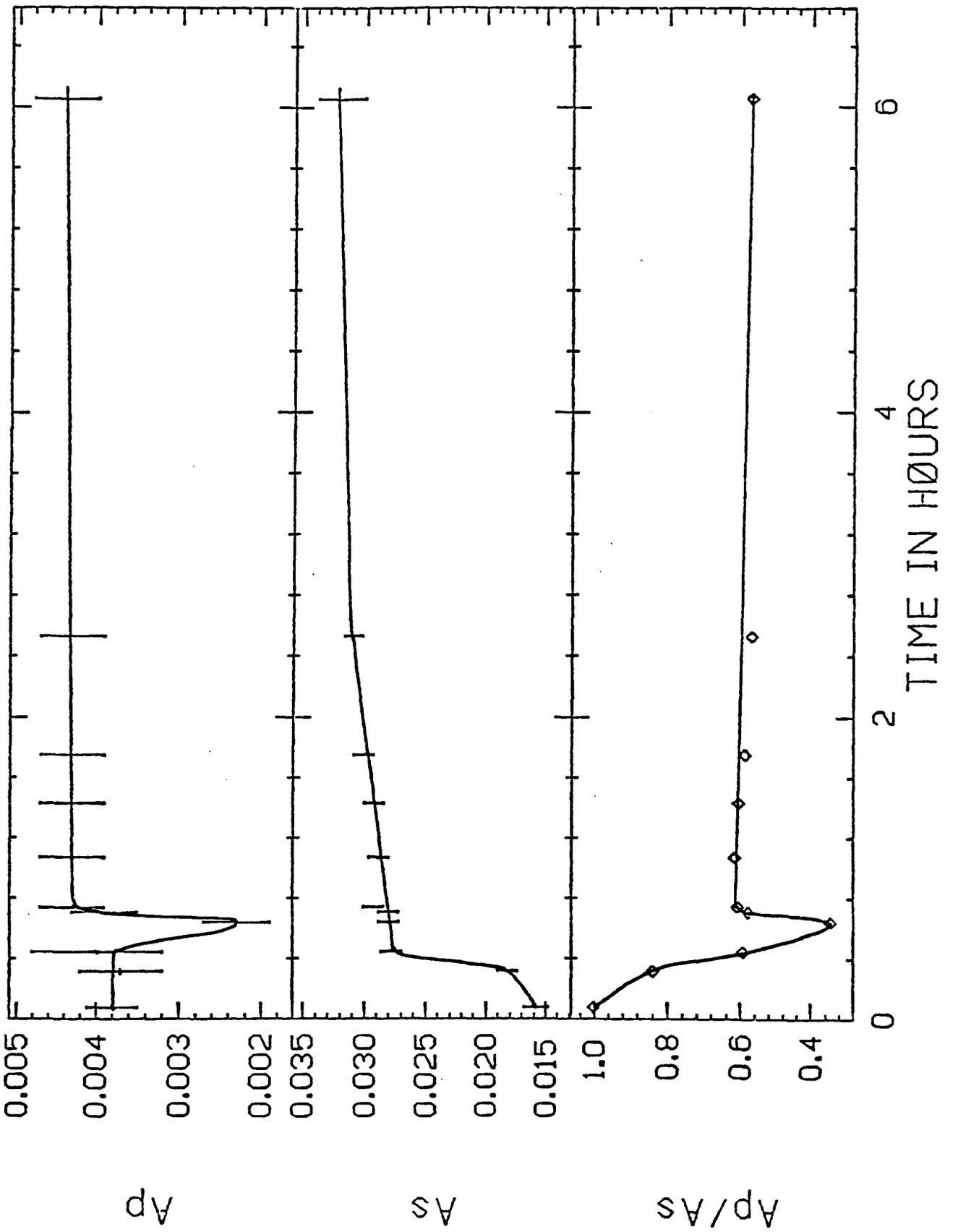

Figure 22b: Ultrasonic measurements of first arrival, zero-to-peak amplitude for fractured Sierra White Granite drying under room conditions from total saturation.

cracks has increased the dispersion associated with the material. Since P velocity is also affected by the effective shear modulus of the rock, it will also experience dispersion in saturated rocks. Our results indicate that the dispersion depends on the permeability of the samples and on the crack density.

Chapter III

DESCRIPTION OF EXPERIMENTAL TECHNIQUES

3.1 INTRODUCTION

In our work, much effort has been placed on the development of experimental techniques to satisfy the demands of the investigations. Measurements of shear velocities at elevated temperatures (>100°C) present technical difficulties that are now being overcomed with the development of more efficient electromechanical transducers, high temperature eupoxies, reliable high temperature seals, and accurate temperature controlers and indicators. Many times, technical-experience knowledge is lost after completion of an experimental research project because the knowledge is not readilly publishable, even though some techniques are essential to successful empirical research. We have taken advantage of the less strict requirements of the dissertation format to include a detailed description of the laboratory procedures, the development of which, consumed most of the time and effort invested in the research. We have listed the instruments and products commercial names in an appendix.

Our first series of experiments required accurate measurements of ultrasonic P and S velocities and relative P and S attenuation at a constant temperature of 150°C, constant confining pressure of 100 bars and variable pore pressure from 1 to 15 bars in highly attenuating rock

samples. We were interested in measuring these acoustic properties under conditions similar to those found in geothermal reservoirs. Subsequent experiments utilized additional instrumentation which is described below.

3.2 OVERVIEW OF PULSE-TRANSMISSION TECHNIQUES

Our water-steam transition experiments presented the greatest technical difficulties. Some of the techniques developed were also used in subsequent experiments.

The samples are cylindrical with diameter ~19 mm and length ~33 mm. The cylindrical surfaces are ground parallel to within .001 in and soaked in slowly circulating dionized water for 24 hours to remove the water-soluble grinding-coolant dilute solution. They are dried in a vacuum oven(60°C,760mm Hg) for several days and then saturated with deionized, distilled, degassed water according to a technique described by Brace, et al. [1965]. Our equipment (see figure 23) permits complete drying of the chamber before the sample is introduced, relatively high vacuums by means of a cold trap between the vacuum pump and the chamber, immediate filling of the chamber with degassed (heated to 100°C and cooled to room temperature), dionized water, and application of up to 1800 psi of pore pressure to push the water into the very small cracks.

Within a sealed, seamless,annealed copper jacket the sample is subjected to a confining pressure Pc of 100 bars and a pore pressure of 15 bars in an externally heated pressure vessell with silicon fluid as

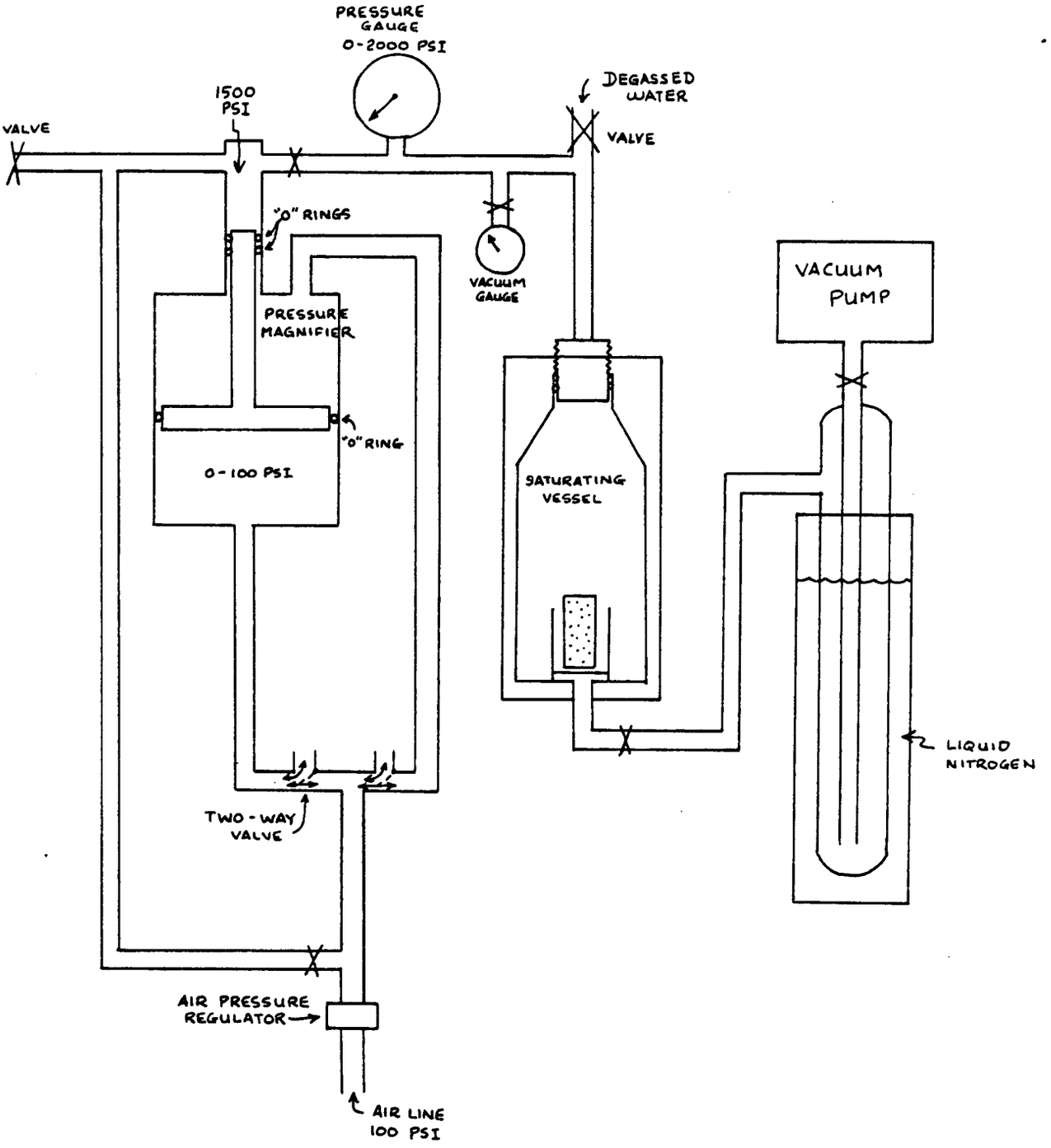

Figure 23: High pressure saturator. The system permits saturation of samples as described by Brace, et al(1965).

the pressure medium [Ito,et al.1979](see figures 24 and 25). After slowly raising the temperature to 150°C keeping both pressures constant, the pore pressure is decreased stepwise at constant Pc and pulse-transmission velocity and first arrival zero-to-peak amplitude measurements are made after waiting for pore pressure equilibrium. At a pore pressure of approximately 4.7 bars, the saturation pressure of water at this temperature, most of the water in the pores evaporates or is displaced by steam. Upon reaching atmospheric pressure the procedure is reversed.

1 MHz piezoelectric PZT-5A transducer mosaics eupoxied unto stainless steel end-plugs that seal the copper jacket are used as sources and receivers of compressional and torsional waves. The torsional transducers are composites of smaller shear plates aligned closely around the circunference of the compressional transducer (See figure 26). Transit times are measured with a time counter by superimposing a variable delayed pulse and the first arrival of the wave on synchronous channels of an oscilloscope. The counter is started with a square pulse to the source transducer and stopped by the variable delayed pulse (See figure 27).

The power to the source transducer is kept constant throughout the experiment to permit the comparison of the amplitude measurements. These are corrected for the change in acoustic impedance at the boundary between the transducer mounts and the sample, produced by changes in velocity. The similar correction due to the density change is

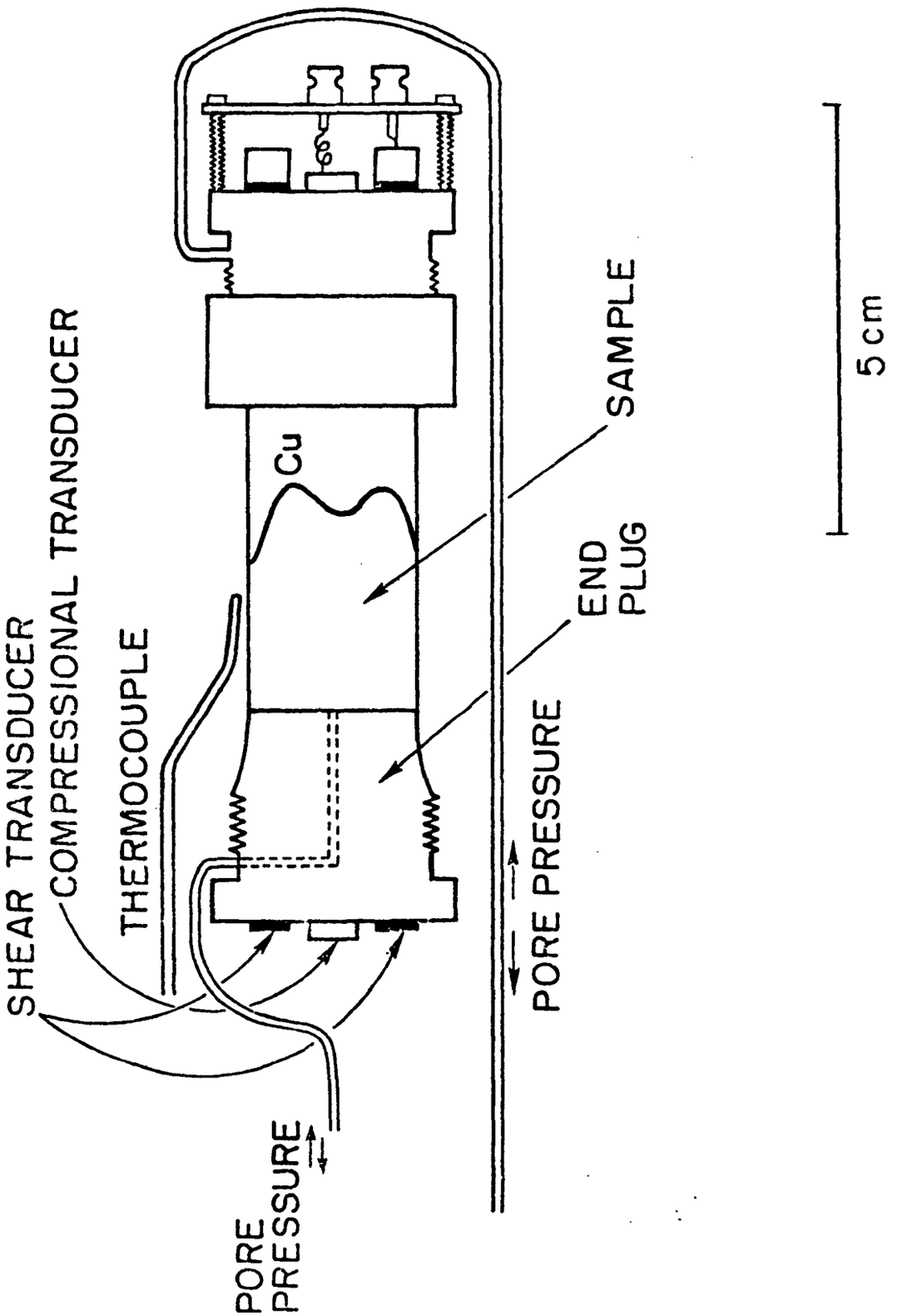

Figure 24: Transducer mounts and sample arrangement for independent application of confining and pore pressure to temperatures below 200°C.

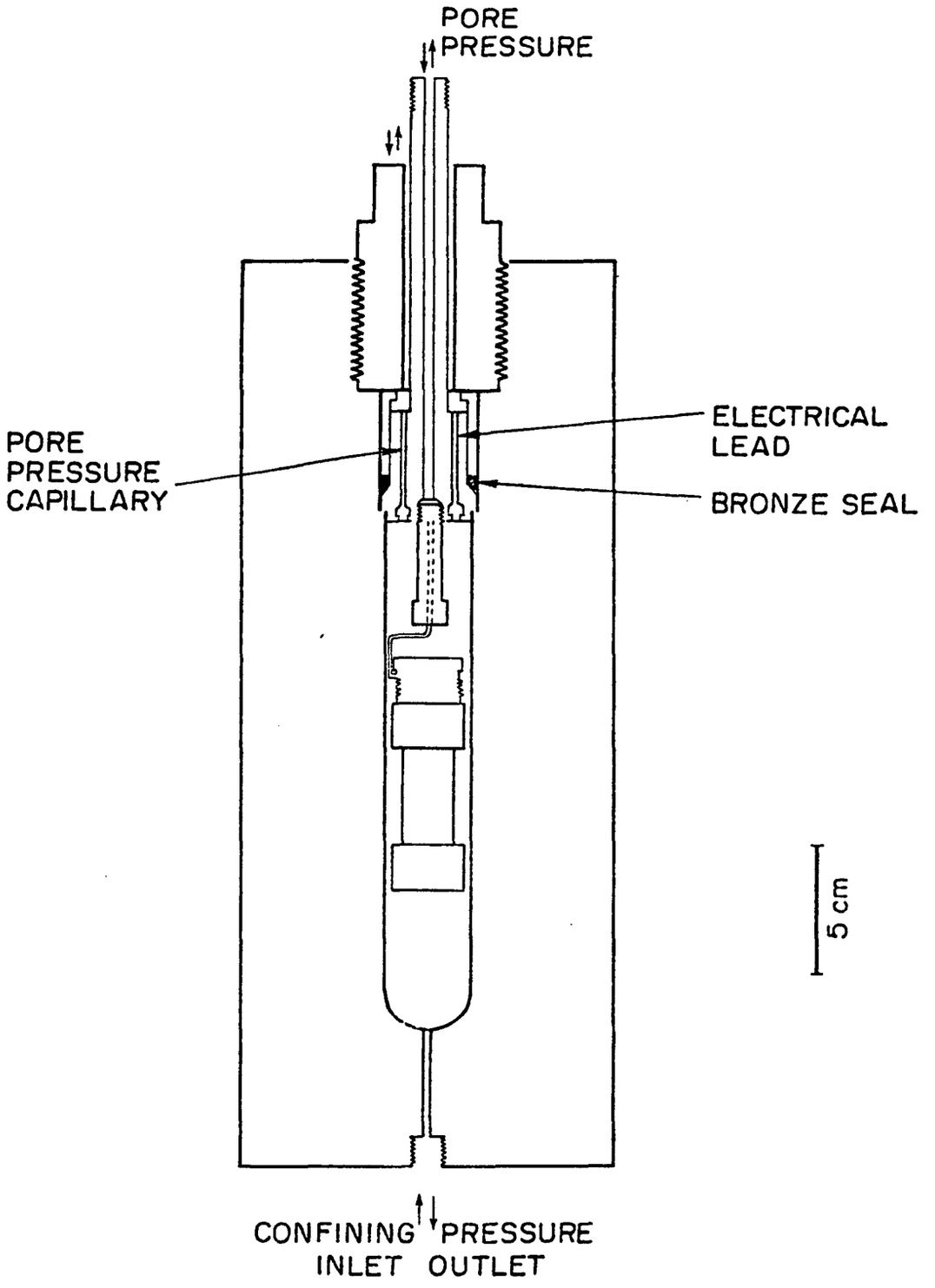

Figure 25: Pressure vessel schematic showing method of sealing for elevated temperature work.

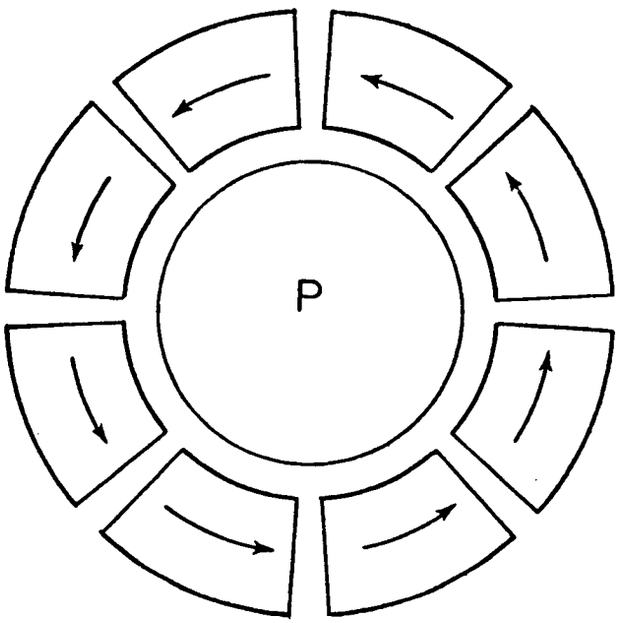

Figure 26: Design of the bi-mode transducer mosaic. Outer transducers are segments of a commercial 1" x 1" shear plate.

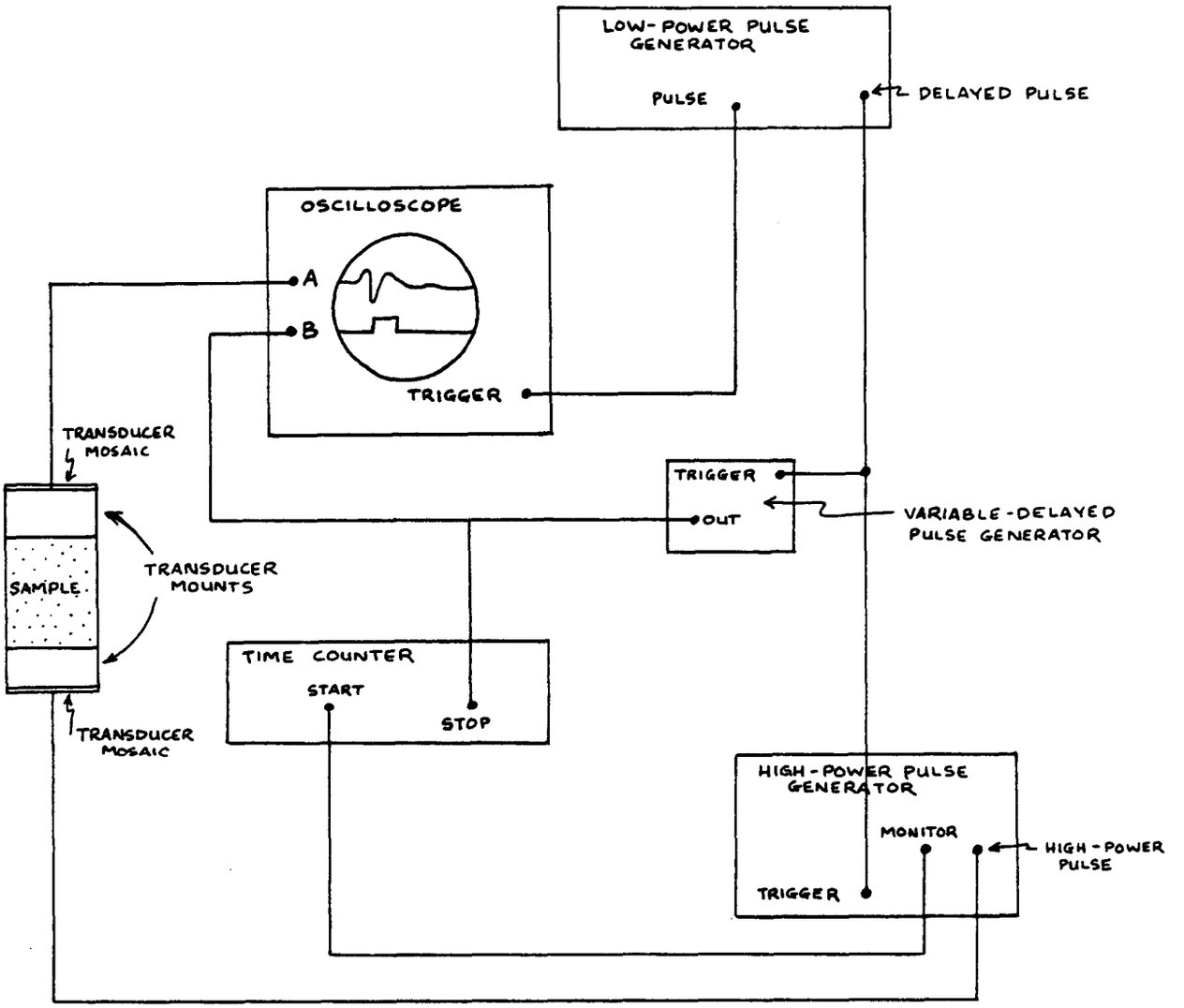

Figure 27: Schematic of Electronic instrumentation used in the pulse transmission measurements.

negligible. Figures 28,29, and 30 compare the amplitude data for the water-steam transition experiments. The acoustic impedance contrast at the boundary between sample and transducer mount changes with a change in density and with a change in wave velocity in the sample. The corrections are derived in an appendix. In our 19% porosity sandstones, the correction related to the density change is approximately equal to the correction related to the wave velocity change independently, and this last correction is seen to be unimportant. Therefore the correction related to the density change is negligible. In the fractured Westerly Granite the correction related to the velocity change is very significant but the correction related to the density change is negligible. We have corrected our values of amplitude changes with the correction related to the wave velocity variation in the sample.

The pore pressure is controled to within 1 psi through two capillary tubes that are silver soldered into the cylindrical end plugs from the side. They communicate through an axial conduit to the ends of the sample. A thermocouple measures the temperature of the silicon fluid around the copper jacket to within 0.5°C, and another one close by is utilized to provide feedback to the temperature controller (See figure 24).

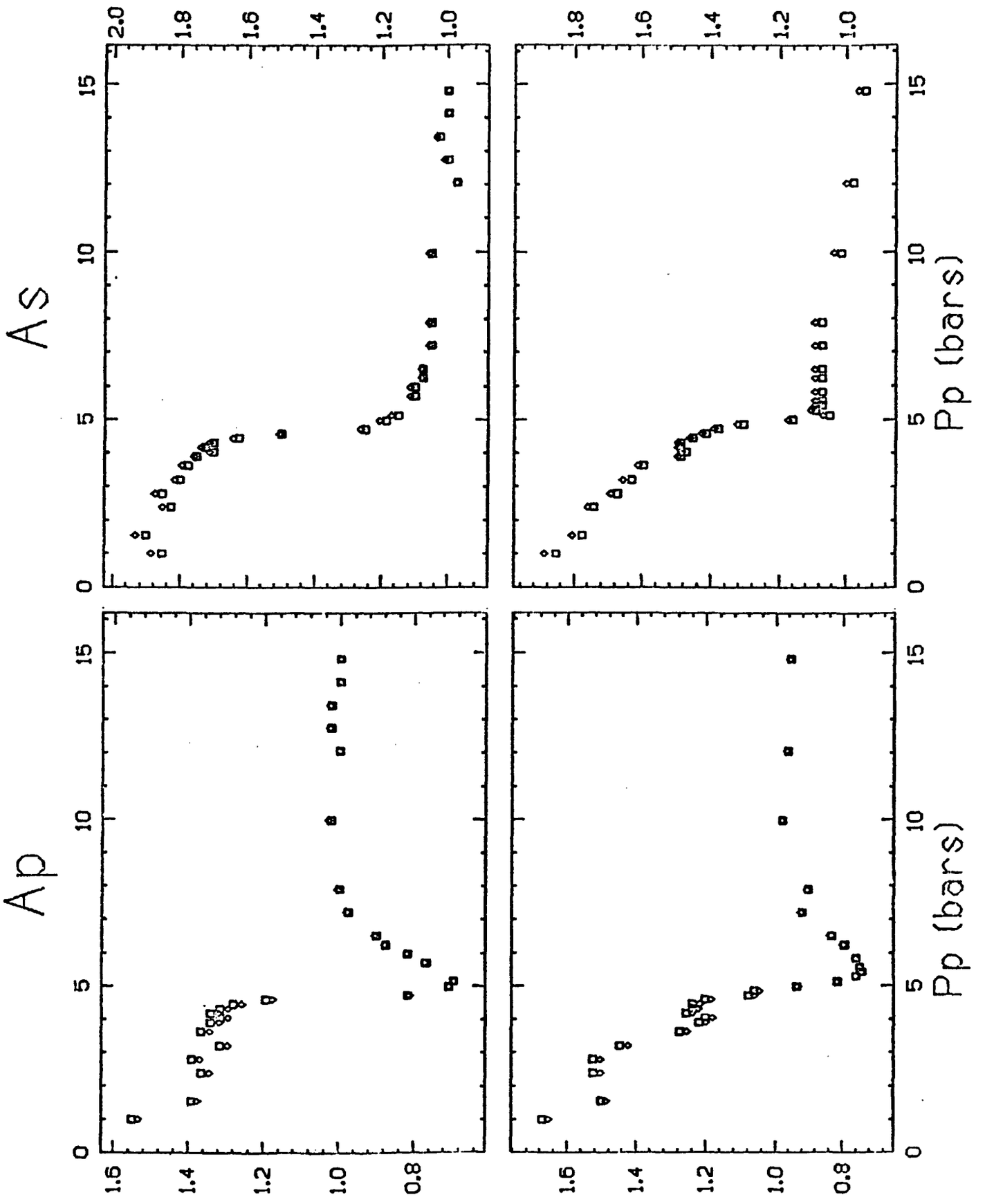

Figure 28: Normalized amplitude data for St.Peter's Sandstone experiment. Diamonds refer to the data after correction for the change of transmission coefficient. Upper windows are for the decreasing pore pressure measurements.

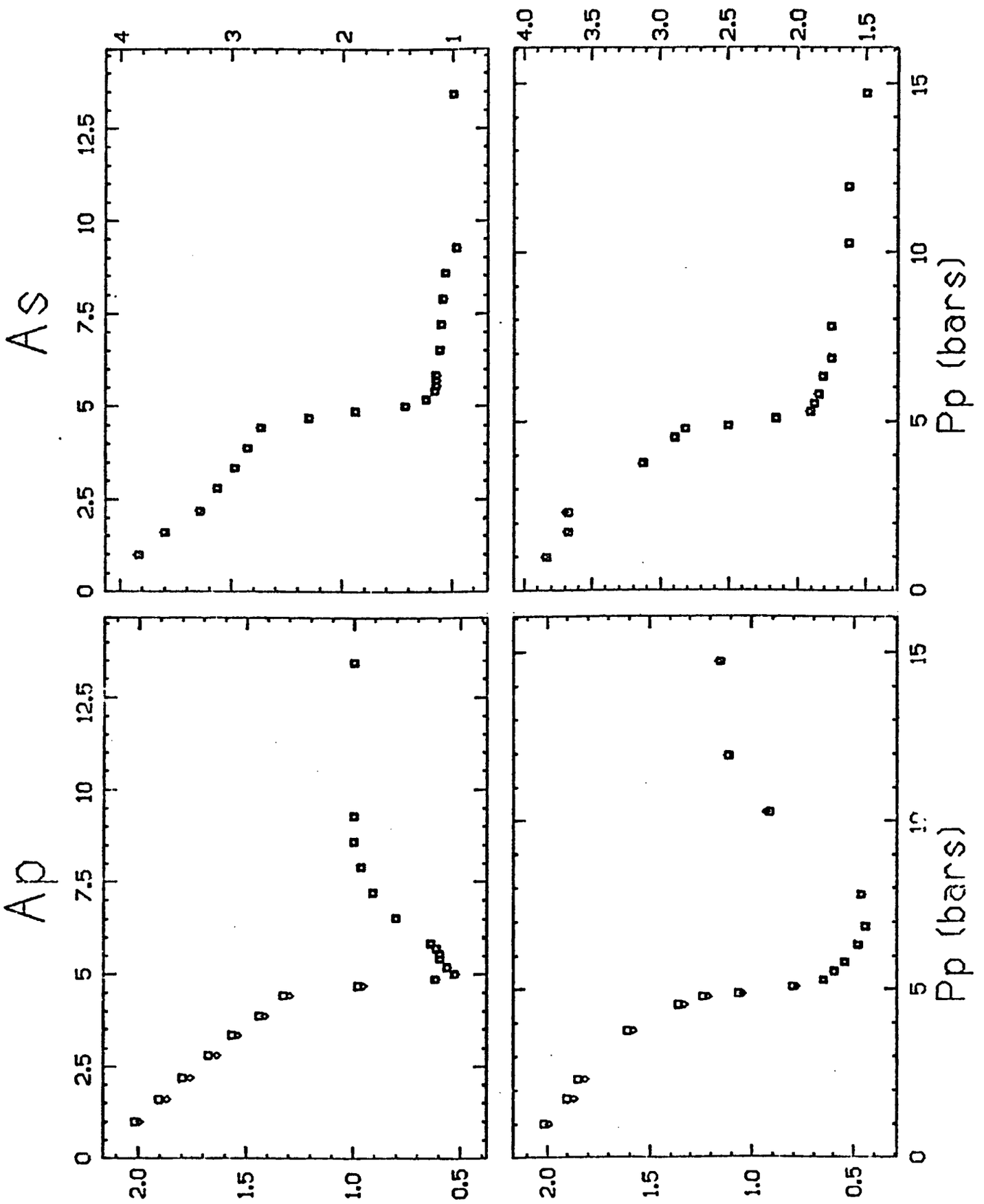

Figure 29: Normalized amplitude data for Berea Sandstone experiment. Diamonds refer to data after correction for the change in transmission coefficient. Upper windows are for decreasing pore pressure measurements.

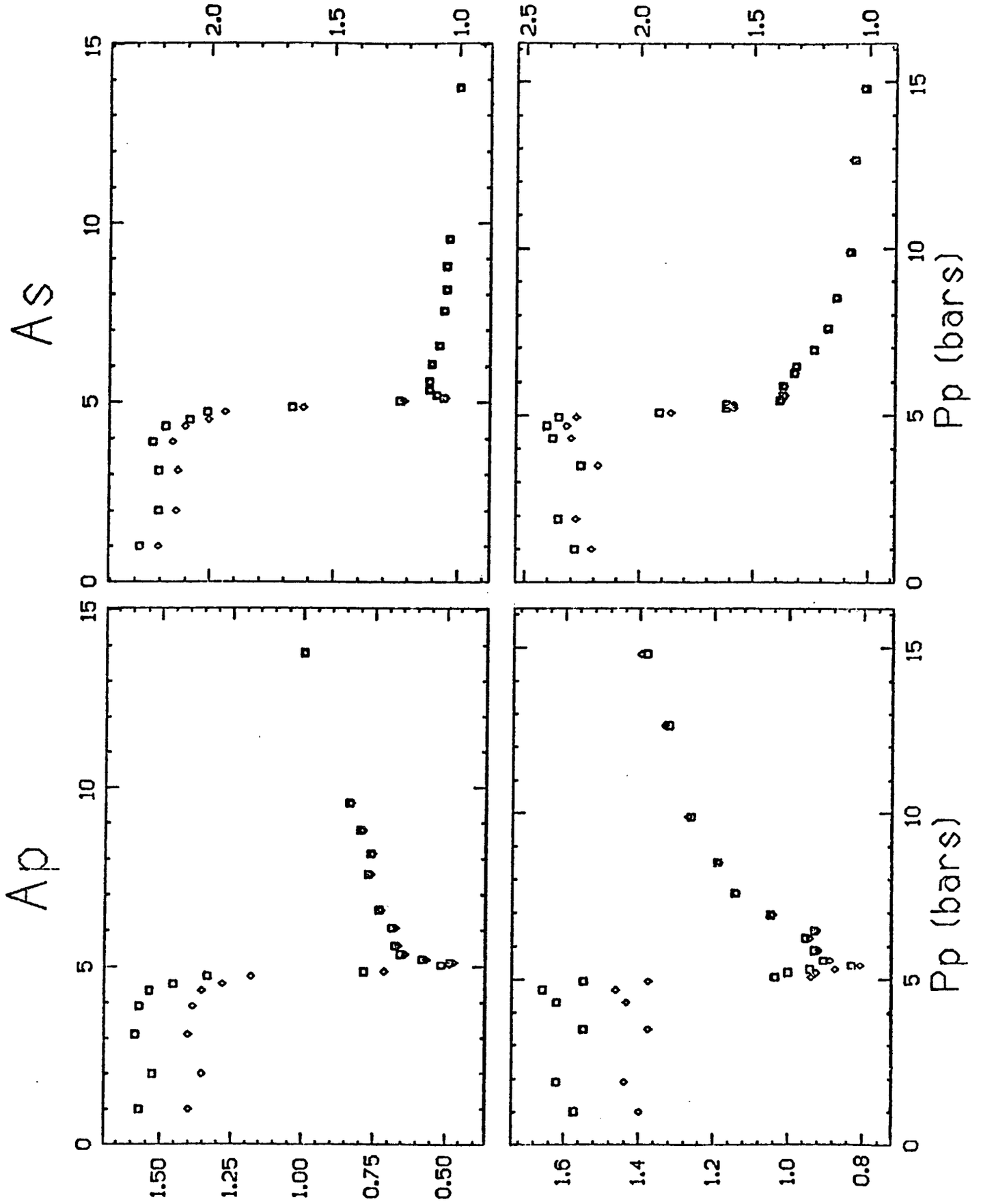

Figure 30: Normalized amplitude data for fractured Westerly Granite. Diamonds refer to data after correction for the change in transmission coefficient. Upper windows are for decreasinf pore pressure measurements.

3.3 SAMPLES

3.3.1 SAMPLE LENGTH

The sample dimensions are constrained by several factors:

a) The attenuation of the rock. The high attenuation of acoustic waves of most partially saturated sandstones decreases the maximum amplitude of an impulse from a transducer to values below the noise level in a few wavelengths. This problem is extreme in conditions of partial saturation where the P wave attenuation is largest, and at total saturation where the S attenuation is largest.

A temperature increase always diminishes the efficiency of the transducers used as sources of energy. Therefore, an adequate length of sample at room temperature may not be adequate at higher temperatures.

b) Wavelength of the transient pulse. When the radius of the sample is less than the wavelength of the compressional pulse it does no longer propagate at the longitudinal wave velocity but at some smaller velocity that tends to the "bar velocity" as the radius decreases with respect to the wavelength. [Schreiber, 1973]

For frequencies of 800 KHz (a higher limit for the compressional pulses as seen at the receiver transducer) and P velocities of 5.5 km/sec a higher limit for saturated granite) the wavelength is 6.8 mm. Our samples are 9 mm. in radius. Therefore in the extreme conditions the requirement is met and the velocities measured are the longitudinal velocities in unbounded media, for these frequencies. We have also

compared our ultrasonic measurements to resonant bar measurements by measuring compressional and shear velocities by both techniques in metals. Table 4 summarizes the results and shows the agreement obtained. A short 12" resonance-bar system was also calibrated with respect to 1m long bars. Short bars were used to measure sonic shear wave velocities in saturated samples for comparison with ultrasonic measurements on the same samples. In addition, we have compared our ultrasonic measurements to published values of the metals utilized. We have found good agreement even though the published values may not be exactly characteristic of the particular metal samples we used. Table 4 also includes the data for this comparisons.

c) Grain size of the rock.- Diffraction studies reveal that the phenomenon becomes important when the wavelength becomes approximatelly equal to the grain size [Plona, 1979]. For 0.5mm maximum grain size and minimum velocities of 1.5 km/sec the lower limit of frequency is 3 MHz.

d) Wavelength of the transmitted pulse.- The length of the sample should be much greater than the wavelength of the transmitted pulse, otherwise a pulse will not be transmitted; the sample will be displaced uniformly [Kolsky, 1963].

From experience we have seen that a 1.2" long sample is appropiate for measuring velocities in partially saturated sandstones above 100 bars confining pressure. A 13/16" diameter was the maximum sample diameter that would fit in our pressure vessel. Theoretically, it is

TABLE 4

COMPARISON OF VELOCITIES AS MEASURED BY THREE DIFFERENT SYSTEMS.

METAL	MEASUREMENT	LONG-RESONANT BAR	SHORT-RESONANT BAR	ULTRASONIC	PUBLISHED*
Stainless Steel	Vs	3.139	3.120	3.12	3.297
	Vp	5.752	-	5.73	5.98
	Vp/Vs	1.83	-	1.84	1.81
Aluminum	Vs	3.195	3.153	3.12	3.111
	Vp	5.962	-	6.25	6.374
	Vp/Vs	1.866	-	2.00	2.05
Copper	Vs	2.246	2.250	-	2.325

* Tables of Physical and Chemical Constants by Kaye,G.W.C. and T.H.Laby Longman,1973. N.Y.

appropiate and then it permitted the use of small, relatively inexpensive shear transducers to produce and receive the taveling pulse.

3.3.2 SAMPLE PREPARATION

Laboratory samples differ in several respects from in situ rock. The release of overburden pressure and the changes in temperature fracture the rock internally [Stokoe, 1978]. Some of these cracks will close at low confining pressures (100 bars) but the effect in some properties may still be significant. The existence of these fractures in laboratory samples should be recognized since it limits the applicability of the data to real life situations. But many times laboratory measurements are apropiate to study economically the nature of the phenomenons. Sometimes it is the only way.

Our laboratory experiments seek to observe the changes in acoustical rock properties predicted by theoretical considerations. Also, parting fron theoretical models we seek to investigate a relationship between acoustical properties and permeability.

Ultrasonic measurements have the great advantages of requiring only small specimens and semi-consolidated material. A large sample is difficult to obtain in porous fractured rock. Approximately 1.2" long, 13/16" diameter cylinders were cored, with water perpendicular or parallel to the bedding plane whenever it was obvious, with water. For the resonance-bar experiments 12"long, 3/4" diameter rods and 40" long, 1" x 1" bars were used, cut parallel to the barely recognizable bedding

planes in the sandstones. The small pulse-transmission samples were surface ground at the ends to within a .03mm in parallel. The griding coolant used was water soluble. (Very smooth sample surfaces are necessary for good coupling of the shear waves across the transducer-mount to sample interphase.) The samples were subsequently immersed in continuous circulating dionized water overnite to dilute out whatever amount of grinding coolant that may have remained in the rock. This was enhanced by a magnetic stirrer. After drying in dryerite for a day, the samples were placed for several days in a vaccum oven at 50-60°C to complete the drying process. It is hard to define when a rock is dry. Measurements of signal amplitude as a sample is vacuumed show that after 20 hours of vacuuming the shear wave amplitude was still increasing slightly. The velocities reached a constant value much sooner. The results of this experiment is contained in an appendix. We assumed then that leaving the samples in the vaccum oven 4 days would not achieve greater degrees of dryness. The object of drying was to open all communicated pores to the passage of air so that it could all be extracted in the saturation process.

3.3.3 SATURATION OF SAMPLES

Our samples were saturated following a procedure described by Brace et al [1965]. The equipment was designed to permeate the sample with degassed water after vaccuming and to permit the application of 1800 psi of pressure upon the water. It is very important to apply large pressures over 1000 psi to the samples for several days since most rocks have very thin pores and clays in sandstones may continue to absorbe water even after 3 days.

A liquid nitrogen cold trap was used to obtain greater vaccums, to completely dry the interior of the saturating vessel before introducing the sample and to protect the vaccum pump. A schematic description of our apparatus is found in figure 23 . It is a very practical, efficient and compact machine. It can be used to saturate 1 inch to 40 in long samples by changing the sample-vessel, and using a combination of valves and the pressure magnifier to act as a water pump to increase, in steps, the pressure in the saturating chamber.

3.3.4 POROSITY DETERMINATION

Porosity is defined as the ratio of pore volume to bulk volume of rock. It is usually given as a percentage. The method we utilized calls for three quantities from the same rock [Sprunt, 1978, personal comunication]: the weight of the saturated rock as it is suspended in water and the weight of the saturated rock. The greatest error in the calculation of porosity occurs in the weight of the saturated rock since its surface dries very fast at room conditions.

As the sample decreases in size, the fraction of pores in the sample that are cut by the exterior surface increases. For our sample dimensions these pores may comprise 15% of the porosity and if they are allowed to dry as the saturated sample is weighed a serious error could be introduced in the porosity determination.

We have alleviated this problem by weighing a weighing-bottle that is partially filled with water and then weighing it again with the

saturated sample. The difference of the two weights gives the weight of the saturated sample. The formulas for the determination of porosity are:

$$Vol_s = \frac{W_{dry} - W_{sus}}{\rho_f}$$

$$\rho_g = \frac{W_{dry}}{Vol_s}$$

$$Vol_p = \frac{W_{sat} - W_{dry}}{\rho_f}$$

$$\phi = \frac{Vol_p}{Vol_s + Vol_p}$$

where: Vol_s = volume of solids

W_{dry} = weight of dry rock

W_{sus} = weight of rock suspended in water

ρ_f = density of the pore fluid at the temperature of measurement

ρ_g = grain density

W_{sat} = weight of saturated rock

Vol_p = volume of pores

ϕ = porosity

Our measurements of porosity are good to within 10% (e.j. $19 \pm 2\%$).

3.4 TRANSDUCER DESIGN AND CONSTRUCTION

The design and construction of high-quality piezoelectric mosaics that permitted the choice in generation and reception of either a compressional wave or a shear wave was a primary contribution of our research group at the Stanford Rock Physics Project.

The idea is to utilize trapezoidal cuts from a 1 MHz chrome-gold platted PZT-5A shear mode electomechanical transducer aligned circularly at the ends of the sample (See figure 26) to produce a quasi-torsional mode of displacement which propagates through the sample at a velocity that is equal to the shear wave velocity in an unbounded medium.

Since most of the displacement (and therefore, energy) of a torsional wave traveling along the main axis in a cylindrical sample travels closer to the circunference than to the main axis, the absence of shear transducers at the center of the mosaics, in practice, does not significantly affect the quality or strength of the shear signals. (By quality we mean that the first arrival of the wave, after crossing the sample and transduer mounts, is very impulsive, has no obvious secondary arrivals in the first peak and has a very high signal to noise ratio. The noise may be caused by S-P conversion at boundaries, bad grounding, electromagnetic interaction, ground loops, etc.) The accuracy of velocity measurements is not affected by the absence of shear source at the center of the transducer mosaics. This can be seen from a comparison of compressional and shear velocities measured with two separate systems: a 1 m. long resonance bar system, and the ultrasonic system. (Table 4).

3.4.1 CUTTING

To construct a torsional transducer for elevated temperatures (<200°C) a (1MHz in this case) chrome-gold platted 1" square commercial transducer plate is cut into 15 small rectangles 0.177" by 0.289" with

the longest dimension parallel to the direction of shear motion of the original transducer plate. The cuts can be accomplished accuratelly with a .014" thick precission diamond wheel cutter by attaching the 1" square plates unto a glass plate and this to a block of graphite using thermoplastic cement at 100°C and then cooling to room temperature. The direction of motion is then marked on each transducer rectangle with a pencil. All the pieces are removed from the glass plate (by heating) and covered on all sides with solid acetone. Then they are stacked vertically, side to side on a smaller 0.25" x 0.289" x 1.5" plate while at 100°C and cooled to room temperature. The stack is put on a steel holder that is in turn held magnetically to the magnetic chuck of a surface grinding machine. The holder positions the long dimension of the transducer pieces at a 67.5° angle to the horizontal and permits grinding off the transducer rectangles into a trapezoidal form with dimensions 0.289" x 0.192" x 0.177" and with the direction of motion parallel to the longest side. 7 of these pieces are arranged in a toroidal form (See figure 26) to make a 0.75" diameter quasi-torsional mosaic with room in the center for a 0.125" diameter compressional transducer. This transducer is also a (1MHz) chrome-gold platted or silver platted PZT-5A electromechanical transducer, with a curie temperature of 350°C.

3.4.2 TRANSDUCER MOUNTS

All transducer pieces in one mosaic are eupoxoied onto a threaded stainless steel transducer mount. These transducer mounts were used as end plugs at the open ends of an annealed copper tube or 'jacket' (.010"

wall thickness) surrounding the sample. The jacket is sealed by deforming each end of the copper jacket between the sides of the threaded transducer mount and a threaded sleeve after lubricating with some graphite.

3.4.3 EUPOXYING

The problem of finding a good conductive eupoxy that retained its rigidity even at temperatures above 150°C was critical to our research. We found that a very good conductive eupoxy for this application was Eupoxy Technology's H-20 silver eupoxy. It is very smooth, fine grained and cures faster than any other eupoxy on the market.

Great care should be taken in the process of eupoxying the transducer pieces to the transducer mounts. The shear transducers should bind perfectly parallel to the surface and the film of eupoxy should be as thin as possible, to achieve strong coupling.

A brief procedure is outlined below:

First of all the transducer mounts and transducers are cleaned with acetone and cotton tips to remove all grease and thermoplastic resin. The transducer mounts are prepared first by fixing a 0.125" high, 0.75" I.D. teflon ring unto each with a ring of two sided masking tape. Then a very thin film of conductive eupoxy is brushed unto the surface of the transducer mount inside the teflon ring and likewise unto the appropiate surface of each shear transducer piece being very carefull to avoid bridging the two electrodes. Each piece is placed lightly inside and

next to the teflon ring. After proper positioning of the 7 pieces a slight pressure is applied unto each to expell the excess eupoxy.

Another teflon ring 0.125" high with 0.74" I.D. is then mounted on the shear pieces and the 0.375" diameter compressional transducer is brushed with eupoxy and placed in the center. The compressional transducer is always thicker than the shear transducers so the second teflon ring serves to position the compressional transducer exactly in the center of the shear pieces leaving an air gap in between.

One cylindrical metal weight with a 0.385" hole through its axis is used to push down on the teflon ring on the shear transducer pieces and another weight supported by a metal rod of diameter 0.380" is used to push down on the compressional transducer through the hole in the first weight. The weights are left on during the curing time of approximately 12 hours at 80°C. When heated, the eupoxy becomes less viscous and the weights are needed to guarantee a parallel bonding. The low curing temperature can be reached with a heat lamp without disturbing the assembly.

After curing has taken place the shear transducers are connected together with a silver platted ring of fine, silver-coated wire eupoxied unto the upper electrodes with a drop of conductive eupoxy on each. The 0.385" I.D. teflon ring is again placed over the shear transducers to flatten the ring unto the upper surfaces of all the shear transducer pieces. The eupoxy is cured at 100°C for three hours.

3.4.4 IMPERMEABILIZING

Since PZT transducers are porous they should be dried in a vaccum oven overnight, filled with dry nitrogen gas, and then covered on all unplatted sides with a thin film of Eccobond 104 non-conductive, high temperature eupoxy diluted with some Toluene and applied with a small brush. It is cured at 100°C for 6 hours. If the transducers are not sealed they will soak-up water from the air or oil from the pressure medium in the pressure vessel and deteriorate rapidly in efficiency. It was found that this procedure would increase the amplitude of the signal of the transducer mosaics by an order of magnitude.

3.4.5 ASSEMBLING

A thin metal plate supported between nuts on three srews driven into the transducer mounts around the transducer mosaics is used to hold 2 small coaxial Teflon connectors. The inside conductor stem is pressed, one unto the compres- sional transducer top electrode and the other to one of the seven shear transducer pieces. This obtains electrical connection through coaxial cables, diminishes electomagnetic noise and guarantees good grounding. Small squares of copper foil pressed between the connector stem and the transducer electrodes are used to prevent arching and to guarantee a good electrical connection within the silicon fluid.

The arrangement permits removal of the connectors to facilitate the sealing of the copper jacket, with or without the sample. Aluminum cups permit the application of a small unaxial force on the end plugs to

couple them to the sample before confining pressure is applied. Otherwise the jacket deforms into any space between the sample and end plugs at low confining pressures, and maintains the separation at higher pressures.

When the transit times through the transducer mounts alone are measured at different confining pressures and temperatures, they are joined by a short copper jacket that is sealed by two beveled rings. This was found to be, by far, the best method.

Figure 31 shows the variation of transit times though the end plugs alone with temperature and confining pressure. The variations are significant. Therefore, the measured transit times were calibrated with end-plug travel times corresponding to the temperature and pressure conditions of the experiment, namely 150°C and 100 bars Pc. Also included are the variations of first arrival amplitude. Absolute ultrasonic measurements of Q require exact knowledge of this variation.

3.5 PRESSURE SYSTEM

The acoustic properties of porous rocks depend not only on the pressure resulting from the weight of the column of rock above it and supported by the crystals or matrix that compose it, but also on the pressure of the instertitial pore fluid. The first is called confining pressure and the second pore pressure. Since the average density of rocks at shallow depths is approximately 2.6 gr/cc and the density of the pore fluids is approximately that of water, assuming an average

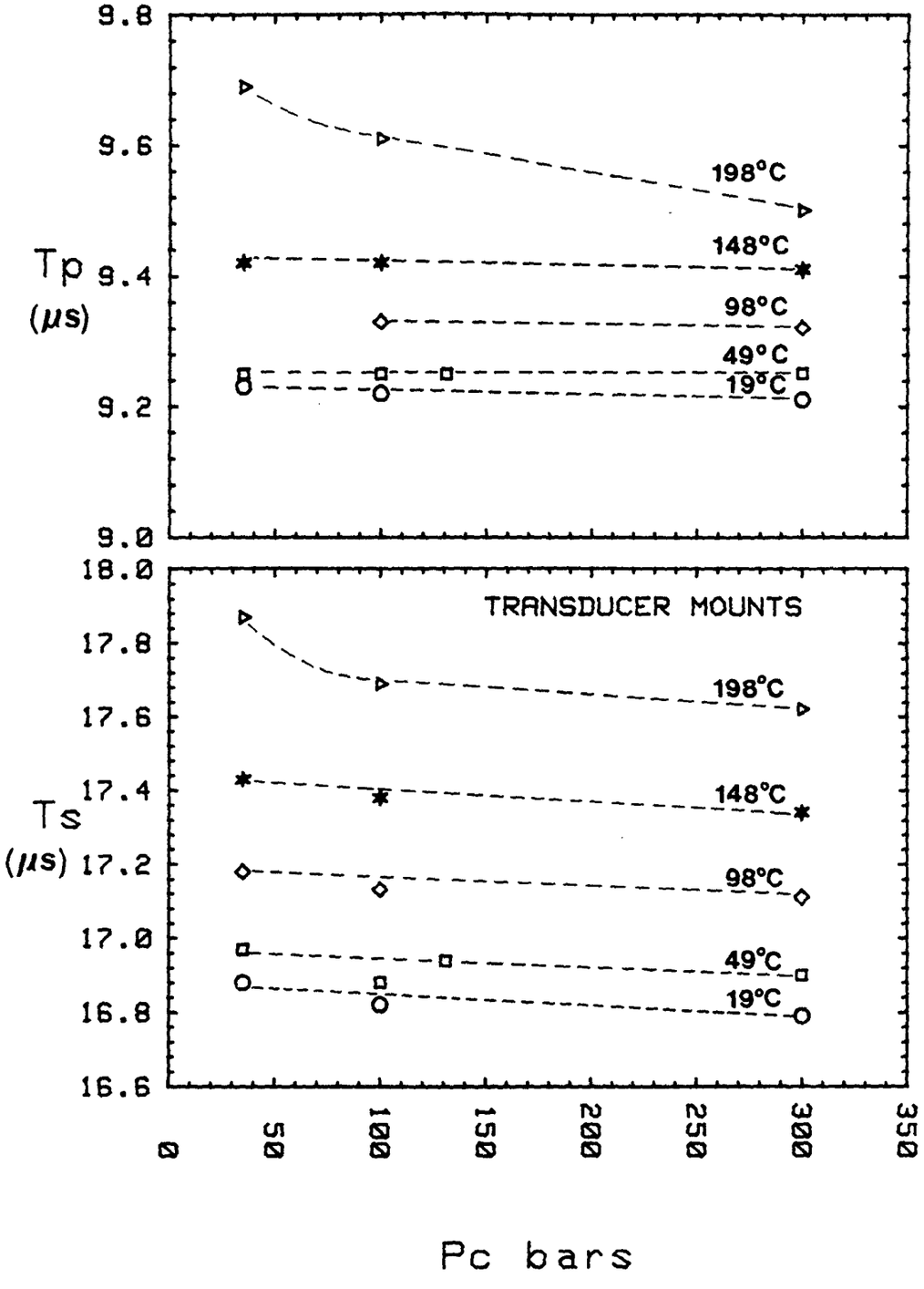

Figure 31a: Changes in Travel time thru the transducer mounts for P and S waves at different temperatures and confining pressures.

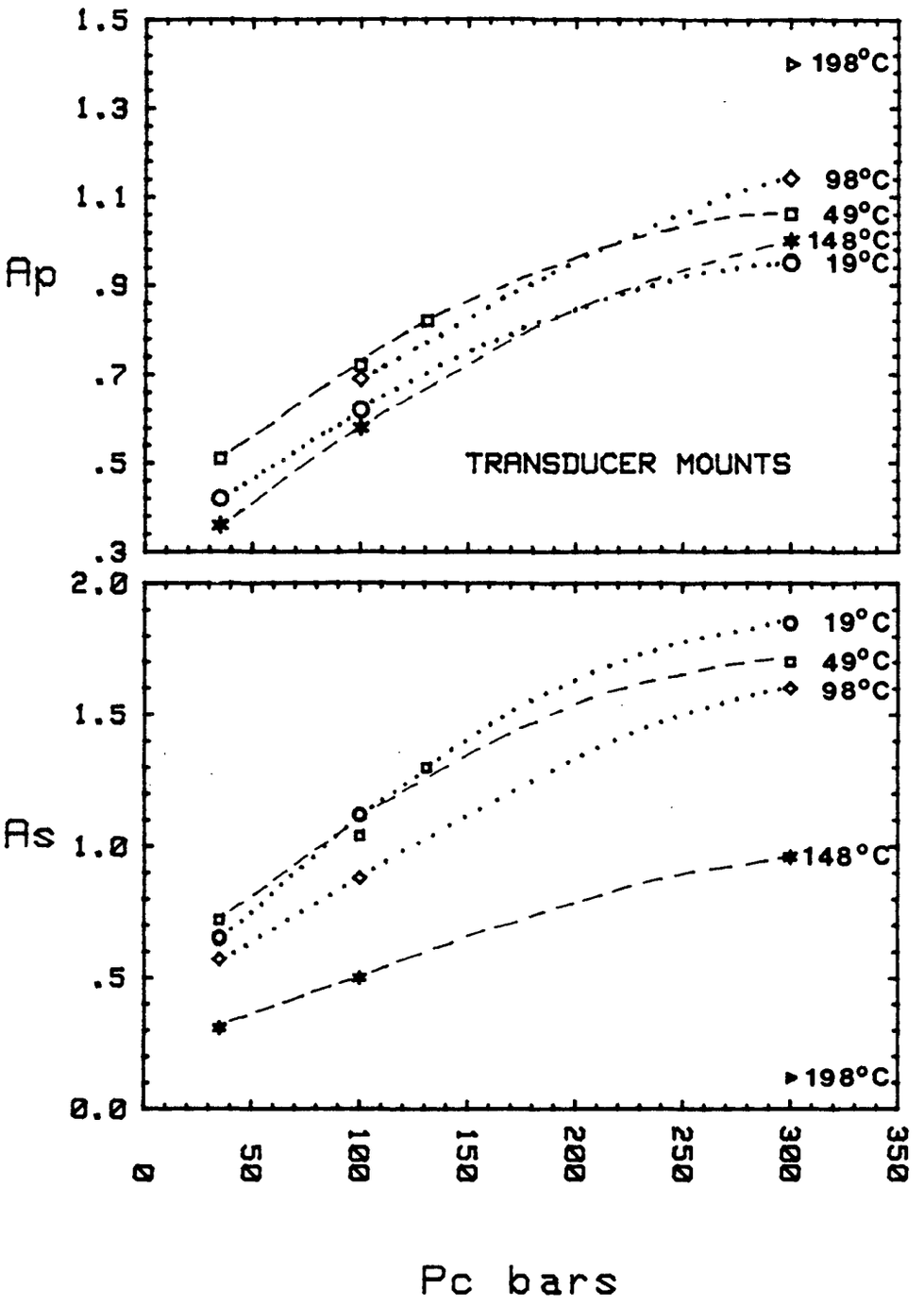

Figure 31b : Changes in amplitudes of the first arrivals for P and S waves through transducer mounts at different temperatures and confining pressures. Symbols same as in figure 31a.

porosity of 20% we can calculate that Pp=.44 Pc. The pore pressure in this simplified model is .44 of the confining pressure. Nevertheless, in sealed systems where the pore pressure can increase due to the generation of gas or an increase in temperature in clay bearing saturated sandstones, the pore pressure can be much larger. Since acoustical properties of rocks are very sensitive to small changes in differential pressure, the difference between the confinning pressure and the pore pressure, when this is low, they can provide diagnostic properties that are valuable in the location of anomalous zones that have either potential as energy sources or that can be dangerous zones for drilling.

Our pressure equipment consists of a pressure vessel with a large opening at the top and openings at the bottom and the side. The opening at the bottom is used to introduce silicon fluid under pressure by means of a hand pump. The other opening is used for a permanent termocouple that provides feedback to the temperature controller. The large opening at the top is machined as in figure 25 to receive the head or cap of the vessel. Sealing at this opening is achieved by a replaceable bronze ring that deforms against the walls of the pressure vessel as it is pulled upward, against another piece that is screwed into the vessel after the bronze ring. This method has been proved to pressures as high as 5 Kbars.

The electrical and fluid comunication through the head of the pressure vessel is the most problematic part of the pressure system. Our

work consisted in part in developing practical techniques to overcome the problems of leaking, grounding, and weakness of electrical connections.

Teflon coaxial cables from the transducer mounts are connected to stainless steel thermocouple wires that pass through the head of the pressure vessel. The thermocouple wires are cut to the right size, and the inner conductor exposed at both ends. The wires are sealed by silver soldering a small stainless steel cone to each about one inch from one of the ends. Each wire is heated to 200°C to evaporate all the water absorbed by the filling, and sealed with high temperature non-conductive eupoxy.The cone is then pressed against the pressure vessel head by a bolt. The problem of connecting the telon-coaxial inner conductor to the delicate inner conductors of the thermocouple wires was a difficult one to solve. The connection was done by flattening a small length of bronze tubing of the appropiate diameter around it, and securing the teflon coaxial wires to the head by the outer conductor net, pressed between small adaptors.

The pore pressure capillary tubes and the thermocouple used to measure the temperature were sealed in the same way to pass through the pressure vessel.

The confining pressure was measured with a Heise gauge. The absolute values of pore pressure were measured with a less expensive gauge that was checked with respect to a new Heise gauge. Table 5 shows the

TABLE 5

Comparison of New Heise Gauge (0-3000 psig) with with Duragauge (0-200 psig) gauge.

0-200 gauge	0-3000 gauge
0	0
10	11
20	21
40	40
60	60
100	98
140	139.5
180	180.5
200	200

correlation between the readings of the two gauges. The values agree to within 1 psi throughout the range from 0 psig to 200 psig (1 bar to 15 bars). The accuracy of the pore pressure gauge is important in the interpretation of the results of the experiments.

The relative pore pressure variation in the experiments was measured with a pressure transducer and recorded on a chart recorder. The continuous measurement was necessary to indicate when the pore pressure in the sample had reached a steady state after each pore pressure drop.

3.6 HEATING SYSTEM

The temperature of the system was controlled within 0.5°C at 150°C by a temperature controller and outside heating coils. The temperature was measured by a thermocouple through the head of the pressure vessel but a permanent thermocouple inserted through the side of the pressure vessel was used as feedback to the temperature controler. Silicon fluid was used as the pressure medium because of its high flashing temperature. It surrounded the sample and guaranteed negligible temperature gradients.

The thermocouple that was used to measure the temperature of the vicinity of the sample was checked in boiling water and was found to be accurate to within 0.5°C. A digital temperature indicator gave readings directly in degrees centigrade.

Temperature cracking was minimized by small heating rates at 300 bars confining pressure.

3.7 ELECTRONIC SYSTEM

The electronic system can be divided into three parts. These are:

a) The pulser

b) Signal viewing

c) Timing

This system was designed to measure wave travel times with an accuracy of at least 1%. A detailed schematic description of the system appears on figure 27.

The primary object of the system was to measure the time difference between the start of the pulse sent to the source transducer and the first arrival of the strain wave at the receiver transducer. Measurements of this time difference for the transducer mounts alone are substracted from the time differences of the transducer mounts and sample together to obtain the time for wave propagation through the sample.

Sometimes it is important to see the driving pulse (In this case, a square pulse) to measure the pulse width or determine if the particular transducer is functioning and if it is well grounded. It becomes necessary to trigger the oscilloscope before the high power pulse generator. This is achieved by triggering both instruments with another low power pulse generator which permits delaying the triggering of the high power pulse generator and changing the repetition rate. The repetition rate needs to be reduced when dealing with low atenuation samples since it takes longer for reflections to die away.

The pulse width of the high power pulse (~500 watts) is variable so that several wavelengths of the first arrival from the receiver transducer are free from the disturbance caused by the termination of the driving pulse. This disturbance travels at the same velocity as the first arrival and therefore, always appears at the same time difference from it. This pulse width and the voltage of the driving pulse was maintained constant throughout the experiment so that amplitudes could be used as a measure of relative attenuation in the sample.

In general, excellent signal to noise ratios in the received signals could be achieved with a driving pulse amplitude of ~500 volts. Higher amplitudes and pulse widths longer than 5 did not obtain much larger response and endangered the piezoelectric properties of the driving transducers.

The signal from the receiver transducer was displayed on a dual-beam oscilloscope after passing through an amplifier. The delays introduced by the amplifier when the amplification was changed from 20 db to 40 db (10x to 100x) were measured using a two volt amplitude square pulse connected both into and pass the amplifier to start and stop the time counter respectively. The difference in delay times is almost negligible in our application. They are .08μ between direct and 20 db amplification and .11μ between direct and 40 db amplification. The frequency response of the amplifier was also checked in the same way. In the superposition of two signals, one through the amplifier at 20 db amplification and the other directly to the oscilloscope on synchronous channels, the delay

produced by the amplifier can be seen directly but no change in the frequency content is seen. This permitted changing the amplification of the received signal without altering the absolute amplitude reading of it, and correcting for the change in travel time when important.

Several investigators have utilized different techniques to measure the travel times through the sample. Some have utilized the first change of slope. Others, the midpoint between the peak amplitude and the baseline or the intersection of two imaginary lines: the base-line and an extrapolation of the line with largest slope that can be fitted to the first arrival. Others have used a mercury delay line to superimpose a signal from it on the signal from the sample. We have found that the first method is the most practical. Velocities in metals, measured by this method agree very well with published values. The main source of error introduced by the method would come from substracting a travel time through metal (the transducer mounts together) from a travel time through metal and rock. The loss of the high frequency components in the rock could result in a slight negative error in velocity. But the other methods also have drawbacks. The change in frequency content as the signal passes through the rock changes the amplitude of the signal and the slope of the first arrival significantly. Comparison with signals that have passed through low attenuation media (mercury, for example) with signals that have passed through porous rock (sandstones) becomes impossible when the period and slope of the first arrival has been changed.

When timing first arrivals, the first change in slope due to the arrival of the wave was shifted horizontally on the oscilloscope screen with an electronic delay line until it was exactly superimposed on a vertical hair line. On another synchronous channel, the first break in slope of a time-variable square pulse was superimposed on the same hair line. The time counter was triggered on by a -.5V monitor signal produced symultaneously with the high power pulse to the driving transducer, at the -.02 V level, and triggerd off, at the .25V level, by the 4V time-variable square pulse that marked the time of the first arrival from the receiver transducer. All timings were done after amplifying the first arrival signals as much as possible, both in amplitude and time so that the very first break in slope could be detected.

Another variable-time square pulse generator is sometimes needed to detain the time counter from triggering on noise (ground loops, or electromagnetic interaction) before the appropiate time.

This method of timing has good accuracy and permits repeatable measurements to within .02μs.

3.8 ADDITIONAL INSTRUMENTATION

For low frequency measurements (<1KHz) of velocity and Q we have made use of a resonance bar measurement system designed and constructed by Winkler [1979] and a smaller version of the equipment has been constructed to measure velocities in 12" long, 3/4" diameter samples.

Only shear velocities and Qs were measured with the resonant-bar systems. Table 4 shows the comparison of shear velocities as measured with the long and short resonant-bar systems. The short resonant-bar system utilizes a Record Cutter Head to produce the vibrations at one end of the sample. The instrument was originally built to cut the matrix for a monoural commercial record. It can set up compressional and shear modes of displacement in bars without loading the bar [Thill, 1974]. In 1m long bars, electromagnets can be used to drive the sample into resonance since the permanent magnets eupoxied to the ends of the samples do not affect the velocities significantly. Nevertheless, we found that in short bars, the weight of the magnets affected the velocities in a way which was very difficult to correct conveniently.

Saturated resonant-bar samples were wrapped in thin plastic as measured to minimize evaporation of the water in the sample during measurements.

Appendix A

BEREA SANDSTONE EXPERIMENT IN VACUUM

A cylindrical sample (diam=19 mm, length=33.42mm) of Berea was cut perpendicular to the bedding plane. After measuring the sample to within .001 inches, P and torsional transducers were attached to it by means of conductive epoxy (This introduces a small negative error in the wave propagation velocities). The epoxy was cured at a temperature of 60 degrees centigrade.

After saturating the sample it was placed in a glass vacuum chamber and measurements were made beforeand after applying a vacuum. (It took about 30 minutes to connect the coaxial wires in the vacuum chamber. This delay parmitted the surface of the sample to dry somewhat).

Measurements for P and shear waves included: time between impulse to source transducers and first arrival from receiving transducers, relative amplitudes pulse width, and slope angle.

OBSERVATIONS

VELOCITIES

P velocity decreased rapidly as soon as the vacuum was applied. The shear wave velocity increased slightly.

The increase in shear wave velocity immediately after vacuum was applied to the sample can be explained by the change in density due to the expulsion of most of the water from the pores.

The P velocity decreased during the first two hours

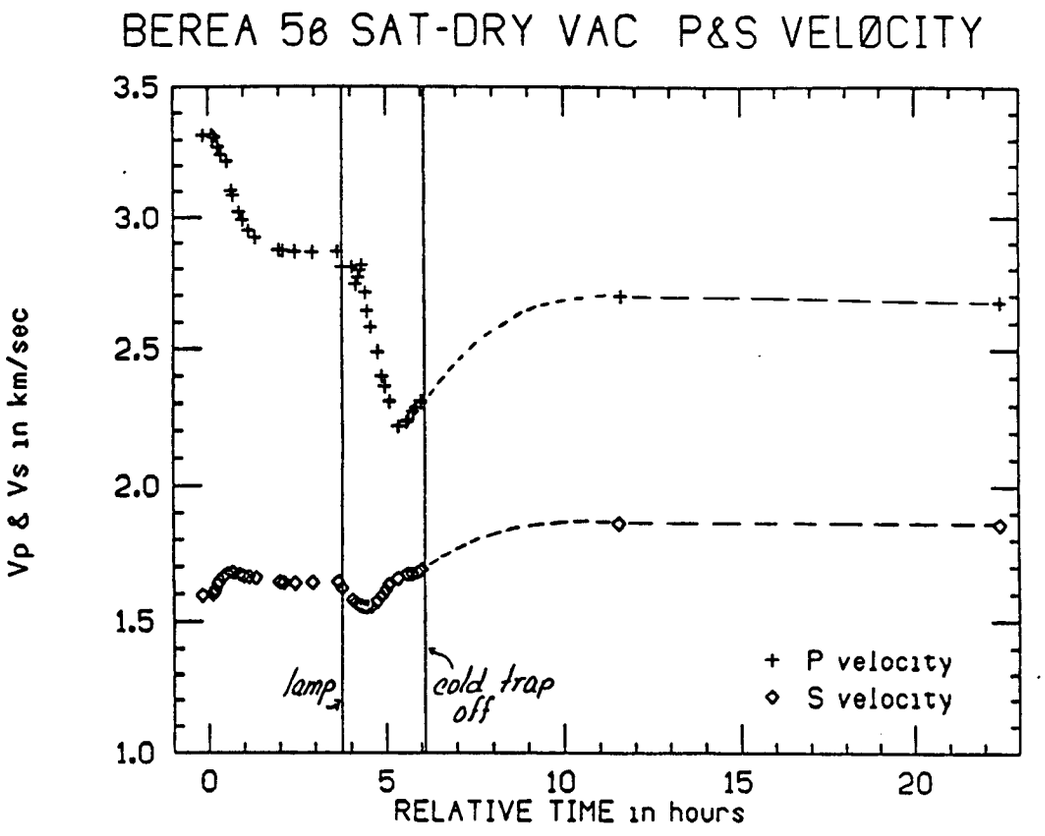
BEREA 58 SAT-DRY VAC P&S VELØCITY
Vp & Vs in km/sec
3.5
3.0
2.5
2.0
1.5
1.0
0
5
10
15
20
RELATIVE TIME in hours
lamp
cold trap off
+ P velocity
◇ S velocity

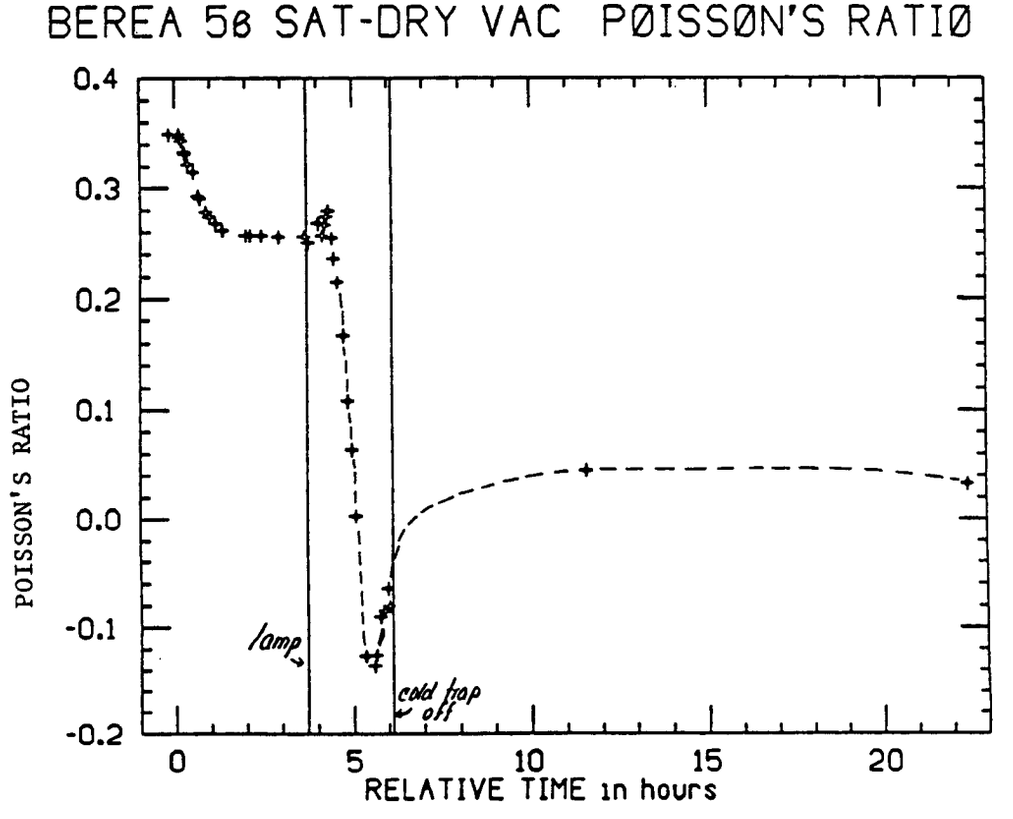
BEREA 58 SAT-DRY VAC PØISSØN'S RATIØ
POISSON'S RATIO
0.4
0.3
0.2
0.1
0.0
-0.1
-0.2
0
5
10
15
20
RELATIVE TIME in hours
lamp
cold trap off

of the experiment but the shear wave velocity reached was decreasing slightly from 0.5 to 2hrs. in the experiment.

The measurements show a change in the variation rate of the P velocity at the time that the shear velocity reached its maximum, suggesting that this time most of the water in the non-capillary pores had escaped (That the density effect had almost terminated) and that later variations were due to very small amounts of water leaving the sample, perhaps water Uretained by the active surface of the clays in the rock.

The values reached at 3 hrs. time are thought to be due to the decrease of heat in the rock by the evaporation process because when at 3.75 hrs. a heat lamp was directed toward the sample, the variations continued for both velocities.

We do not know how much of the changes are due to the change in temperature of the sample but we certainly cannot explain the velocity minima nor the great change in P velocity as just a temperature effect (The sample probably remained below 30 degrees centigrade during the experiment. A temperature controled experiment could resolve the question of the temperature effect).

A possible explanation: Just before the minima, water is still leaving the very small pores (These small pores can have a large effect on the velocities) and decreasing the elastic moduli. The increases after the minima are due to changes of the clays in the rock in the dehydration process.

Regardless of the magnitude of the temperature effects, both shear and bulk moduli had to be decreasing shortly after the heat lamp was installed. This is the first time that the change in effective shear modulus with saturation is observed at ultrasonic frequencies.

At the end of the experiment an intermediate value had been reached by the P velocity and a maximum value by the shear velocity.

Velocity minimus were obserfed for both types of waves but at different times. The shear wave velocity minimum was reached before the P velocity minimum.

The shear modulus reaches its minimum before the bulk modulus. This can be appreciated in the plot of Poisson's ratio for the experiment since it depends on the ratio of bulk modulus to shear modulus. Poisson's ratio is quite insensitive to small systematic errors of the same sign in the velocities.

POISSON'S RATIO

Poisson's ratio was found to decrease abruptly as most of the water left the pores before 2 hrs. A much greater change was observed after the heat lamp was applied. It may be that rocks in the field never loose the water retained in the clays (or by the clays) and that this drastic contrast of Poisson's ratio does not occur naturally. On the other hand, it may occur in very dry geothermal systems. Note the minimum at around 5.5 hrs.

Negative values of Poisson's ratio have been observed before in dry low porosity rocks at low confining pressures (Nur and Simmons, 1969). By definition, a negative Poisson's ratio indicates that a sample would contract sideways under vertical uniaxial compression.

this happens when:

$$K = \frac{2}{3}\mu \qquad \text{or} \qquad V_p = \sqrt{2}\, V_s$$

AMPLITUDES

The amplitude and slope measurements are a relative measure of the attenuation of the waves in the sample. (The power to the source transducer was kept constant throughout the experiment.)

Soon after vacuum was applied to the sample, the P amplitude decreased by more than a factor of 3 while the shear amplitude remained constant at this time. After this time, the shear amplitude increased slightly but continuously until the heat lamp was applied. After heat was provided and evaporation of water in the pores and clays continued, both P and S amplitudes increased by a factor of 16.

The following series of photographs show the oscilloscope traces for P and shear waves during the experiment. Note the second arrival in the P trace that catches up to the first pulse as the sample is drying. The shear wave does not show this phenomenon in the photographs.

Note that the shear wave amplitude continues to increase even after 22 hrs, while the P wave amplitude is constant after 11 hrs.

PULSE WIDTH

A plot of the pulse width of the first arrival, measured at one fifth of the amplitude follows.

Larger pulse widths indicate more attenuation of the higher frequencies of the received signal and therefore a decrease in Q, and viceversa. (High frequencies would attenuate more than low frequencies for a certain drop in Q because they travel through more wavelengths in the rock.) pulse width relative to that of the P wave before 4 hours. This plot shows that pulse width for a shear wave decreases with the amount of water in the pores, while for P waves, there is a sharp

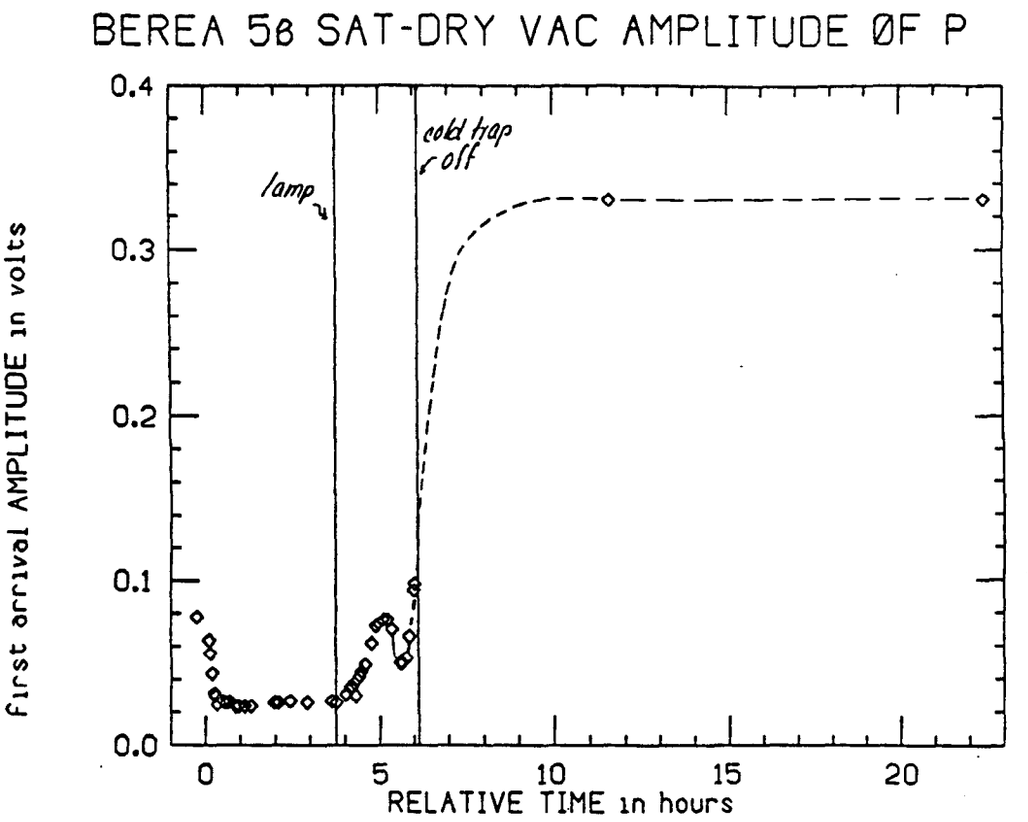
BEREA 58 SAT-DRY VAC AMPLITUDE ØF P
first arrival AMPLITUDE in volts
0.4
0.3
0.2
0.1
0.0
lamp
cold trap off
0
5
10
15
20
RELATIVE TIME in hours

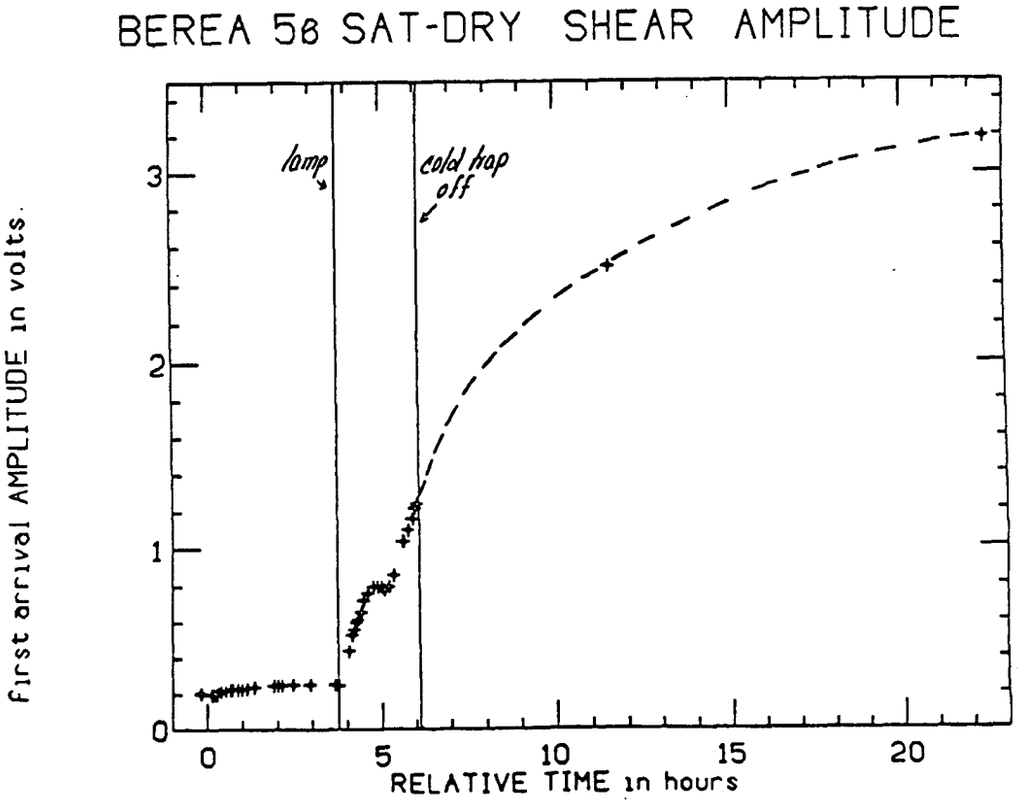
BEREA 58 SAT-DRY SHEAR AMPLITUDE
first arrival AMPLITUDE in volts
3
2
1
0
lamp
cold trap off
0
5
10
15
20
RELATIVE TIME in hours

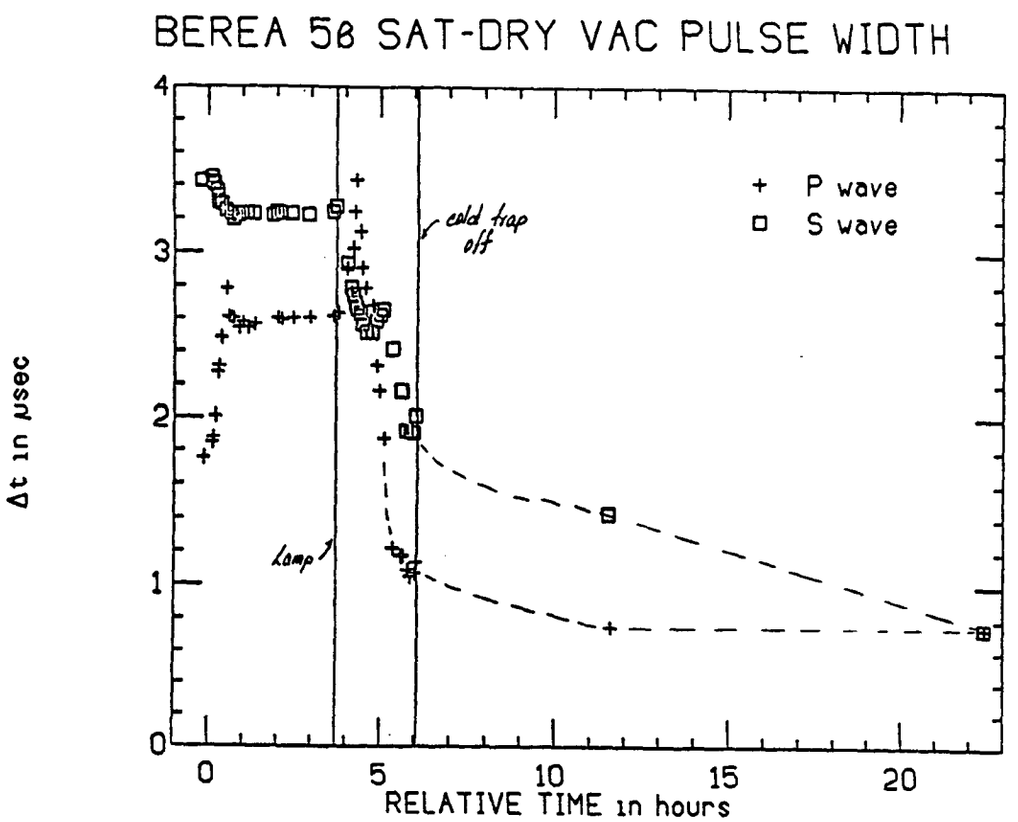
BEREA 58 SAT-DRY VAC PULSE WIDTH
Δt in μsec
+ P wave
□ S wave
cold trap off
Lamp
0
1
2
3
4
0
5
10
15
20
RELATIVE TIME in hours

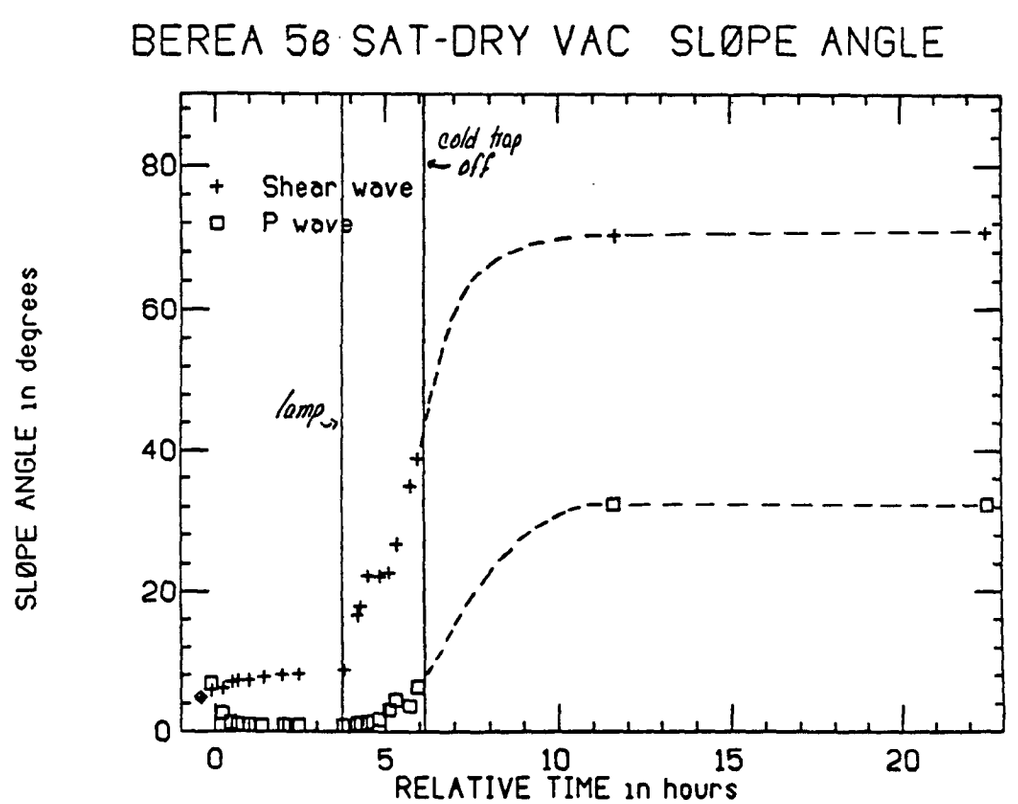
BEREA 58 SAT-DRY VAC SLØPE ANGLE
SLØPE ANGLE in degrees
+ Shear wave
□ P wave
cold trap off
lamp
0
20
40
60
80
0
5
10
15
20
RELATIVE TIME in hours

increase at the partial saturation condition and a sharp decrease when the last drops of water leave the pores.

MAXIMUM SLOPE ANGLE

The maximum slope angle of the first arrivals was measured from photographs of the oscilloscope screen. It is interesting to see how prescisely it can be measured. It follows very closely the amplitude data before 5 hrs. It is different afterwards in that the shear wave slope is constant from 11hrs. on while the shear amplitude continues to increase between 11 and 22 hours.

The maximum slope angle also differs from the pulse width plot in the same way, but in addition both maximum shear wave slope angle and shear amplitude, in contrast to pulse width, do not change significantly within the first 30 minutes. Note how much higher the maximum slope is for the shear wave than for the P wave ar the end of the experiment, even though they started at the same level.

The photographs of the P and S wave first arrivals show a second arrival only for the P wave. A possible explanation of the fact that this arrival catches-up with the first arrival is that the second arrival is Biot's [1956] second wave. This second wave propagates as a diffussion wave through the pore fluid of the rock and therefore is slower than the first arrival. The observation that the second wave catches up with the first as the sample dries in vacuum, a condition where the evaporation process would be homogeneous, suggests that the identification of this second wave may be correct.

P WAVE SIGNALS

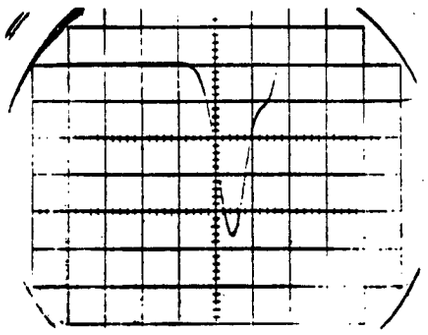

-0.41 hrs.

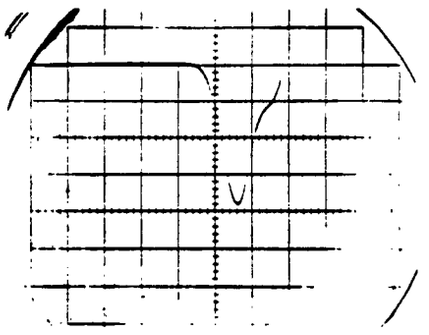

-.12 hrs.

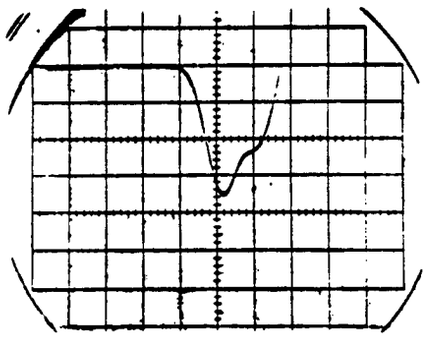

0.22 hrs.

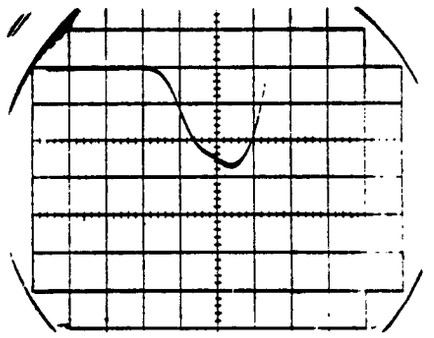

0.47 hrs.

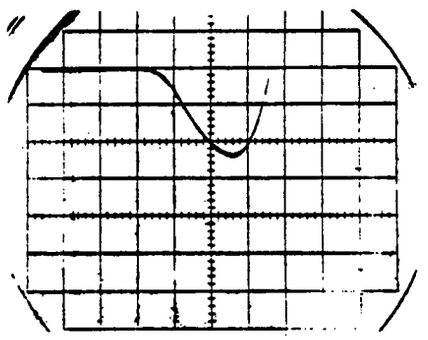

1.01 hrs.

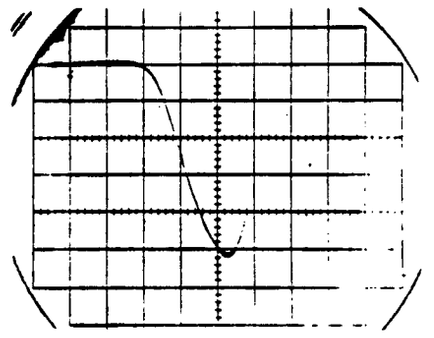

2.04 hrs.

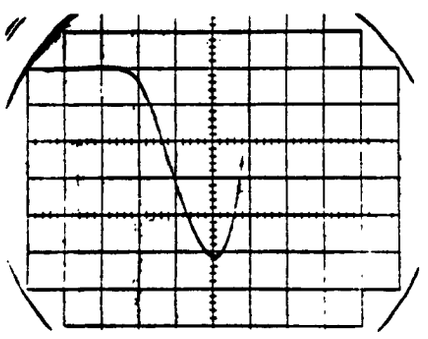

3.79 hrs.

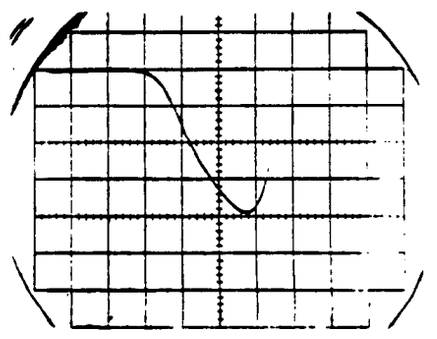

4.31 hrs.

S WAVE SIGNALS

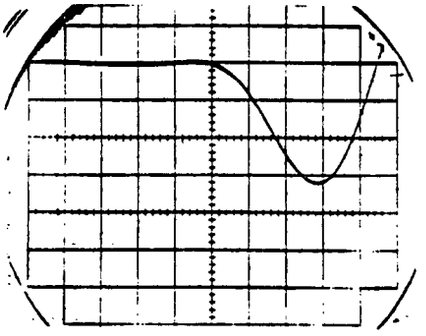

-0.39 hrs.

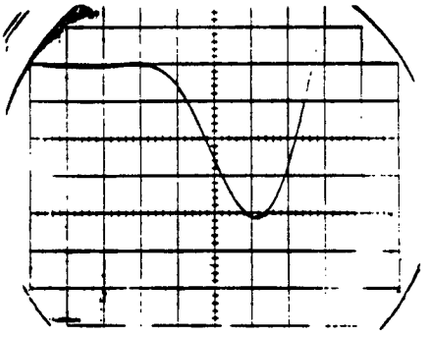

0.24 hrs.

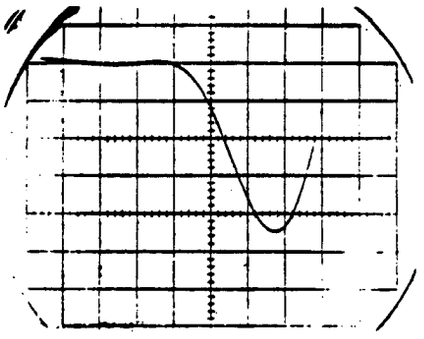

0.50 hrs.

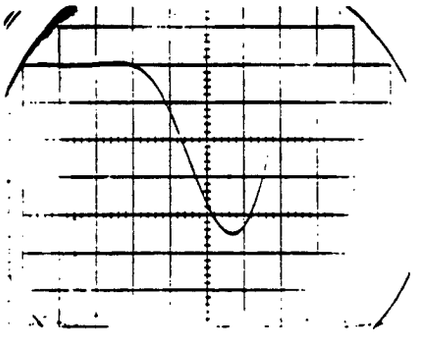

0.67 hrs.

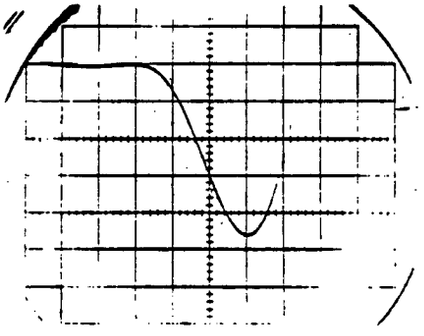

0.99 hrs.

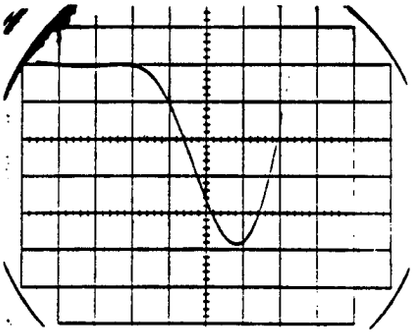

1.45 hrs.

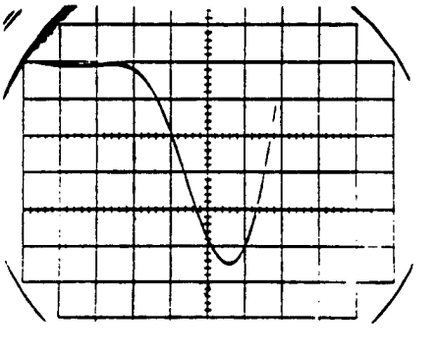

3.80 hrs.

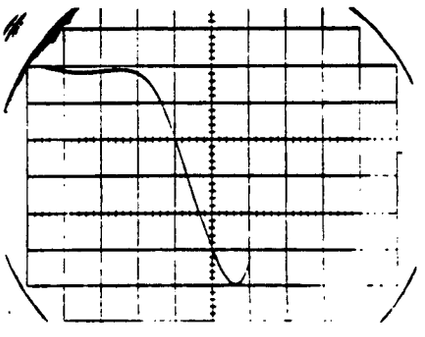

4.29 hrs.

Appendix B

DATA FROM WATER-STEAM TRANSITION EXPERIMENTS. COMPARISON BETWEEN THE DOWNWARD GOING PORE PRESSURE DATA WITH THE UPWARD GOING PORE PRESSURE DATA. SOLID DOTS REFER TO PORE PRESSURE DECREASING. CIRCLES REFER TO PORE PRESSURE INCREASING.

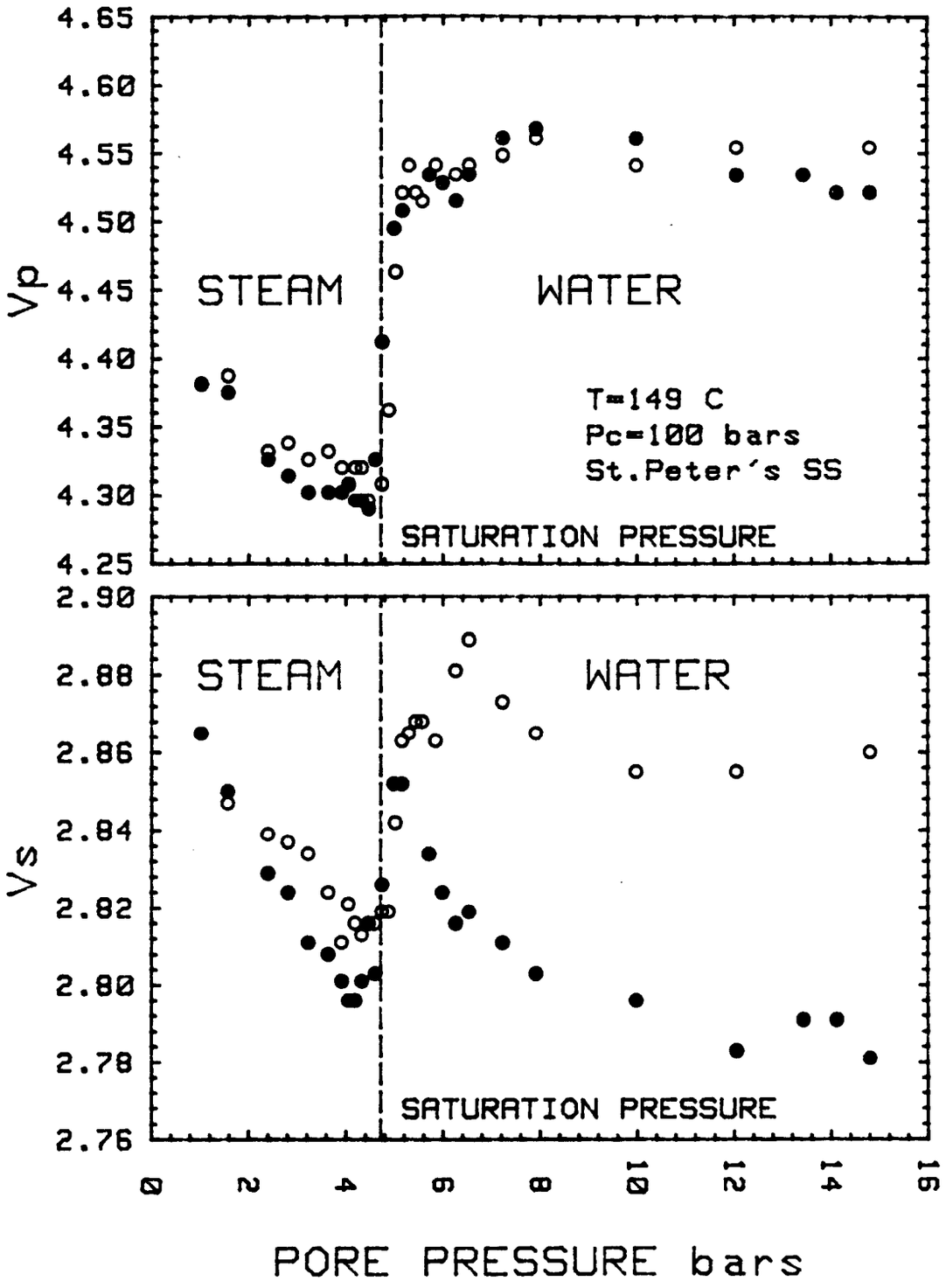
4.65
4.60
4.55
4.50
4.45
4.40
4.35
4.30
4.25
Vp
STEAM
WATER
T=149 C
Pc=100 bars
St.Peter's SS
SATURATION PRESSURE
2.90
2.88
2.86
2.84
2.82
2.80
2.78
2.76
Vs
STEAM
WATER
SATURATION PRESSURE
0
2
4
6
8
10
12
14
16
PORE PRESSURE bars

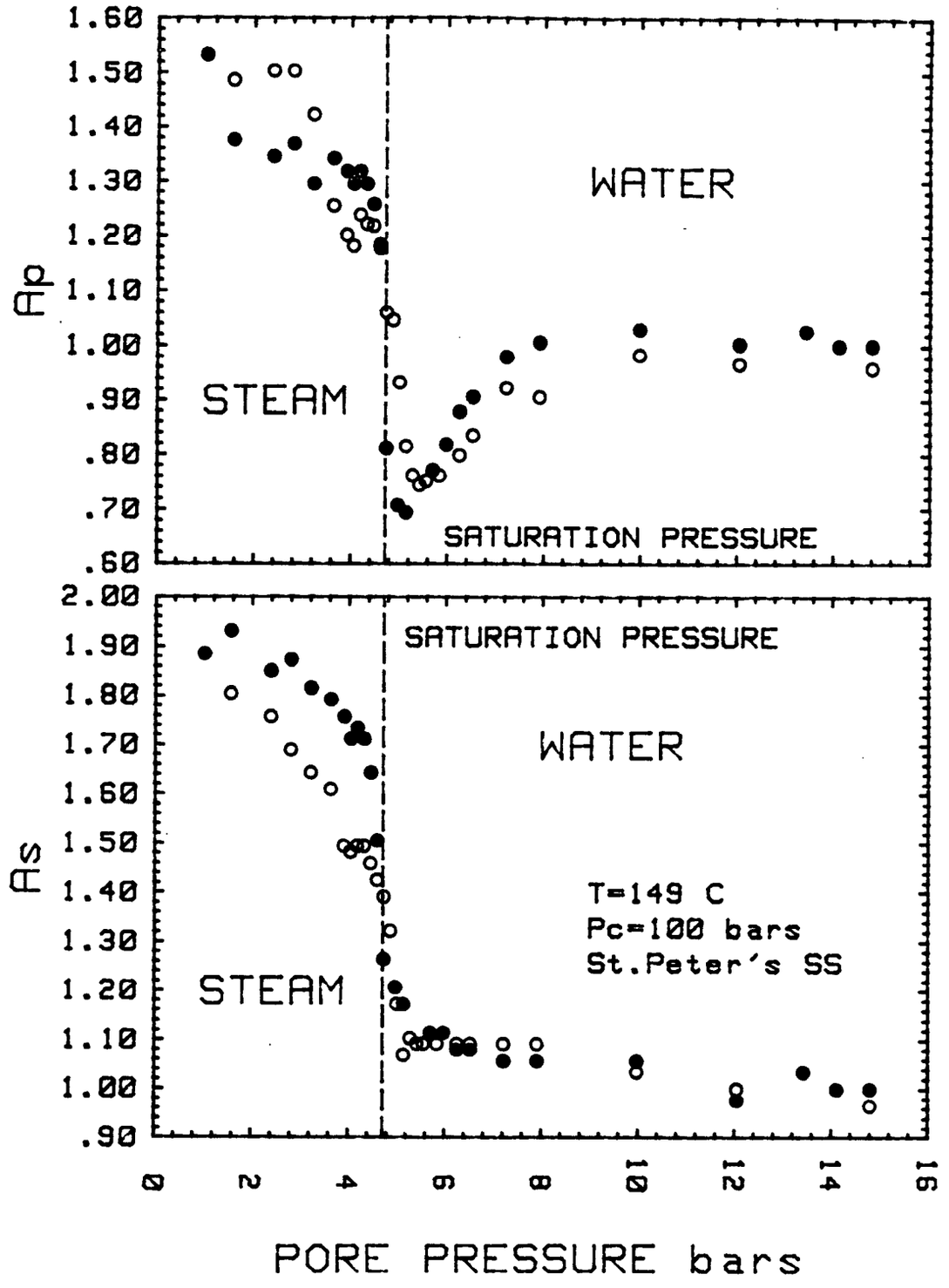
1.60
1.50
1.40
1.30
1.20
1.10
1.00
.90
.80
.70
.60
Ap
WATER
STEAM
SATURATION PRESSURE
2.00
1.90
1.80
1.70
1.60
1.50
1.40
1.30
1.20
1.10
1.00
.90
As
SATURATION PRESSURE
WATER
T=149 C
Pc=100 bars
St.Peter's SS
STEAM
0
2
4
6
8
10
12
14
16
PORE PRESSURE bars

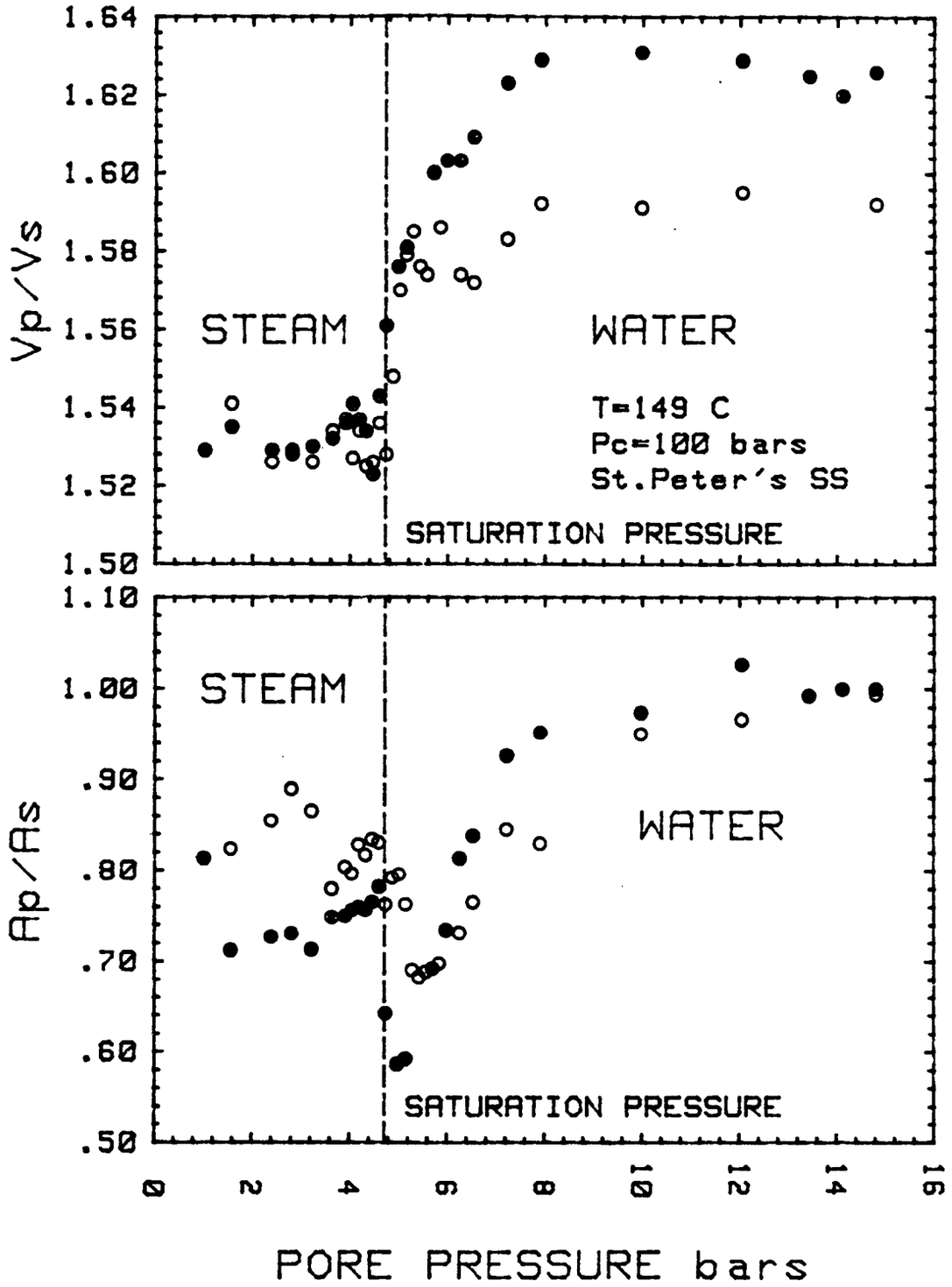
1.64
1.62
1.60
1.58
1.56
1.54
1.52
1.50
Vp/Vs
STEAM
WATER
T=149 C
Pc=100 bars
St.Peter's SS
SATURATION PRESSURE
1.10
1.00
.90
.80
.70
.60
.50
Ap/As
STEAM
WATER
SATURATION PRESSURE
0
2
4
6
8
10
12
14
16
PORE PRESSURE bars

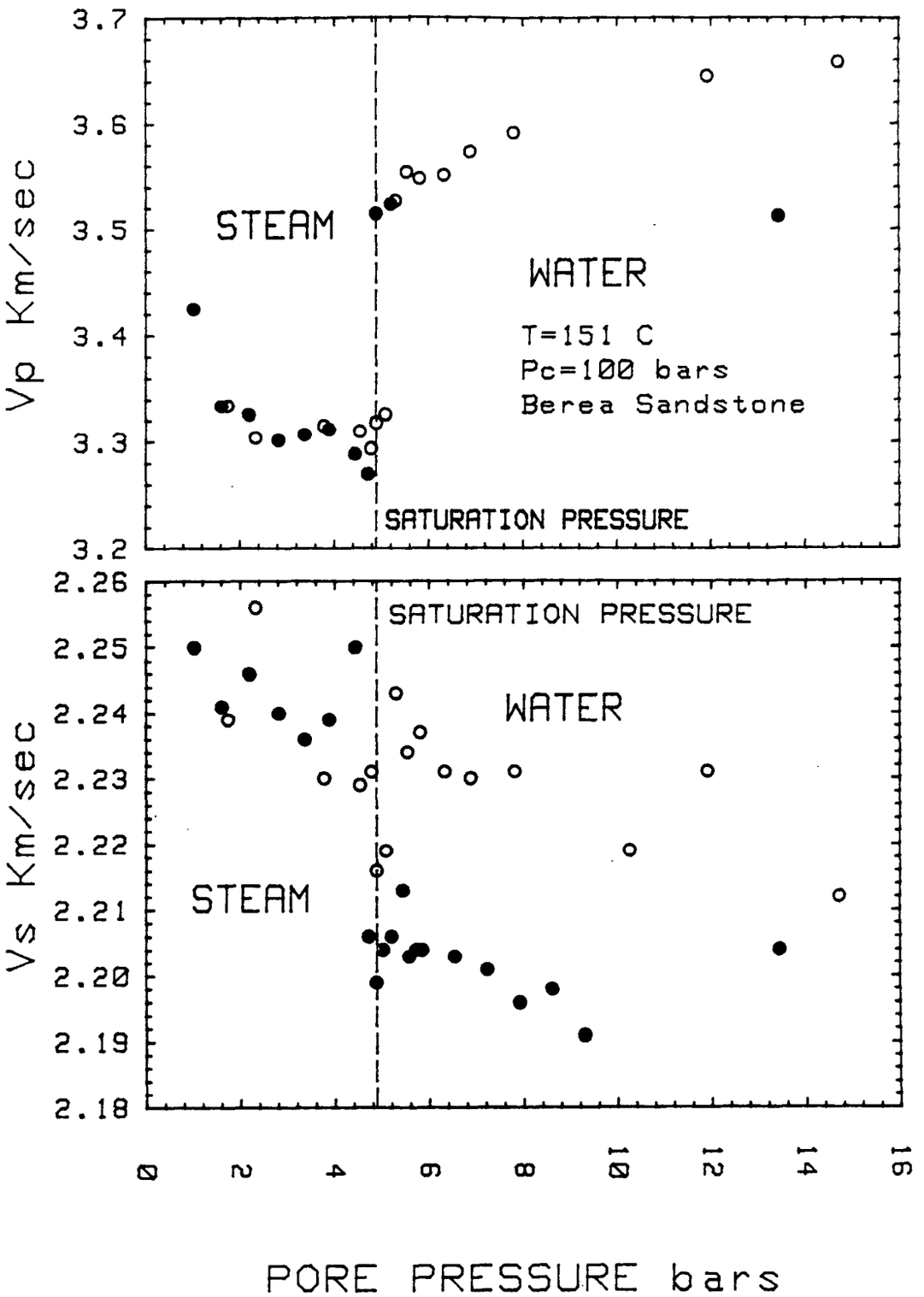
3.7
3.6
3.5
3.4
3.3
3.2
Vp Km/sec
STEAM
WATER
T=151 C
Pc=100 bars
Berea Sandstone
SATURATION PRESSURE
2.26
2.25
2.24
2.23
2.22
2.21
2.20
2.19
2.18
Vs Km/sec
SATURATION PRESSURE
WATER
STEAM
0
2
4
6
8
10
12
14
16
PORE PRESSURE bars

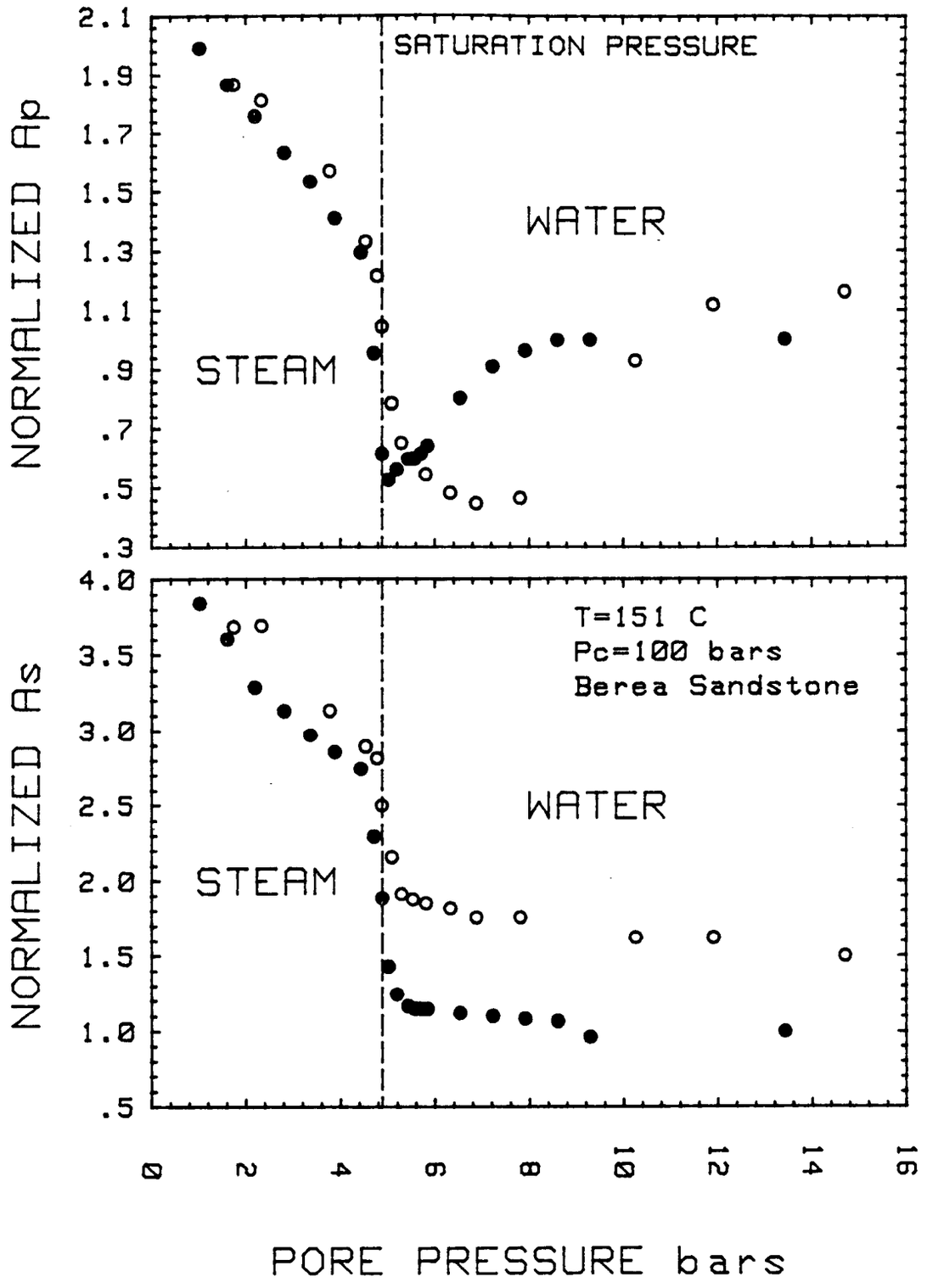
SATURATION PRESSURE
WATER
STEAM
NORMALIZED Ap
2.1
1.9
1.7
1.5
1.3
1.1
.9
.7
.5
.3
T=151 C
Pc=100 bars
Berea Sandstone
WATER
STEAM
NORMALIZED As
4.0
3.5
3.0
2.5
2.0
1.5
1.0
.5
0
2
4
6
8
10
12
14
16
PORE PRESSURE bars

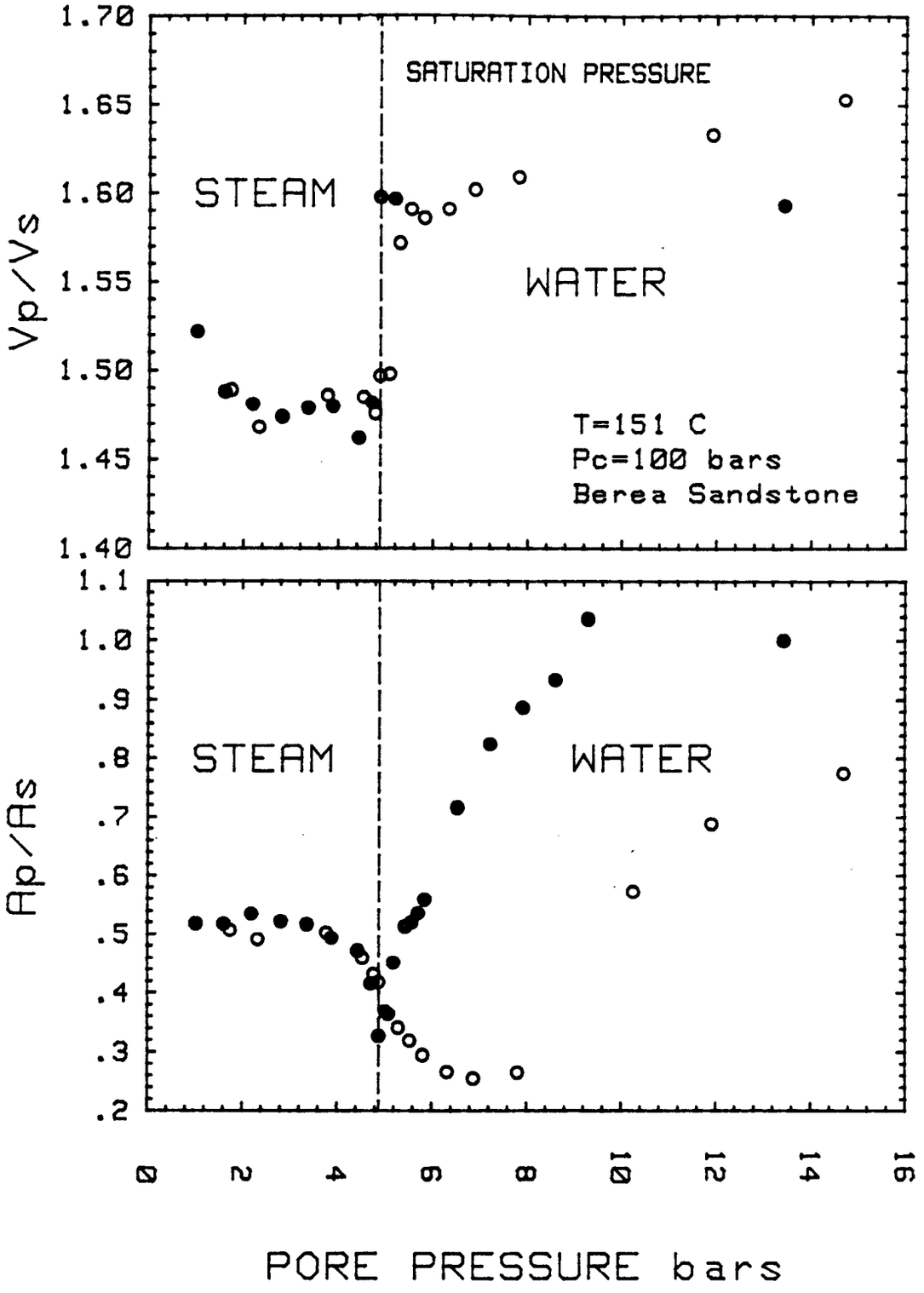
SATURATION PRESSURE
STEAM
WATER
T=151 C
Pc=100 bars
Berea Sandstone
Vp/Vs
Ap/As
STEAM
WATER
PORE PRESSURE bars

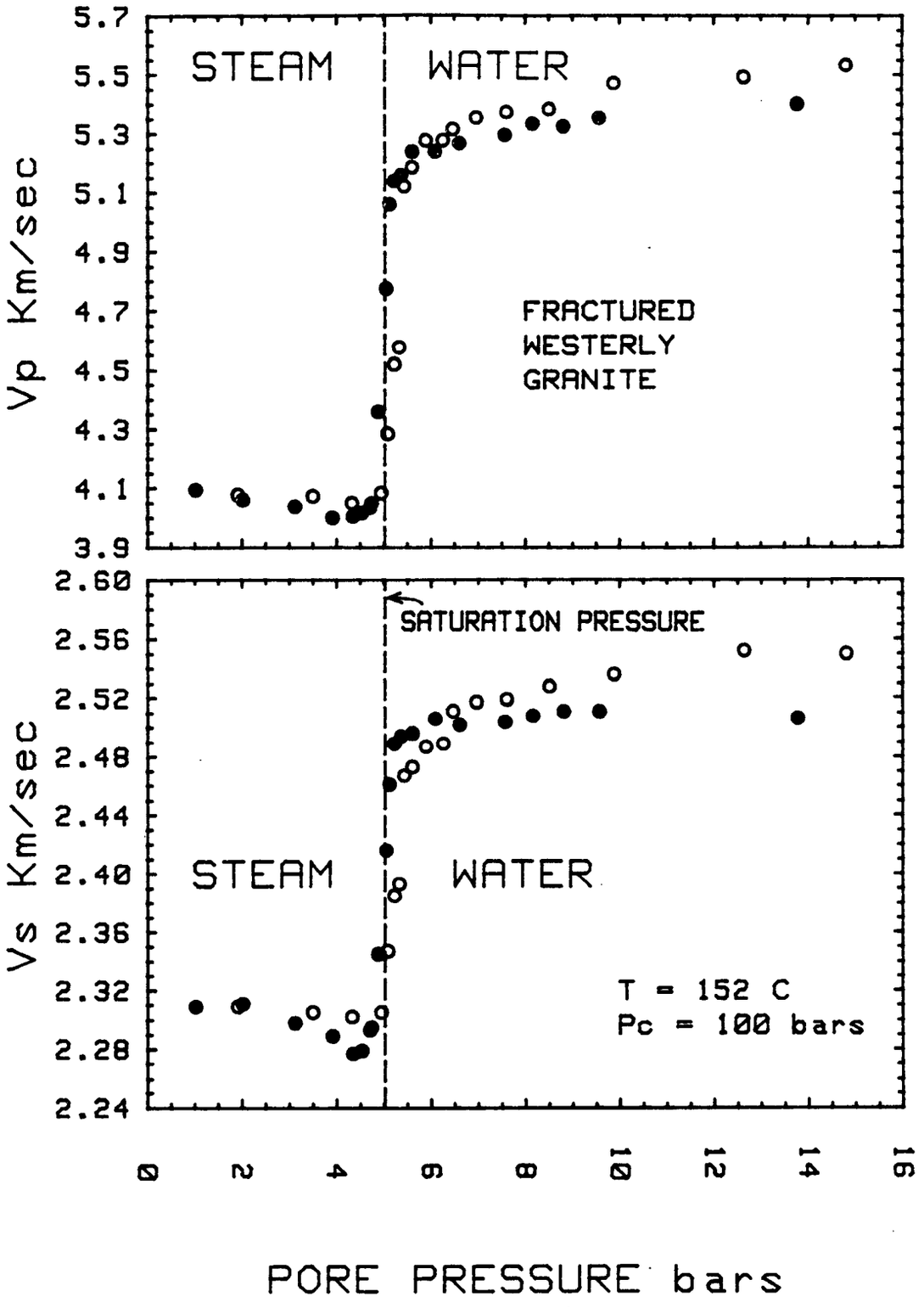
STEAM
WATER
FRACTURED
WESTERLY
GRANITE
Vp Km/sec
5.7
5.5
5.3
5.1
4.9
4.7
4.5
4.3
4.1
3.9
SATURATION PRESSURE
STEAM
WATER
T = 152 C
Pc = 100 bars
Vs Km/sec
2.60
2.56
2.52
2.48
2.44
2.40
2.36
2.32
2.28
2.24
0
2
4
6
8
10
12
14
16
PORE PRESSURE bars

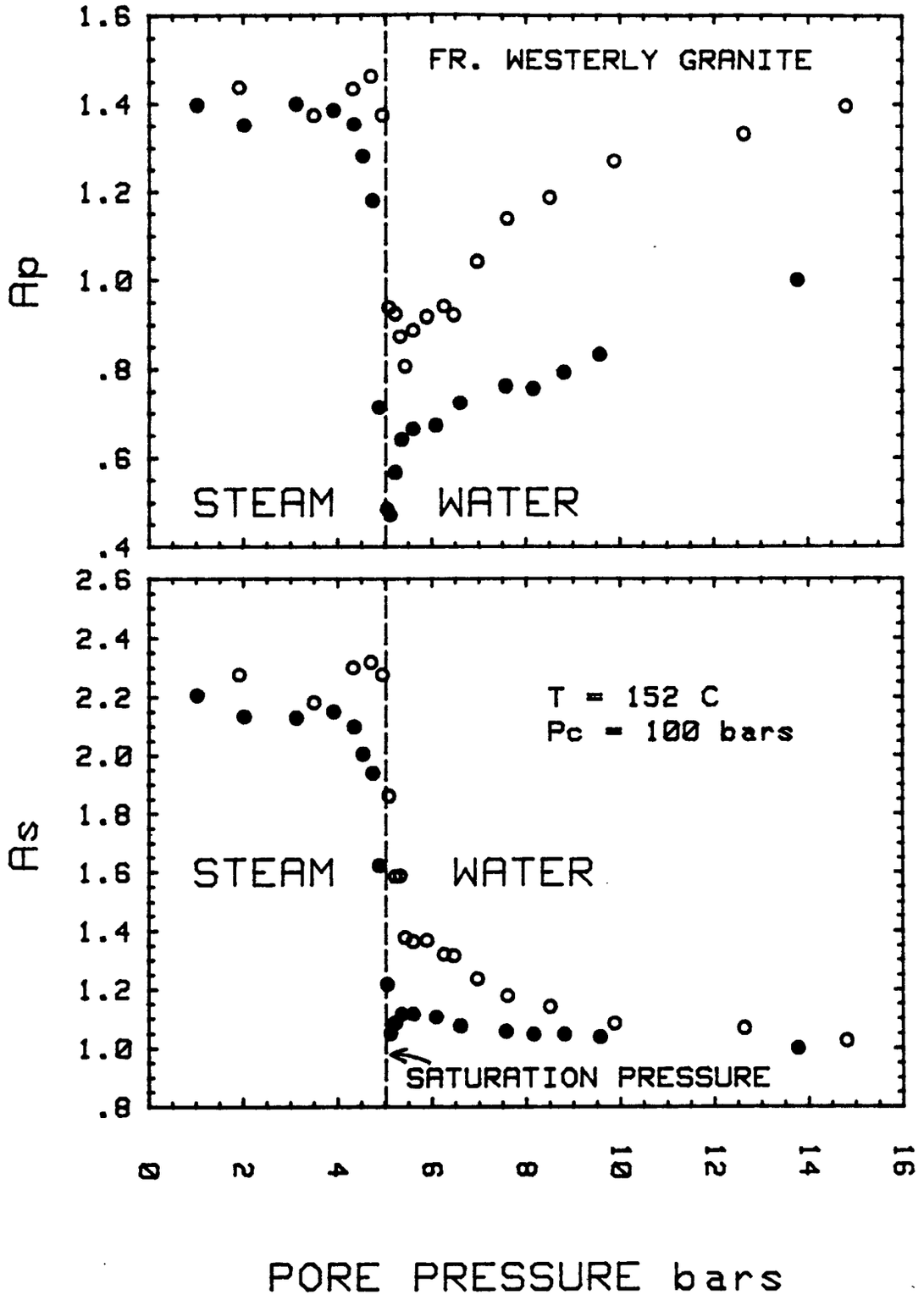
FR. WESTERLY GRANITE
STEAM
WATER
Ap
T = 152 C
Pc = 100 bars
STEAM
WATER
As
SATURATION PRESSURE
PORE PRESSURE bars

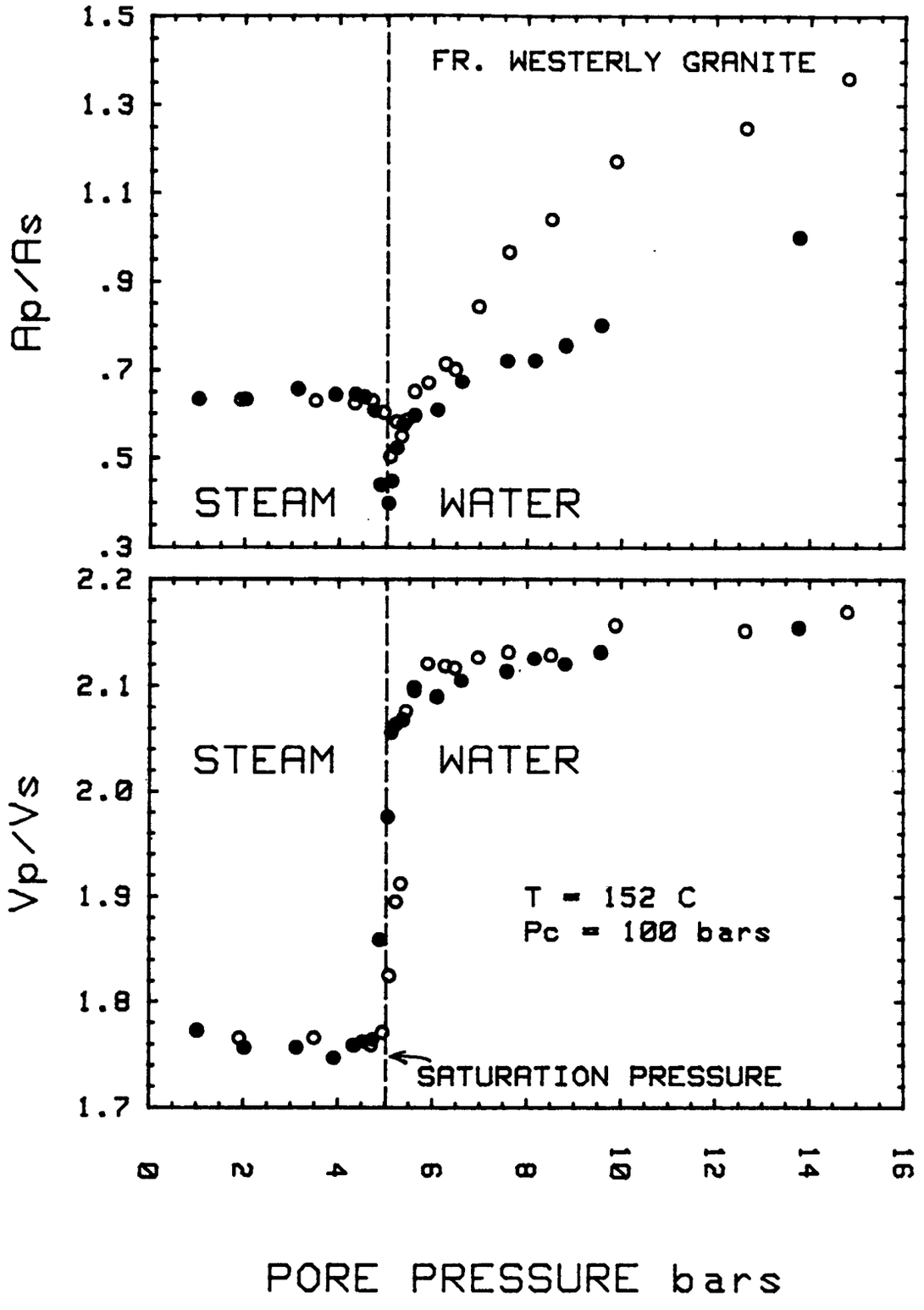
FR. WESTERLY GRANITE
Ap/As
1.5
1.3
1.1
.9
.7
.5
.3
STEAM
WATER
Vp/Vs
2.2
2.1
2.0
1.9
1.8
1.7
STEAM
WATER
T = 152 C
Pc = 100 bars
SATURATION PRESSURE
0
2
4
6
8
10
12
14
16
PORE PRESSURE bars

Appendix C

CALCULATION OF DENSITY CHANGE EFFECT ON SHEAR VELOCITY.

$$Vs^2 = \frac{\mu}{\rho}$$

$$dVs = \frac{\partial Vs}{\partial \rho} \, d\rho + \frac{\partial Vs}{\partial \mu} \, d\mu$$

$$\frac{\partial Vs}{\partial \rho} = -\frac{1}{2}\left(\frac{\mu}{\rho^3} \right)^{\frac{1}{2}}$$

if $\mu = \mu_o$ = constant,

$$dVs = -\frac{1}{2}\left(\frac{\mu_o}{\rho^3} \right)^{\frac{1}{2}} d\rho$$

from saturated to dry conditions:

$$d\rho = \frac{M_R}{V_R + V_P} - \frac{M_R - M_P}{V_R + V_P} = -\phi$$

where: M_R = mass of solids

M_P = mass of pores

V_R = volume of solids

V_P = volume of pores

ϕ = porosity

therefore:

$$dVs = \frac{\phi}{2} \cdot \left(\frac{\mu}{\rho^3} \right)^{\frac{1}{2}} = \frac{\phi Vs}{2\rho}$$

Appendix D

Substitutions into Walsh (1969) Equations.

Change of notation:

$$\left.\begin{aligned} \mu_o &= \mu_1 \\ K_o &= K_1 \\ \bar{\mu} &= \mu' \end{aligned}\right\} \text{ Walsh}$$

Walsh's expression for the effective shear modulus [1969]:

$$\left(\frac{\mu_o}{\bar{\mu}} - 1\right) = \frac{2G}{45}\frac{d^3}{v}\,\frac{2 - A(\omega/\omega_d)^2}{1 + (\omega/\omega_d)^2} +$$

$$+ \frac{c}{10}\,\frac{\dfrac{4}{3}\cdot\dfrac{3K_2 + 2\mu_o}{3K_2'} + 3(\omega/\omega_c)^2\cdot\dfrac{K_2' - 2K_2}{2\mu_o}}{1 + (\omega/\omega_c)^2}$$

where:

$$G = \frac{3K_o + 4\mu_o}{3K_o + 2\mu_o} \qquad C = \text{porosity}$$

$$K_2' = K_2 + \pi\alpha\mu_o\cdot\frac{3K_o + \mu_o}{3K_o + 4\mu_o}$$

$$A = \frac{3\pi\alpha}{4}\cdot\frac{3K_o + 2\mu_o}{3K_o + 4\mu_o}$$

$$\frac{\omega}{\omega_d} = \frac{\omega\eta}{\alpha\mu_o} = \frac{4G\omega\eta}{3\pi\alpha\mu_o} \quad ; \quad \frac{\omega}{\omega_c} = \frac{4\omega\eta}{3K_2'}$$

Assume:

$$K_o = K_{quartz} \sim 44 \times 10^4 \text{ bars}$$

$$\mu_o = \mu_{quartz} \sim 37 \times 10^4 \text{ bars}$$

For air in pores:

$$K_2 \approx 0$$

$A = 1.73\alpha$

$G = 1.361$

$$K_2' = 71 \times 10^4 . \alpha \text{ bars}$$

$\frac{\omega}{\omega_d} = 8 \times 10^{-6} \frac{f}{\alpha}$ (f in MHz)

$\alpha \left(\frac{\omega}{\omega_d}\right)^2 = 7 \times 10^{-11} \frac{f^2}{\alpha}$

} Both insignificant for $f < 1$ and $\alpha > 10^{-4}$

$$\therefore \left(\frac{\mu_o}{\mu} - 1\right) \approx 0.12 \frac{d^3}{v} + 0.141 \frac{c}{\alpha}$$

but $\frac{c}{\alpha} = \frac{\pi}{6} \frac{d^3}{v}$ For an ellipsoidal inclusion where two axes are equal.

$$\therefore \left(\frac{\mu_o}{\mu} - 1\right) = 0.12 \frac{d^3}{v} + 0.024 \frac{d^3}{v}$$

For 150°C water in pores:

$$K_2' = K_2 \text{ since } \frac{3K_o + \mu_o}{3K_o + 4\mu_o} \sim \frac{4}{7} \text{ for } K_o \sim \mu_o$$

$$A = 1.73\alpha$$

$$\frac{\omega}{\omega_d} = \frac{4G\omega\eta}{3\pi\alpha\mu_o} \text{ and } \frac{\omega}{\omega_c} = \frac{4\omega\eta}{3K_2}$$

$$G = 1.36$$

$$\eta = 0.183 \ \frac{mNs}{m^2} \ @ \ 150^0C$$

$$K_2 = 2.13 \times 10^4 \text{ bars}$$

$$\left(\frac{\omega}{\omega_d}\right)^2 = \left(\frac{.01\ \eta f}{\alpha}\right)^2 \ (f \text{ in MHz}) \text{ significant for } \alpha << 1$$

$$\alpha\left(\frac{\omega}{\omega_d}\right)^2 = \left(\frac{.01\ \eta f}{\alpha}\right)^2 \text{ not significant}$$

$$\left(\frac{\omega}{\omega_c}\right)^2 = \left(\frac{.84\ f\eta}{K_2}\right)^2 \text{ not significant}$$

$$\therefore \left(\frac{\mu_o}{\mu} - 1\right) = 0.12 \frac{d^3}{v} \cdot \frac{1}{1 + (\omega/\omega_d)^2}$$

$$= 0.12 \frac{d^3}{v} \cdot \frac{1}{1 + \left(\frac{.0018\ f}{\alpha}\right)^2}$$

Appendix E

ERROR ESTIMATION AND AMPLITUDE CORRECTION.

Maximum errors were estimated by:

$$dV(p_1,p_2)= \frac{\partial V}{\partial p_1} dp_1 + \frac{\partial V}{\partial p_2} dp_2$$

where V is some variable calculated from two measured parameters p_1 and p_2 (for example: travel time and length for velocity computation.). Since p_1 and p_2 can be both positive and negative, all (4) combinations of p_1 and p_2 were used to calculate dV and the maximum was chosen as the estimated error for the measurement. Velocities and the velocity ratio were treated in this way. 2/3 of the maximum estimated errors were plotted.

The travel time error was read off the oscilloscope screen as the maximum and minimum possible travel time minus the observed travel time. The length error was determined by measuring the sample at the center of the circular faces and at four points close to the circunference. All these measurements of length were then averaged to give the observed value and the standard deviation used as a measure of the error in the length of the samples.

The amplitude correction consisted in removing the effect of the change in transmission coefficient at the boundaries between the sample and the transducer mounts due to changes in velocities as the degree of saturation changes occured. The transducer mounts and sample arrangement can be modeled as a wave incident on two boundaries, one after the other. The transmission coefficient, T, is calculated from the known densities and velocities of the materials. The change in amplitude at the receiver transducer due to changes in velocity in the sample can be calculated by assuming constant Q for the sample and a linear relationship between strain and the amplitude of the electronic signal at the receiver transducer.

The amplitude at the receiver transducer is:

$$A=B_o T_1 T_2 = B_o T$$

where T_1 is the transmission coefficient at the first boundary, T_2 the transmission coefficient at the second boundary and B_o is a constant. Since T changes with wave velocity in the sample, we multiply the observed amplitudes by T_o/T to cancel the effect. T_o is the initial transmission coefficient and T is the compounded transmission coefficient for the particular observation. T is known to be, for normal incidence:

$$T = \frac{2\rho_1 V_1}{\rho_1 V_1 + \rho_2 V_2} \cdot \frac{2\rho_2 V_2}{\rho_2 V_2 + \rho_1 V_1} = \frac{4\rho_1 \rho_2 V_1 V_2}{(\rho_1 V_1 + \rho_2 V_2)^2}$$

where subscript 1 refers to the transducer mount material while subscript 2 refers to the sample.

The correction related to the change in density with saturation was seen to be of the same magnitude as the correction related to the velocity change. This last correction was calculated and seen to be insignificant for the sandstones, therefore the amplitude data is presented corrected only for the change in trasmission coefficient due to velocity changes in the sample.

Appendix F

Listing of Instrumentation.

High Power Pulser.	Velonex, Model 570 and 350-12 High Power Pulse and Burst Generator.
Low power Pulser.	HP 222A Pulse Generator.
Time counter.	Dana series 9000 Microprocessing Time/Counter.
Oscilloscope.	Tektronix, Type RM 565, Dual-Beam Oscilloscope.
Temperature Indicator.	Doric Trendicator 400A, Type K/^{o}C.
Temperature Controler.	Research, Inc. 640U process Controller.
Pressure Gauges	Heise CM-7084 (0-3000 bars) Heise CM 24348 (0-3000 psi) Duragauge (0-200 psi)
Pressure Transducer.	Pace Wiancko, model KP15.
Chart Recorder.	HP model 17502A.
Record Cutter Head.	Grampian Recording Head, Type B1/D Obtained from: International Cutter Head Repair. 194 King's Ct. Teanack, N.Yersey 07666 201-837-1289
Amplifier.	HP 465A
Oscilloscope Camera.	Tektronix C-12.

Other resonance equipment is listed in Winkler (1979 thesis, Stanford University, Geophysics.).

Non-conductive eupoxy	Ecco-bond]04, Emerson and Cumming.
Conductive eupoxy	H-20, Eupoxy Technology

BIBLIOGRAPHY

Amyx,J.,D.Bass,R.Whitning Petoleum Reservoir Engineering Physical Properties. McGraw-Hill Book Co,Inc.,p.13,1960

Auberger,M.,J.S.Rinehart, Ultrasonic Velocity and Attenuation of Longitudinal Waves in Rocks. J.Geophys.Res.66,191-199,1961

Biot,M.A. Theory of Propagation of Elastic Waves in a Fluid-Saturated Porous Solid. I.Low-Frequency Range J.Acoust.Soc.Am. v.28,2,March,1956.

Birch,F. The Velocity of Compressional Waves in Rocks to 10 Kb. Part 2, J.Geophys.Res.66,p.2199, July 1961.

Birch,F.,D.Bancroft, New Measurements of the Rigidity of Rocks at High Pressure, J.Geol.,v.48,pp.752-766,1940

Born,W.T. The Attenuation Constant of Earth Materials. Geophysics,6,132-148,1941

Brace,W.F.,A.S.Orange and T.R.Madden, The Effect of Pressure on the Electrical Resistivity of Water Saturated Crystalline Rocks. J.Geophys.Res. 70,p.5669,1965.

Collins,R.E. Flow of Fluids through Porous Materials. Reinhold Pub. Corp.N.Y.p.33, 1961

Gregory,A.R. Fluid Saturation Effects on Dynamic Elastic Properties of Sedimentary Rocks. Geophysics 41,5,895-921, 1976

Gretner,P.E.F., An Analysis of the Observed Time Discrepancies Between Continuous and Conventional Well Velocity Surveys, Geophysics,26,1-11,1961.

Hsieh,C.H. Ph.D. Dissertation. Petroleum Engineering Department Stanford University,in preparation,1979

Ito,H.,J. DeVilbiss and A. Nur Compressional and Shear Waves in USaturated Rock During Water Steam Transition. J.Geophys.Res.,84,b9, August,1979

Kanamori,H. and D.L. Anderson Importance of Physical Dispersion in Surface Wave and Free Oscillation Problems: Review, Rev.Geophys.Space.Phys.,15,pp.105-112 1977

Keenan J.H., F.G. Keyes, P.G. Hill, J.G. Moore, Steam Tables Thermodynamic properties of Water Including Vapor,Liquid, and Solid Phases. John Wiley & Sons,Inc.,N.Y.,1969

King,M.S. Wave Velocities in Rocks as a Function of Changes in Overburden Pressure and Pore Fluid Saturants. Geophysics v.31,1,pp.50-73, Feb.1966

Kjartansson,E., Generalized Viscoelastic Models of Wave Propagation. Stanford Rock Physics Project Report. v.5,1978.

Kjartansson,E. Constant Q-Wave Propagation and Attenuation, J.Geophys.Res.84,B9p.4737, Aug.1979

Kolsky,H. Stress Waves in Solids, Dover Publications, Inc. N.Y. p.47,1963.

Liu,H.P.,D.L.Anderson,and H.Kanamori, Velocity Dispersion due to Anelasticity; Implications for Seismology and Mantle Composition, Geophys.J.Roy.Astron.Soc.,47,41-58,1976.

Mavko,G. and A.Nur Wave Attenuation in Partially Saturated Rocks, Geophysics v. 44,2,161-178, Feb. 1979.

McEvilly T.V.,G.A.Mahood,E.L.Majer,B.Schechter,A.H.Truesdell Seismological/Geological Field Study of the Sierra la Primavera Geothermal System. Univ. of Callif. Berkeley,1978.

Nur,A. and G. Simmons. The Effect of Saturation on Velocity in Low Porosity Rocks. Earth and Planetary Science Letters 7, 183-193 1969, North-Holland Publishing Comp., Amsterdam.

Nur A.,G. Simmons, The effect of Viscosity of a Fluid Phase on Velocity in Low Porosity Rocks. Earth Planet. Sci. Lett.,7, 99-108,1969b

O'Connell,R.J.,B.Budiansky Viscoelastic Properties of Fluid-Saturated Cracked Solids. J.Geophys.Res.v.82,36,pp.5719-5735, Dec 1977.

Peselnick,L.,W.F.Outerbridge, Internal Friction in Shear and Shear Modulus of Solenhofen Limestone Over a Frequency Range of 10&seven Cycles per Second. J.Geophys.Res.,66,581-588,1961

Plona,T.J. and L.Tsang, Determination of the Average Microscopic Dimension in Granular Media Using Ultrasonic Pulses: Theory and Experiments. Presented at the Society of Exploration Geophysicists 1979 Annual Convention, New Orleans, Louisianna, U.S.A. Schlumberger-Doll Research, Ridgefield, Conn.

Schreiber,E. Elastic Constants and their Measurement, McGraw-Hill Book Co. N.Y.,1973.

Simmons,G.,and W.F.Brace, Comparison of Static and Dynamic Measurements of Compressibility of Rocks, J.Geophys.Res.,70,5649-5656 1965.

Spinner S.,W.E.Tefft A Method for Determining Mechanical Resonance Frequencies and for Calculating Elastic Moduli from these Frequencies, ASTM proc.,v.61,1961

Stokoe,K.H.,II,E.J.Arnold,R.J.Hoar,D.J.Shirley and D.G.Anderson. Development of a Bottom-Hole Device for Offshore Shear Wave elocity Measurement. OTC 3210 Presented at the 10th Offshore Technology Conference, Housto, Tex. May 8-11,1978.

Toksoz M.N.,C.H.Cheng,A.Timur Velocities of Seismic Waves in Porous Rocks. Geophysics,v.41,4,pp.621-645 Aug. 1976.

Thill R.E.,S.S.Peng, Statistical Comparison of the Pulse and Resonance Methods for Determining Elastic Moduli. Report of Investigations 7831 U.S. Dept. of the Interior Bureau of Mines

Walsh, J.B. New Analisis of Attenuation in Partially Melted Rock. J.Geophys.Res.,74,17, August 1969

Winkler,K.and A.Nur, Pore Fluids and Seismic Attenuation in Rocks. Geophys.Res.Lett.,6,1-4,1979,

Winkler, K., The Effects of Pore Fluids and Frictional Sliding on Seismic Attenuation. Theses, Stanford University Geophysics Department, 1979. Also in Stanford Rock Physics Project v. 7, 1979 report.

Wyllie,M.R.J.,A.R.Gregory,G.H.F.Gardner, An Experimental Investigation of Factors Affecting Elastic Wave Velocities in Porous Media. Geophysics v.23,3,pp.459-493,1958